A STUDY ON ENCLOSURE FIRES WITH MECHANICAL VENTILATION SYSTEM

KUI Qiao

BEng (Hons), The Beijing Polytechnic University

A thesis submitted to The Hong Kong Polytechnic University

in accordance with

the requirements for the degree of Doctor of Philosophy

ABSTRACT of thesis entitled "A Study on Enclosure Fires with Mechanical Ventilation System" submitted by KUI Qiao for the degree of Doctor of Philosophy at The Hong Kong Polytechnic University in July 2003.

Enclosure fires with forced ventilation were studied in this thesis with three stages. Stage one is on reviewing fire codes in China, Hong Kong, USA and other countries for identifying the fire safety aspects in enclosures with mechanical ventilation. Theoretical background of airflow induced by mechanical ventilation system appeared in the literature was studied. New concepts on performance-based fire codes were discussed. Stage two is on evaluation of different system designs. Possible fire hazard scenarios in relation to ventilation requirements were identified. Consequences of those hazard scenarios on the occupants, the building and its contents were assessed by fire models. Results are useful for designing appropriate fire services systems to provide better fire safety. Stage three is on developing a practical air flow model for forced ventilated fire.

Cabin design, a safety concept commonly used in big halls in Hong Kong, was selected for a more detailed evaluation. This was taken as an example with provision of mechanical ventilation system. Concepts of zone models with some fire plume equations available in the literature were studied. Models were then applied for scenario analysis. The principles of ventilation system design and aspects of smoke movement in a chamber were studied. In the zone model simulations, both natural ventilation and forced ventilation conditions in a cabin

were considered. The associated developed equations were solved by symbolic mathematics which have greater flexibility in changing the parameters concerned; and more transparent to the users. The two-layer zone model ASET was used for enclosures without openings. 'Bare cabin' fires with operation of smoke extraction system were solved by FIREWIND program. The Computational Fluid Dynamics (CFD) package PHOENICS was also applied to simulate several cases of cabin fire. In verifying the model, CFD results are compared with those experimental results reported in the literature including the ISO room-corner fire test and other compartment fires. Simulations with different geometrical aspects of the chamber, fire sizes, zone models, and plume models were carried out. Results are useful to identify the possible fire hazards, as well as to determine the zone model with suitable sub-models such as the plume model for different types of chamber.

Air flow induced by a point heat source in a natural ventilated compartment was studied. Three models, fully-mixed model, water-filling box model and emptying air-filling box model, on air flow in a chamber reported in the literature were reviewed. With a point heat source located at the center of the compartment, two zone models were developed: Model 1 is for a compartment without any walls and Model 2 is for an enclosed compartment with adiabatic walls; but with two openings. Equations in the developed zone models were solved by symbolic mathematics. The relationship between the neutral plane height and the outlet area was drawn. Results of the two new models are compared with those predicted by CFD, and fairly good agreement was found.

Thermally-induced plume in a chamber under forced ventilation was also studied. Plume equations derived under natural ventilation available in the literature were reviewed first. CFD was then applied to study two 'models' induced by a heat source in a chamber with forced ventilation. They are the parallel flow model and the jet flow model. Based on the plume expression in a chamber with natural ventilation, two plume equations under forced ventilation were then derived from seven sets of CFD simulations. Those are four cases with different thermal power of the point heat source; and three cases on different air speeds. Again, symbolic mathematics was used to solve some equations concerned. These developed air flow models and derived plume equations have the potential to be used in fire assessment for compartments with mechanical ventilation.

As a summary, originality and contribution to fire science and engineering can be summarized into three parts. The first part is on attempting to apply performance-based fire code in China with carpark as an example. The second part is on demonstrating zone models and CFD field model as simulation tools for fire safety assessment. Lastly, new zone models for studying aerodynamics in chambers and plume equation under forced ventilation were developed.

DECLARATION

I hereby declare that, apart from the sources quoted, this thesis represents my own work under the supervision of Professor W.K. Chow when I studied in the Department of Building Services Engineering at The Hong Kong Polytechnic University. The material of this thesis has not been submitted to The Hong Kong Polytechnic University or any other institution in an application for admission to a degree, diploma or any other qualification.

Kui Qiao

July 2003

ACKNOWLEDGMENTS

CONTENTS

Chapter 1 INTRODUCTION

In the Hong Kong Special Administrative Region (HKSAR, formerly Hong Kong), the usable land area in the downtown is quite limited. Numerous areas are enclosed, say in commercial establishments such as shopping malls, underground car parks, halls and atria. Ventilation must be provided and usually, only a small portion of volume space at the occupant levels would be ventilated for large enclosures. Mechanical ventilation (forced ventilation) and air conditioning systems are installed to supply adequate fresh air and to remove the air contaminants within a reasonable amount of time. An acceptable level of air quality in those enclosed commercial buildings can then be maintained. Hazard assessment in such enclosure buildings with forced ventilation system installed was focused in this project.

1-1   Review of earlier studies

Earlier studies of fire ventilation were concentrated on carbon monoxide, oxides of nitrogen, oxides of sulphur, odorous substances and smoke in open area. It is because those are generally considered to be the major factors affecting health. In the United States, as quoted by Stankunas (1989), the basic design criteria are 4 to 6 air changes per hour, with a minimum ventilation rate of 10 to 15 $ls^{-1}m^{-2}$. The maximum recommended carbon monoxide concentration is 50 ppm for an eight-hour time-weighted average; and 125 ppm for a one-hour time-weighted average. The minimum flow rate of fresh air to be maintained as specified in the

Australian Standard 1668.2 (1991) is 3,000 ls^{-1}. This would give an indoor carbon monoxide level of about 136 ppm if a loading value of 0.4 ls^{-1} or 1.4 m^3hr^{-1} of carbon monoxide is discharged, as proposed and used by Ball and Campbell (1973). The average driving lengths of cars for a heavy-load car park are also specified in Australian Standards. Similar standards are also found in Japan, Finland and other countries.

However, fire in a building with forced ventilation is different from those in other buildings with natural ventilation. First, a thermal stratified hot smoke layer might not be formed due to the interaction between the air flow induced by the fire and that of the ventilation system. Locations of air intake at a higher level would be an obvious example. In this instance, assumptions made in traditional zone models would not apply. Second, even if a hot smoke layer is formed, say for the case with air intake at a low level and air exhaust at a high level, the air entrainment rate toward the plume might be neglected by plume expressions available in literature describing natural ventilation fires. Estimation of the fire temperature inside such compartments using the theories for a natural ventilated fire is then not accurate enough. The forced-ventilation induced air flow would interact with the flow due to the fire, making the smoke layer unstable. In fact, whether or not a smoke layer can be formed depends on many factors. If hot gases cannot rise, sprinkler heads and fire detectors installed at higher levels would not be actuated. Another important factor is the ventilation rate which provides the necessary air for combustion. The ventilation rate is dependent on the floor area and usually, the smaller the floor area, the larger the ventilation

2

rate per unit floor area. Understanding the effects of ventilation design and the ventilation rate on enclosure fire properties is therefore important.

1-2   Outline of main works

The objectives of this research project are to study the possible hazard scenarios in relation to ventilation and fire aspects in enclosures with forced ventilation, the consequences of those scenarios on fire safety and how good building services engineering systems can be designed for improving the situation.

Zone models (Cooper 1982a & 1982b) have been developed to simulate compartmental fires. Chow and coworkers (Chow 1995a) have worked with full-size and scale models. The application of Computational Fluid Dynamics (CFD) is a powerful technique in the simulation of the resultant air flow pattern in field models (Chow 1997a, 1997b, 1998b & 1998c). These have been validated through larger fires and it is interesting to see the use of CFD performance in simulating enclosures with forced ventilation fires.

The following aspects are focused:

- Possible hazard scenarios in relation to ventilation requirements and fire safety in enclosures with forced ventilation.
- Consequences of those hazard scenarios to the occupants, the building and its contents.

3

- How good building services engineering systems can be designed for improving the safety aspects.

- Application of mathematical fire models in fire hazard assessments.

- Performance evaluation of fire protection systems.

Fire codes were reviewed and forced ventilation design was studied. Key equations in a two-layer fire zone model were analysed by referring to the popular model Available Safe Egress Time ASET (Cooper 1982a & 1982b). Results predicted by ASET (Cooper 1982a & 1982b) and from a model based on symbolic mathematics program MATLAB (1997) were compared. Also, natural ventilation and fire simulations on 'cabin' with FIREWIND 3.4 (FMC 1997) were studied. 'Bare cabin' fires (Chow 1997a, 1997b, 1998b & 1998c) were predicted by zone model with and without operation of smoke extraction system. Time to flashover with smoke extraction system in a 'bare cabin' was studied. In addition, results were compared by CFD studies (Chow 1997a, 1997b, 1998b & 1998c). Thermally-induced indoor aerodynamics in compartment with natural ventilation was investigated and plume equation in a chamber with forced ventilation was studied.

Estimates of doorway flow rates are required for smoke control in fires and forced ventilation design. Literatures and papers about doorway ventilation were reviewed and studied. The scope of the Code is expanded from a prescriptive-based code for stairs, doors and fire escapes to a performance-based and prescriptive-based code addressing myriad factors affecting life safety in the

4

event of fire. Every item in the fire code comes from series of lessons or experiments.

Fire codes in Hong Kong (Chow 1995c, NFPA 1994 & 2001) might become more closely related to those of the Mainland after the smooth reunification in 1997. Updated fire codes in China and in Hong Kong are studied. Meanwhile, the study on forced ventilation is not isolated, but should be applied to practical situations. One of the main aspects of the application is to amend and change the prescriptive fire codes into performance-based fire codes (Bressington 1999a, Buchanan 1998, Hadjisophocleous 1998). Fire codes of China (Ministry of Public Security 1995 & 1997, Ministry of Construction 1999), particularly on carparks (Ministry of Public Security 1998, GB50067-97), were reviewed and compared with those in Hong Kong. Cabin fire simulations for airport terminals and railway stations were carried out, in order to study how good building services engineering systems can be designed for improving the safety aspects. It is well known that airport terminals and railway stations have long escape routes with large spaces. Smoke extraction systems are provided to enhance fire safety where travel distances for escape are extended or compartment volumes exceeded the regulation limits.

In order to have a better understanding of fire development and the smoke spread, so as to provide safety to people, simulations with natural ventilation were carried out by using FIREWIND 3.4 (FMC 1997). The time to flashover for fires in a 'bare cabin' with smoke extraction system was studied by using the

FIREWIND program as a simulation tool. The FIREWIND simulation on cabin was started with natural ventilation, and then with different fires and with or without forced ventilation system installed to evaluate their performance. Over 14,400 simulations were carried out with results reported in literature (Kui & Chow 2000, Chow & Kui 2000).

CFD, a powerful but practical technique was applied to simulate the resultant air flow induced by fire in enclosures with forced ventilation. CFD studies were carried out on 'bare cabin' fires with and without the operation of smoke extraction system. The popular CFD package – PHOENICS (PHOENICS 2000) was selected as the simulation tool for data analysis. ASET (Cooper 1982a) model was developed and combined with MATLAB.

1-3   Outline of thesis

As described above, this chapter gives an introduction including a review of previous works and fundamental knowledge on fire safety aspects in enclosures with mechanical ventilation system. A pictorial presentation of the thesis is shown in Figure 1-1. The fire aspects identified in enclosures with mechanical ventilation were reported from Chapters 2 to 4. Performance-based fire codes were attempted to be implemented in China. Application of zone models and CFD field models as simulation tools for fire hazard assessment were studied from Chapters 5 to 7. Performance of fire protection system were evaluated. For Chapters 8 and 9, innovations of two zone models of both natural ventilation and

forced ventilation aspects were studied for optimizing the fire safety aspects by improving the design of building services engineering system. Finally, a conclusion is given in Chapter 10.

Chapter 2 PRELIMINARY REVIEW ON FIRE SAFETY CODES IN CHINA

Fire code study is important because in any country, building design should follow building fire codes and related regulations. Fire codes integrate both former fire science research achievements and experiences. Both the fire codes of China and Hong Kong studied are of the latest versions.

Upon smooth reunification of Hong Kong to Mainland China, local fire codes (Fire Services Department 1994a & 1994b, Buildings Department 1995, 1996a, 1996b & 1998) might be more closely related to those in the Mainland. Understanding the fire codes in the Mainland and how they can be upgraded to suit the requirements in this new century would be essential. To satisfy the requirements for new buildings, some changes have been made in other places (Chow 1995c, NFPA 1994 & 2001). The scope of building fire codes is moving from prescriptive-based codes (e.g. for stairs, doors and escapes) towards 'performance-based', with some specification codes addressing factors affecting life safety in case of fire.

The objective of establishing building fire codes is to ensure life safety in case of fire and other similar types of emergency (NFPA 1994 & 2001) with minimum requirements, taking into account the function, design, operation and maintenance of the buildings and structures concerned. The level of fire safety can be worked out (NFPA 1994 & 2001) through the requirements on:

prevention of ignition; detection of fire; control of fire spreading; confinement of fire and smoke; extinguishment of fire; provision of refuge and/or evacuation facilities; staff responses; and provision of fire safety information to occupants.

2-1   Basic fire codes in China

Over the last 50 years, China has actively participated in the global fire research activities and has played an important role in the field of fire engineering on the international platform. Fire codes in China are quite complicated but can be classified in two main ways: by legal effects and by contents. The details are shown in Table 2-1.

Many fire codes in China are related to buildings, among which the three most popularly used are: Code for fire protection design of buildings (GBJ-16-87, Ministry of Public Security 1995), Code for fire protection design of tall buildings (GB50045-95, Ministry of Public Security 1997), and Design code for residential buildings (GB50096, Ministry of Construction 1999). A critical review on the requirements on the design of building in the China fire codes can be found in Appendix A.

2-2   Comparison with NFPA Life Safety Code, USA

Building fire codes in the USA are made by different non-benefited individual organizations and associations such as: American National Standards Institute

(ANSI), American Society of Heating, Refrigerating and Air-Conditioning Engineers (ASHRAE), National Fire Protection Association (NFPA) and American Society for Testing and Materials (ASTM). A building code cannot become a regional law unless going through legislation program and approved by most members of the city council. The copyright of building codes does not belong to the US government, but the individual associations and organizations. The US government has the authority to announce emendation clauses or items of each building code (Shen 2001).

The purpose of the performance-oriented language used in the NFPA Life Safety Code (NFPA 1994 & 2001) is specified as protecting the occupants not intimate with the initial fire development from loss of life while also improving the survivability of those who are intimate with the fire.

2-2-1   Comparison of fire hazard classification

Fire hazards are divided into four classes in the China code and three classes in the NFPA code. The criteria for classification of fire hazard are listed in Table 2-2.

According to the comparison above, the classification in the US code and the China code are similar. They are all based on the burning performance of the building materials and structure of the buildings.

2-2-2 Comparison on means of egress

Occupants of a building must be protected from obstacles to safe egress. To achieve this goal, the protection of each component in the egress system must be considered. The principal factors governing the provision of means of escape are the number of occupants in the compartment, and the maximum time needed for an occupant to escape from a given compartment. To determine the number, width and location of exits, three vital points are considered in both the China code and the US code: alternative egress, travel distance and number of occupants, the width and the number of exits and the location of exits limiting the time of escape.

The egress capacity requirements of common buildings in the China code and in performance-based code are shown in Table 2-3 and Table 2-4 respectively.

The comparison of travel distance limits is shown in Table 2-5. The comparison of width requirements on assembly and other occupancies of performance-based code is shown in Table 2-6, and the comparison of the requirements of width and exit of buildings is shown in Table 2-7.

The classification of fire class for industrial buildings in the China code depends on the production of the factory; while for the US code, it depends on the burning and explosive characteristics of the materials contained in a building, not on the quantity of combustibles. The different definitions of the two codes are shown in

Table 2-8.

The number of stories and occupancy area of industrial buildings are also limited by their classification of danger. Requirements in the China code are shown in Table 2-9.

Obviously, the China code is more detailed than the US code on this part. The China code has a clear classification on industrial buildings, because a large series of experiments and tests have been done in China for setting those requirements.

2-3 Comparison with fire codes in Hong Kong

In Hong Kong, the fire code is called as Code of Practice (Buildings Department 1997a). There are mainly four codes:

- Code of Practice for Means of Access for Firefighting and Rescue (Buildings Department 1995)

- Code of Practice for the Provision of Means of Escape In Case of Fire (Buildings Department 1996a)

- Code of Practice for Fire Resisting Construction (Buildings Department 1996b)

- Codes of Practice for Minimum Fire Service Installations and Equipment (Buildings Department 1998a)

"Code of Practice for Means of Access for Firefighting and Rescue" seeks to achieve the objective of assisting in firefighting and in saving lives of people in buildings by ensuring adequate access for firefighting personnel in the event of fire and other emergencies. The following parts are included: access staircase; fireman's lift; firefighting and rescue stairway.

"Code of Practice for the Provision of Means of Escape In Case of Fire" is to announce provisions for the protection of buildings from the effects of fire by providing adequate means of escape in the event of fire and other emergencies. It includes: requirements of exit routes, direct distance and travel distance, doors in relation to exits, etc.

"Code of Practice for Fire Resisting Construction" is to announce provisions for the protection of buildings from the effects of fire by inhibiting the spread of fire and ensuring the integrity of the structural elements of buildings. It includes: compartmentation (zoning), protection of adjoining buildings, protection against spread of fire and smoke between floors, roofs, etc.

"Codes of Practice for Minimum Fire Service Installations and Equipment" provides detailed fire design requirements of the following: basements, boiler rooms, carparks, commercial buildings, domestic buildings, garages, hotels, etc. Hong Kong is a part of China, but before the handover in 1997, Hong Kong has developed its own fire codes far different from those of China. Most parts are incomparable, only because they belong to different systems. The comparison of

specified requirements of width and exit of common buildings, and travel distance limits are listed in Table 2-5 and Table 2-7.

2-4   Conclusion

As learned from the above study, China's fire code is a prescriptive-based fire code paying more attention to industrial buildings. This is because the industrial development has been the central focus of the country in the past 50 years. That is necessary, but no longer suitable for the new situation. Compared with the US code, protection of human lives should be considered more. The following practice and circumstances are analyzed carefully in both the US code and the China code: volume and height of the building, use of the basement construction, the degree of natural ventilation or without natural ventilation, the provision of adequate smoke control, the distance from the boundary or the distance to other buildings, the use category of other parts of the same building or adjacent buildings, the accessibility of the fire fighting appliances, the spacing and adequacy of fire-protected pedestrian escape stairs.

Compared with the US code, some advantages of the performance-based fire code would be good for the improvement of the China code.

2-5   Future directions

Performance-based fire codes are developed from prescriptive-based codes and

widely used by municipal departments of government, fire department and relative institutions. China can learn more from this to improve the existing fire code. Now, with the development of new buildings, it should be amended to suit the new situation. More new types of buildings should be considered such as underground carparks, enclosure buildings and atria or even new high-technology Artificial Intelligence (AI) buildings.

Cars, ships, trains and planes are similar to buildings in the way that they have an enclosure area, several entrances and exits. They are more dangerous than low-rise buildings because most fire cases occur on their moving, thousands of meters high in the air or in the middle of the ocean. Their problems are the same as buildings on escape, fire alarm, fire resistance and so on. Future fire codes would be applicable to those vehicles.

Multi-disciplines are involved in the study of fire code, such as fire engineering, building services, calculation with the new performance-based code, and even humanity factors engineering and social sciences. Scientists are needed to break the barriers in language and limits and to accept different concepts. International conferences can help fire engineers and scientists get together to exchange their viewpoints.

Chapter 3 REVIEW OF VENTILATION SYSTEM DESIGN

This Chapter is focused on two parts: ventilation system design review and ventilation system design methodology (see Figure 3-1). Ventilation system design can be better understood by reviewing the fire codes. That is because ventilation system design in the building would follow building regulations. To study the fire safety in enclosures with forced ventilation conditions, acquiring more knowledge of ventilation system design in different building types is necessary. Both natural ventilation design and forced ventilation design in different building type are reviewed. Basic knowledge of forced ventilation system model design methodology was then studied. Underground carpark in the commercial building is always designed as a typical large enclosed space. The study on carpark is very important to get the basic concepts of fire safety in enclosures with forced ventilation conditions. Carpark ventilation system requirements in different countries are reviewed in order to show the common ground.

3-1 Objectives of installing ventilation system in a building

The ventilation control system and smoke control system must accomplish one or more of the following objectives (NFPA 92A 1992 & 2001, NFPA 92B 1995 & 2001):

- Maintain a tenable environment in the means of egress from large-volume building spaces during the time required for evacuation.

- Control and reduce the migration of smoke between the fire area and adjacent spaces.

- Provide conditions within and outside the fire zone that will assist emergency response personnel to conduct search and rescue operation and to locate and control the fire.

- Contribute to the protection of life and reduction of property loss.

- Aid in post-fire smoke removal.

To achieve these objectives, sprinkler systems are provided in most commercial buildings in Hong Kong. Smoke management systems such as smoke extraction systems, or staircase pressurization systems might also be provided (Wong 1999).

Smoke extraction systems serve to prevent a smoke layer from reaching a critical level, reduce its temperature and improve visibility by diluting the smoke with cooler air. The spread of smoke is limited by fire compartments, or smoke barriers.

3-2   Natural ventilation system

Natural ventilation system includes all natural ventilation facilities installed in a building, such as windows, doors and so on. Natural ventilation design of residential buildings in Hong Kong and Mainland China are compared below.

3-2-1 Natural ventilation design of residential buildings in Hong Kong

Regulations on ventilation design in a building were set up in Hong Kong with most of them listed in Chapter 123, Hong Kong Building (Planning) Regulations (Buildings Department 1997b). Requirements for planning, design and construction of buildings and associated works were provided as in Hong Kong Building Ordinance (Buildings Department 1997b). This will make provision for rendering safety of dangerous buildings and land; and make provision for matters connected therewith.

Windows and doors are basic installations for natural ventilation. The minimum requirements of windows are listed clearly in The Hong Kong Buildings Ordinance Chapter 123F 31 and also shown in Table 3-1.

In this regulation, "window" includes french window; and the sill of a prescribed window shall be deemed to be at a level 1 m above the level of the floor of the room for which the prescribed window is provided, whether or not the sill is at such level (Buildings Department 1969).

To make sure the function of window is effective, there are restrictions on distance between the prescribed windows, to any part of the room.

The minimum requirements of doors are listed in Chapter 123, Hong Kong Buildings Ordinance (Buildings Department 1997b) and also shown in Table 3-2.

Since the living space in Hong Kong is quite limited, there are no specifications on the size of door, but general requirements on the position and type. No door, gate, window or shutter opening on or over any street shall be so hung or placed as to project over such street at a height of less than 2.5 m above the ground. Emergency exit doors, electrical transformer room doors, plant room doors, refuse storage chamber doors and doors leading to similar types of utility rooms or chambers may open outwards over such a street if such doors when fully opened do not cause an obstruction to any person or vehicle using the street (Buildings Department 1992).

3-2-2   Natural ventilation design of residential buildings in Mainland China

Requirements of natural ventilation design of residential buildings in China are listed in three regulations, namely Code for fire protection design of buildings (GBJ-16-87, 1995), Code for fire protection design of tall buildings (GB50045-95, 1997) and Code for fire protection design of commercial buildings (JGJ48-88, 1989) (Ministry of Public Security 1995, 1997 & 1989).

It is required that the window open to staircase and fire elevator should be at least 2 m^2. Smoke extraction window should be installed on the ceiling or on the top of the room and easy to open. In the Design code for residential buildings of China (GB 50096-1999) (Ministry of Public Security 1999), it is required that in both the living room and bedroom, the inlet-outlet area for natural ventilation should be 1/20 of the floor area at least. In bathroom and kitchen, the inlet-outlet

area for natural ventilation should be at least 1/10 of the floor area and no less than 0.6 m^2.

Minimum requirements of the size of windows in China code are listed in Table 3-1, where the window area A_c in a room corresponds with the room floor area A_f (GB 50096-1999). The requirements are found to be similar to the Hong Kong Buildings Ordinance, but China design code has more details on the requirements of different types of room. That is because other countries' building fire codes (NFPA 1994 & 2001, BCA96 1996, Ministry of Construction 1995) are referred to for the China design code.

Minimum requirements of the size of doors in China code are listed in Table 3-2. The width of the door is varied from 1.2 to 0.7 m and the height of door is always 2.0 m. The requirements are again similar to the Hong Kong Buildings Ordinance.

3-3   Forced ventilation system

Forced ventilation system includes all kinds of forced ventilation facilities installed in a building like fans, ventilation pulps, inlets and outlets of ventilation, etc. Forced ventilation design of residential buildings in Hong Kong and Mainland China are compared below.

3-3-1 Forced ventilation design of residential buildings in Hong Kong

Regulations on smoke control and forced ventilation are specified in: Smoke Extraction Systems, Code of Practice for Minimum Fire Service Installations (Buildings Department 1998), Equipment and Inspection, Testing of Installations and Equipment. Forced ventilation system for smoke extraction can be exempted if any one of the following conditions is satisfied (Wong 1999).

- The compartment does not exceed 7,000 m^3; or

- The aggregate area of open window of the compartment exceeds 6.25% of the floor area of that compartment; or

- The design fire load does not exceed 1,135 MJ m^{-2}.

- For atrium, the compartment does not exceed 28,000 m^3.

- For internal means of escape for hotels, if the route is provided with openable windows connected to open air and the aggregate area of such windows exceeds 6.25% of the floor area of the route.

- For basement area, if the compartment does not exceed 7,000 m^3; or the design fire load does not exceed 1,135 MJ m^{-2}.

Two options of smoke extraction system can be employed: Dynamic smoke extraction system and static smoke extraction system.

Dynamic system is a mechanical ventilation system capable of removing smoke and the products of combustion from a designated fire compartment, and also

supplying in fresh air, to maintain a specified smoke free zone below the smoke layer.

Static system has been applied in natural ventilation, utilizing smoke reservoirs, located ducting and openings actuated by smoke detectors.

In Chapter 123 of Hong Kong Buildings Ordinance, it is specified that the mechanical means of ventilation shall be capable of supplying fresh air to all parts of a room at a rate of not less than 5 changes of air per hour.

3-3-2   Forced ventilation design of residential buildings in Mainland China

Requirements of forced ventilation design for buildings in China are illustrated in the three regulations mentioned earlier. They are Code for fire protection design of buildings (GBJ-16-87, 1995), Code for fire protection design of tall buildings (GB50045-95, 1997) and Code for fire protection design of commercial buildings (JGJ48-88, 1989) (Ministry of Public Security 1995, 1997 & 1989).

In China Building Code (Ministry of Public Security 1989, 1995, 1997 & 1998), forced ventilation system and smoke extract system should be installed in the following buildings:

- Subway individual department stores, hospitals and motels which usable area exceeds 500 m^2;

- Restaurants, exhibition centers, gymnasiums, ball halls, skating ranks which the usable area exceeds 1000 m^3 and decorated by noncombustible materials. Or, the usable area exceeds 500 m^3 and decorated by difficult combustible materials;

- Cinemas, auditoriums;

- Libraries, chanceries and workshops in class C and D (see Table 2-17) which the usable area exceeds 1000 m^3;

- Underground buildings with smoke proof staircases installed.

Minimum requirements of forced ventilation for residential buildings in the China code are shown in Table 3-3. The largest difference with the Hong Kong code is in the requirements of extraction rate in industrial buildings. The extraction rate in the China code is much larger than in the Hong Kong code, that is because most industrial buildings in mainland China are for heavy industry, they need higher air change rate to maintain the air quality inside the factory.

3-3-3 Requirements from prescriptive codes for dynamic smoke extraction system

Generally, in the prescriptive codes, the requirements for smoke extraction system are:

- Smoke extraction rate is 8 air changes per hour in general, 10 air changes per hour for internal means of escape for hotel areas, with minimum smoke extract sizing based on 7,000 m^3. Atria are not included.

- Minimum make up air rate is 80% of the extraction rate in general.

- Requirements on smoke detection system can be made reference to BS 5839 (British Standard 1995).

3-4   Fire in an enclosed chamber

Smoke is the real enemy to life safety in most fire accidents. Smoke management system is important to defend life safety. The basic knowledge of smoke, smoke layer, and requirements on ventilation system are introduced in this section.

Once a fire is started, a convective plume of heated gases would rise upward to the compartment ceiling. The driving force is buoyancy and 1 m^3 of hot air at flame temperature would only have density of a quarter of that of surrounding ambient air. The upward buoyancy is about 1 kg force. The higher the ceiling above the fire source, the greater the volume of smoke, but the cooler the resulting gases at ceiling level with less buoyancy. This is because cooler air at ambient temperature is entrained into the plume as it rises. The upward buoyancy will be decreased and hence the vertical velocity decelerated. Smoke in the smoke layer has over 95% of entrained air. The rate of air entrainment is a function of several variables, notably the base perimeter of the plume at spout level, the ceiling height and the flame temperature. Large amount of air is drawn into the plume in the near field around the base of the fire.

A smoke layer would be formed in a compartment fire when the ceiling jet strikes a vertical wall. It will become hotter and thicker to descend downward. This is analogous to water filling a sink but turned upside down. Values of typical layer lift forces or upward pressure are around 3 to 6 Pa (ASHRAE 1985). There will be problems on evacuation and fire fighting when the smoke layer descends to the occupant zone. Visibility of occupants will be reduced and toxic gases will bring ill-health effects. In fact, most deaths in fires were due to smoke, not heat.

3-5   The well-mixed model: carpark

The basic design method is based on the "well-mixed model" described as follows. Suppose a carpark is an enclosed space of volume V_{Room}, and the fresh air intake rate and the exhaust rate are the same, at a value of M (expressed in kgs^{-1}). Sources of carbon monoxide are taken to be of emitting rate S_t (expressed in kgs^{-1}), giving an instantaneous carbon monoxide concentration of C(t) (expressed in kg per kg of air). The air density is ρ (1.2 kgm^{-3} at 20 °C and 101.325 kPa; it is taken to be the same as the density of carbon monoxide of 1.25 kgm^{-3} at 0°C and 101.325 kPa (ASHRAE 1985). The fresh air injected into the car park enclosed space has a carbon monoxide concentration of C_{in} (expressed in kg per kg of air).

The mass balance equation for thorough mixing of carbon monoxide and air gives:

$$\rho V_{Room} \frac{dC_t}{dt} = S_t + MC_{in} - MC_t \qquad (3\text{-}1)$$

The expression of the equation was developed by Chow (1995b).

In a carpark, cars might move in or out within a time interval while measuring the emission rate. The carbon monoxide level in the carpark can be very high if mixing between the fresh air and the carbon monoxide is poor (Chow 1995b).

Concentration of carbon monoxide C(t) can be expressed as a "filling up" part when a source is discharging; and a "decay" part when there are no cars with engines running to emit carbon monoxide. The variation in carbon monoxide concentration against time for three cars is shown in Figure 3-2. It can be seen that the carbon monoxide level increases to only about 32 ppm, which is much less than the maximum value of 240 ppm calculated by the ventilation rate of 6 air changes per hour with the well-mixed model. In this example, the filling up period for carbon monoxide in the car park resulting from the discharge of carbon monoxide from car 1 is from 0 to 5 minutes, and the decay period is from 5 to 10 minutes, followed by a decay period of 15 to 30 minutes. Another filling-up period, resulting from car 3, is between 30 and 35 minutes, and the carbon monoxide is diluted after 30 minutes.

3-6 Ventilation requirements of carparks in different countries

Mechanical ventilation systems are installed in large enclosed carparks to supply adequate fresh air and to remove the air contaminants within a reasonable amount of time, in order to maintain an acceptable level of air quality. Many design guides on ventilation are available in the literature such as ASHRAE (1985) and Australian Standards (1991). Ventilation requirements of these standards are commonly expressed in terms of the fresh air flow rate per unit flow area.

Carbon monoxide is discharged by motor vehicles that have internal combustion engines. The amount of carbon monoxide discharged depends on the completeness of the combustion process. Therefore, the type of fuel used, the age and working condition of the engine, the driving behavior of the driver, and the quantity of fresh air supplied will all affect the concentration of carbon monoxide in an enclosed space.

Because the potential health effects of carbon monoxide on human beings are quite significant, keeping the carbon monoxide level below a certain value is used as a criterion in many ventilation design guides. The volume of carbon monoxide discharged per time period is a varying parameter: it varies even for the same car, if it is driven under different operating conditions. A loading volume of 0.4 ls^{-1} or 1.4 m^3 hr^{-1} is the standard used for a five-passenger car by

Ball and Campbell (1973); 0.2 gs^{-1} per car is required in ASHRAE standards (1985).

The studies of air quality are not only concentrated on carbon monoxide, but also other pollutants, such as oxides of nitrogen, oxides of sulphur and odorous compounds.

In the United States, the basic design criteria as quoted by Stankunas (1989) are: 4 to 6 air changes per hour, with a minimum ventilation rate of 7.5 $ls^{-1}m^{-2}$ and a maximum ventilation rate of 10 to 15 $ls^{-1}m^{-2}$. The maximum recommended carbon monoxide concentration is 50 ppm for an eight-hour, time-weighted average; and 125 ppm for a one-hour, time-weighted average.

In Japan, as quoted by Matsushita (1993), the mean carbon monoxide level per eight-hour average is 20 ppm and the environmental standard for inhabitable rooms is 10 ppm over the same period.

In Finland, the ventilation requirement for carparks is determined by the carbon monoxide concentration (Koskela 1991). The limit for carbon monoxide concentration is 30 ppm for an eight-hour average, and 75 ppm for a 15-minute average. The minimum supply air flow rate is 2.7 $ls^{-1}m^{-2}$. This rate would require 9.72 air changes per hour per metre-length of ceiling height.

In Australia, the standard 1668.2 (1991) specifies that a minimum flow rate of fresh air of 3,000 ls^{-1} is to be maintained. This would give an indoor carbon monoxide level of about 136 ppm if a loading value of 0.4 ls^{-1} or 1.4 m^{3}hr^{-1} of carbon monoxide discharged, as proposed by Ball and Campbell (1973), is used. Australian standards also specify the average driving lengths of cars for a heavy-load carpark.

The carbon monoxide load in a given carpark is a key parameter for modeling the carbon monoxide level. The number of cars exhausting toxic gases is a transient phenomenon that depends on many factors. For this reason, modeling the carbon monoxide level contour due to a single source is not especially useful, because the positions of the cars and the amount of toxic gases discharged from them are uncertain.

In the investigation of the design of lighting, heating and ventilation in multi-story and underground carparks reported by Ball and Campbell (1973), a five-passenger car might produce up to 1.44 m^{3}hr^{-1} (or 0.4 ls^{-1}) of carbon monoxide. This means that if a carbon monoxide level of 50 ppm is to be maintained, the ventilation rate should be 8 m^{3}hr^{-1}(NFPA 92A 1992 & 2001).

The technique of computational fluid dynamics is used to verify those existing models and then to compute the mixing factors concerned.

In addition, a study of doorway ventilation is shown in Appendix B.

3-7   Conclusion

The objective of installing ventilation control system in a building is illustrated in this chapter. Basic knowledge of smoke development is introduced. Both Hong Kong Buildings Ordinance and China buildings code are reviewed on natural ventilation design on windows and doors, forced ventilation design and air change per hour or fan extraction speed. Requirements of smoke extraction system in prescriptive codes are introduced. The ventilation aspects of underground carparks are also studied. The ventilation theory of well-mixed model is reviewed. For the well-mixed model, the maximum carbon monoxide can be obtained by dividing the emission strength of the source by the ventilation rate. This is the asymptotic value of the transient carbon monoxide concentration curve derived by solving the mass balance equation analytically.

In order to understand the different requirements on natural ventilation design and mechanical design in Hong Kong and China Mainland, the China Building Code (Ministry of Public Security 1989, 1995, 1997 & 1998) and Hong Kong Building Code (Buildings Department 1997b) are compared in this chapter. The results are very useful for further simulation modeling design. These results are used to study the air movements in a building in the following chapters.

Chapter 4 PRELIMINARY FEASIBILITY STUDY ON APPLYING ENGINEERING PERFORMANCE-BASED FIRE CODES IN CHINA: CARPARK AS AN EXAMPLE

This Chapter is focused on performance-based fire code study of ventilation requirements on carpark. According to the studies above, three fire safety aspects are focused: smoke control (ventilation), fire control and egress, where smoke control and fire control in enclosure are the focus of study, which is most important to both egress and property protection. Study of existing ventilation requirements on ventilation in enclosures, especially requirements on underground carparks, is very useful to learn the method for identifying the possible hazard scenarios in relation to ventilation requirements and fire safety in enclosures with forced ventilation, which is also considered in the design of performance-based fire code. In addition, how to make the fire science research achievements be accepted by public and be transferred to the form of fire codes as an application is very important, which has been discussed in this chapter. Performance-based fire codes have now become the most popular topic among fire engineering and safety scientists. More and more countries are introducing this concept to rebuild their fire codes. The essence of performance-based fire code is brought out, and feasible ways to apply in China are suggested.

4-1   Introduction to fire codes of carpark in China

Fire codes of carpark in China (GB50067-97, Ministry of Public Security 1998) are one of the important parts of the building codes under the Technical Law branch. It is constituted by the Ministry of Public Security and approved by Planning Committee of PRC. It was first issued for test on 1 January 1985. The following areas of interest in the fire codes of carpark in China are introduced.

There are eight chapters in the fire codes of carpark:

- General principles: the purpose and application of this code.

- Fireproof classification and fire resistant class.

- Plane planning: general requirements, fire space and fire engine track.

- Fire separate and building structure: requirements on fire separate, fire wall, separate wall, elevator well, pipes' tunnel and other fire resistance structure.

- Egress: requirements on safety escape for occupancies.

- Fire water supply, alarm and extinguishing equipment.

- Heating and ventilation.

- Electric equipment.

The code is used for new carparks, enlarged carparks and rebuilt carparks.

Carparks are classified into the following three types in China:

- Enclosure garage, including high-rise garage, enclosed or open garage, compound garage and underground garage.

- Motor repair shop.

- Open parking area.

Another way of classifying carparks is by the nature of cars:

- Carparks for cars of special use.

- Carparks for important cars needed to be protected or cars carrying valuables.

- Carparks for cars carrying combustibles or explosives.

In order to extinguish the fire more effectively, carparks are classified into four types of fireproof by the number of cars as shown in Table 4-1.

In order to make the design of carparks easier, they are also classified into three classes of fire resistance as listed in Table 4-2.

It is also clarified in the code that it is better to classify a carpark at a higher level to make stricter requirements.

4-2   Requirements on ventilation in carparks

The two main areas of particular interest are the fire separate and structure on tunnel and other facilities for ventilation. In order that the ventilation system works effectively,

- Ventilation system in carparks should be set up individually. Ventilation pipes should be made of non-combustible materials, and should not run through fire wall and fire separate wall.

- If it must be done that way, space around pipes should be filled by non-combustible materials, and fire valve is needed.

The structure requirements of elevator well and tunnel in carparks are:

- Elevator well, pipes' well, cable tunnel and staircase should be arranged separately.

- The walls of those tunnels should be built of non-combustible material with 1 hour minimum fireproof time.

- If the height of the multi-story carpark exceeds 24 m, the wall of the elevator well should be constructed of non-combustible material with at least 2.5 hours minimum fireproof time.

The aim of setting up these requirements is to stop the fire spread in vertical direction (Ministry of Construction 1995). The data were referred to the Life Safety Code (NFPA 1994 & 2001).

- In places where pipe well and cable tunnel run through the floor, the same fire resistant materials as that of the floor should be used.

- A fire door with 0.6 hours minimum fireproof time should be used for the inspecting door on the wall of well and tunnel.

That is because in China, fire doors are classified into three classes. The fire resistant time for Class A is 1.2 hours, Class B is 0.9 hours and Class C is 0.6 hours. Normally, fire door for carparks is designed as Class C. Drive road in enclosed multi-story carparks and underground parking should be separated from the parking zone by fire wall.

- Fire wall belongs to the part of fire separate and structure. Firewalls should be built on the base of the frame of reinforced concrete.
- No ventilation pipes and windows are permitted to run through the firewall except fireproof window with minimum fire resistant time of 1.2 hours.
- Firewalls in entrances and exits should have a minimum fire resistant time of at least 1.2 hours, or rolling doors protected by water screen, in spite of sprinklers are installed.
- The requirements of ventilation and fire separates are no different from those of other buildings.

In China, to maintain the carbon monoxide level in carparks under the standard (GB50067-97, 1998), it specifies that a minimum flow rate of fresh air should be at least 50% of the smoke extraction rate. The minimum supply air velocity in pipe should be 15 to 20 ms^{-1}. This rate would require 6 air changes per hour for a 2000 m^2 carpark or garage with a ceiling height of 3 m. This requirement is referred to the US Life Safety Code (NFPA 1994 & 2001).

4-3   Performance-based fire codes vs current fire codes

In this new millennium, code officials can anticipate the first generation of performance-based fire codes to be in effect in the world. The reason why the present system has to be changed though it does work is, more and more building designers agree that the present system of prescriptive codes does not always apply to today's new design of buildings. A set of rules and guidelines is needed which can be used to test the validity of a particular design. Therefore, people can make clear about the designs and assumptions which they based on. The basic concept and structure of performance-based fire code are introduced, and the advantages are pointed out in this section.

Specific rules are spelt out in prescriptive codes for everything needed for an acceptable system: exits, fire sprinklers, fire-containment doors, etc. Authority Having Jurisdiction (AHJ) follows prescribed codes when inspecting systems and approving the final plans.

In a performance-based code system, requirements are stated as goals rather than concrete requirements. For instance, the current prescribed code might state that "The maximum distance to a building exit shall be less than 45 meters". The revised wording, when stated as a performance goal, would read like "All occupants must have time to reach a safe place". The performance-code language has the advantage that it applies whether the occupants are high school athletes

or nursing home residents. Then, fire testing facilities and capabilities can be used to verify specific approaches to performance-based design.

During the past 20 years, there have been a great deal of research on how fires behave and how people can be better protected. Performance-based fire codes are being developed through computer models that predict heat transfer, fluid movement and fire spread. Some of the groups leading the fire research in this area are National Institute of Standards and Technology (NIST) and Society of Fire Protection Engineers (SFPE).

4-3-1   Basic knowledge of performance-based fire codes

In the classical study on fire codes, standards are of three types generally (ISO 6241 1984): Materials standards, Engineering practice standards (for basic design) and Testing standards.

Differing from the old prescriptive-based code, the new legislation allows any solution provided that it complies with the performance requirements. It concerns about how the building behaves instead of how the building is built.

Thus, the definition of performance factors (illustrated in ISO 6241, 1984) are:
- User's requirements;
- Uses of the building and spaces;
- Sub-systems of the building;

- Agents relevant to the building performance.

Four basic use groups are specially considered. They are sleeping use, unfamiliar use, familiar use and nursing.

The main performance requirements are (Buchanan 1998, Hadjisophocleous 1998):

- Provision of safe egress for occupants.
- Provision for safety of fire fighters.
- Prevention of fire spread to neighboring properties.
- Safeguarding the environment from the adverse effects of fire.

4-3-2 Advantages of " performance-based"

In the past practice, shortcomings in the classical prescriptive codes are found, such as:

- Non-uniform fire levels in buildings.
- Confusion between code objectives and methods.
- Little recognition of wide variation in real hazard within a given occupancy.
- Lack of focus on occupancies.
- Difficulty in interpretation.
- Complexity in handling.
- Lack of the applicable code requirements.
- Low efficiency.

- Overlapping fire safety measures.

- Low flexibility in architectural design.

- Difficulty in the use of new technology.

Following the earlier studies, more advantages can be found in performance-based fire codes as follows:

- Facilitate innovation

- Cost effective

- Lower construction costs

- Increase fire safety

- Enhance hazard recognition

- Allow free design

- Clear safety goals

- Eliminate technical barriers

- Follow universal regulation system

- Facilitate use of new technology

- Non-complex

To meet the new requirements of today, performance goal on selected chapter will be applied in the updated China code. The following are proposed as examples.

- "All cars and people in carparks must have enough time to escape to a safe place during the fire."

1   "Entrances and exits must be designed to let people and cars move to a safe place during the fire."

"Entrances for cars and exits for people should be installed individually. At least two exits should be installed except that there would be at maximum 25 persons at the same time. Enclosure staircases are required as well with the minimum width of 1.1 m. The shortest distance from the carpark to the safety exit is limited to 45 m to 60 m depending on whether sprinklers are installed."

"Fire walls in Entrances and Exits should have minimum fire resistant time of at least 1.2 hours, or rolling doors protected by water screen, in spite of sprinklers are installed."

2   "Drive road must be well protected from fire."

"Drive road in enclosed multi-story carparks and underground parking should be separated from the parking zone by fire wall."

The above is a preliminary study of the new performance-based fire code for China.   The first sentences in the above two examples are the performance requirements, outlining a suitable level of performance which must be met by the building materials, components, design factors, and construction methods for a building to meet the relevant functional statements and, in turn, the relevant

objectives. The performance requirements are the core, and are the only parts of the code with which compliance is mandatory. The following sentences contain the building solutions, setting out the means of achieving compliance with the performance requirements. Two methods that can be followed to develop a building solution are: (a) deemed-to-satisfy provisions, including examples of materials, components, design factors, and construction methods; and (b) alternative solutions. The key to performance-based fire code is that there is no obligation to adopt any particular material, component, design factor or construction method. An approval authority may still issue an approval if it differs in whole or in part from deemed-to-satisfy provisions described in the code if it can be demonstrated that the design complies with the relevant performance requirement. The final assessment methods include documentary evidence, verification methods, expert judgment and comparison to deemed-to-satisfy provision (BCA96 1996). More researches based on experiments are needed for the new buildings to face the new challenge of the new era.

4-3-3 Improvement in performance-based fire code

Performance-based fire code is not perfect. The change of design brings about disadvantages as well. The disadvantages are listed as follows (Hadjisophocleous 1998):

- Lack of measurable fire safety objectives.
- Calculation uncertainty and difficultly in evaluation.
- Gaps in existing technical knowledge (need education).

- AHJs (Authority Having Jurisdiction) problems.

Therefore, compared with performance-based fire code, the advantages of prescriptive codes are still:

- Straightforward evaluation of compliance with established requirements.

- With/without higher level of engineering expertise.

However, it does not mean that there is no need to upgrade the old codes but it serves as a reference for scientists to evaluate prescriptive codes and the design of new code.

4-4   Conclusion

More professionals are talking about performance-based fire codes in China. Collaboration projects among government departments, private sectors and overseas institutions have been developed rapidly. For example, performance-based fire code for atria is a good starting point. The collaborative venture of "Fire Safety and Technology Research Center for Large Space" between The Hong Kong Polytechnic University (PolyU) and the University of Science and Technology of China (USTC) is now operating smoothly (Chow and Fong 1998, Chow 1999c). Many tests are conducted with the aim of developing new performance-based fire code, though prescriptive codes are still useful for typical buildings.

Chapter 5   NUMERICAL STUDIES ON 'BARE CABIN' FIRES

5-1   Introduction

The concept of 'cabins' for fire protection (Law 1990, Beever 1991 & 1995, Bressington 1995 & 1999b) is commonly used in the big halls in Hong Kong. There, areas storing lots of combustibles and places identified with higher fire risk are put in cabins.   Sprinkler system and smoke extraction system are installed in each cabin for controlling fires.

This is no doubt a good design which can use the hall spaces efficiently without installing big smoke extraction systems; and it has been used in many airport terminals and big railway terminals (Law 1990, Beever 1991 & 1995, Bressington 1995 & 1999b).   However, a point to be considered in this design concept is the likelihood of flashover in a cabin and its consequences of occurrence.   The fire load density associated with the nature of the shop, smoke extraction and sprinkler systems design in the cabin, and fire safety management are key factors.   Note that the sprinkler systems are not so reliable as experienced locally (Fire Services Department 1994b).   In case of the sprinkler system in a cabin does not work, a 'small' cabin might become a big hot object.   Nothing was mentioned on the storage of alcohol in 'duty free shops' and other combustibles.   The local upper limit on fire load density is 1135 MJm^{-2} (Fire Services Department 1994b), which is also being criticized (Jones 1998).   Putting in factors on poor operation of retail shops such as excessive storage of goods

because of high rental prices, blocking the sprinkler heads, and covering the extraction vents by goods, a very big fire might be resulted. What will happen if the 'cabin' becomes a big burning object, giving large production of smoke?

This point was briefly discussed where the sprinkler system and smoke extraction system in a 'bare cabin' did not work (Chow 1997a, 1997b, 1998b & 1998c). Analysis on flashover was carried out using the fire protection engineering tool FASTLite (NIST 1996) version 1.0 released in 1996. Unfortunately, that earlier version did not give physically consistent results as criticized (Law and Beever 1998, Law 1998, Beever 1998), though the tool is now modified and should be very suitable for studying practical fire problems in buildings. However, results derived earlier on the flashover time were not physically correct (Chow 1998d, 1998e & 1998f).

This point is now further investigated using another software FIREWIND (FMC 1997). Correlation equations between the time to flashover in each cabin and the geometry of the cabin are derived. Those equations are useful in understanding the possibility of flashover and the time required to achieve it.

The flashover criteria during a compartmental fire was reviewed clearly by Thomas (1995) and updated recently as well by Peacock et al. (1999). The problem can be investigated using a heat balance equation for the compartment. In the equation, the difference between the heat gain and the heat loss would determine the rate of temperature rise of the compartment. The term describing

heat gain is basically the heat release rate of the fire. At the initial stage of a compartmental fire, the fire is fuel-controlled and the heat gain depends on the temperature. As the fire proceeds, it will be changed to a ventilation-controlled fire with the burning rate becoming roughly independent of the compartment temperature, giving an almost horizontal line in the heat-temperature curve.

Heat loss includes the heat transfer through the wall surfaces and the heat taken away by the air. This term is roughly proportional to the compartment temperature.

Quasi-steady states can be found when the heat gain is the same as the heat loss. Plotting the two terms against the average smoke temperature would give something similar to Semenov's diagram in classical thermal explosion theory (Thomas 1995) for determining the criteria for flashover. The heat release rate of a fire $\dot{Q}(t)$ and the heat loss rate Q_L can be plotted against the average increase of compartmental temperature. From the intersection points of these two curves, criteria for flashover can be developed. For example, radiation heat flux of 20 kWm^{-2} at floor level, or upper layer temperature of 500°C to 600°C are practical criteria (Thomas 1995).

To study the likelihood of flashover in a compartment fire, using a two-layer zone model seems reasonable (Peacock et al. 1999, Chow 1998d). The flashover

time for fires in a 'bare cabin' is studied in this chapter using the new fire protection engineering tool FIREWIND (FMC 1997).

Numerical studies on 'bare cabin' fires with a fire zone model were carried out. Two cases are studied:

5-2   Numerical experiments

Assume that the heat source induces a thermal plume and yields a rather stable thermally stratified upper hot layer. There are two zones in the cabin, an upper hot zone and a lower cool zone. The air inside each zone is assumed to be mixed thoroughly, and there is no layering effect.

Case 1

Cabins of different sizes and natural ventilation conditions are considered under four sets of NFPA t^2-fires. Time to flashover is simulated by the new fire protection engineering tool FIREWIND with those four sets of fires, each of 440 simulations. From the results, correlations for the flashover time with the geometry of the cabin are derived. Effects of operating the smoke extraction system at different ventilation rates are studied. The relative time of operation of the sprinkler system and the smoke extraction system are discussed.

Case 2

Fires in 'cabins' with only the smoke extraction system operating are studied. Cabins of length up to 10 m, width up to 8 m and height up to 5 m, and with different ventilation conditions under a NFPA t^2-fire with cut-off value of 5 MW are investigated. The fire environments due to all the four sets of slow, medium, fast, and ultra-fast t^2-fires are tested. The fire zone model FIREWIND is selected as the simulation tool. The total number of simulations is 14,400, including four smoke exhaust rates. The time to flashover is computed for two different times of operation of the smoke extraction system. It is found that without operating the sprinkler system, flashover would occur under many conditions with the time to flashover as fast as 200 s.

5-3   Simulations for case 1

The fire environment in 'bare cabins' inside the big halls is predicted. Cabins with different dimensions are studied with length L taken as 4 m, 6 m, 8 m and 10 m, width taken as 4 m, 6 m, 8 m and 10 m and height H taken as 2 m, 3 m, 4 m and 5 m.

Different ventilation conditions with opening heights H_v from 1.5 m to 2.5 m and width W_v from 1.5 m to the cabin's width (i.e. up to 10 m) are considered. The number of openings is varied from 1 to 4, depending on the design conditions. Larger ventilation area would increase the air intake rate which would give higher burning rate.

A fire of size 1 m by 1 m is located at the centre. Four sets of heat release rate curves are used with the initial stage following NFPA slow-, medium-, fast-, and ultra fast- t^2-fires (NFPA 92B 1995 & 2001), then at cut-off values of 5 MW, 7.5 MW and 10 MW until 2000 s, and drop to 0 MW at 2100 s.

Simulations were performed for the four sets of fires, each of 11 cases, each case of 40 configurations (giving a total of 1760 simulations) using FIREWIND (FMC 1997) with initial temperature taken to be 20°C. Flashover in the enclosure is said to occur when the upper layer gas temperature reaches 500°C as listed in p. 6 of the User's Manual (FMC 1997). Values of the flashover time t_f for some cases are shown in Table 5-1.

The following are observed:

- Values of t_f increased as the dimensions of cabin increased, i.e. 952 s for the cabin of size 4 $\times$ 4 $\times$ 2 m to 1245 s for the cabin of size 4 $\times$ 6 $\times$ 2 m with one opening of size 4 $\times$ 1.5 m.

- The flashover time t_f slightly changed with the ceiling height for a slow t^2-fire with cut-off value 5 MW, i.e. increased to 997 s for a 4 $\times$ 4 $\times$ 5 m cabin, when there is one opening of size 4 $\times$ 1.5 m as in above (t_f of 952 s when the ceiling height is 2 m).

- Flashover did not occur for cabins longer than 8 m and wider than 8 m for a slow t^2-fire.

- Very similar results on t_f are found with the medium t^2-fire, fast t^2-fire and ultra fast-t^2-fire with other opening arrangements as shown in Table 5-1.

- Results are similar for the 7.5 MW cut-off fires.

- Flashover occurred in very few cases as shown in Table 5-1 when the opening is big enough, such as the width is equal to the cabin width, even for the big fire with cut-off value of 10 MW.

5-3-1   Correlation relations

The flashover criteria for fires in a 'cabin' are studied using the two-layer zone model of FIREWIND (FMC 1997), a new fire protection engineering tool by taking the flashover criteria on the hot layer temperature as 500°C. Note that those flashover criteria are only for practical application without physical basis (Thomas 1995, Peacock et al. 1999).

Predicted flashover time t_f (in s) for the above simulations are correlated with floor area A_f in the range of 16 m^2 $\leq$ A_f $\leq$ 60 m^2 and cabin height H of 3 m, 4 m and 5 m:

$$t_f = a_h H + a_f A_f + a_0 \qquad\qquad (5\text{-}1)$$

For a slow t^2-fire:

$$a_h = 10.4 \text{ m}^{-1}\text{s} \ ; \ a_f = 8.9 \text{ m}^{-2}\text{s} \ ; \ a_0 = 795 \text{ s}$$

with a correlation coefficient r^2 of 0.994; and the range of t_f simulated from 951 s to 1361 s.

The results predicted by FIREWIND for the three ceiling heights are plotted together with the fitted lines as in Figure 5-1. It is observed that the derivation between the two sets of data is very small, as r^2 is 0.994.

For a medium t^2-fire:

$$a_h = 5.4 \text{ m}^{-1}\text{s} \ ; \ a_f = 5.2 \text{ m}^{-2}\text{s} \ ; \ a_0 = 375 \text{ s}$$

with r^2 of 0.983; and the range of t_f simulated from 476 s to 732 s.

For a fast t^2-fire:

$$a_h = 7.7 \text{ m}^{-1}\text{s} \ ; \ a_f = 4.0 \text{ m}^{-2}\text{s} \ ; \ a_0 = 130 \text{ s}$$

with r^2 of 0.949 and the range of t_f from 241 s to 451 s.

For an ultra-fast t^2-fire:

$$a_h = 3.2 \text{ m}^{-1}\text{s} \; ; \; a_f = 1.6 \text{ m}^{-2}\text{s} \; ; \; a_0 = 105 \text{ s}$$

with r^2 of 0.987 and the range of t_f simulated from 135 s to 210 s.

It can be seen that the flashover time increased with the cabin height H. This is more reasonable than the simulations reported (Chow 1997a, 1997b & 1998f) previously. Further, values of the flashover time t_f are shorter than the duration of burning (of 2000 s) of the fire. The thermal penetration time might be quite long for some materials such as thick timber. But it is possible that flashover occurs before heat penetrates through the wall reaching steady state.

5-3-2 Smoke extraction

It is important to install smoke extraction system in a cabin. The effect of operating the system is simulated by FIREWIND (FMC 1997). A cabin of length 4 m, width 4 m and height 3 m, with an opening of size 2 × 2.5 m is taken as an example. Extraction rates of 40, 80, 120 and 180 air changes per hour (ACH) are simulated. The system is not expected to operate as soon as the fire has started. Two values of time to operate the smoke extraction system t_{op} are considered. The first case is t_{op} at 37 s, when the smoke layer thickness is 0.45 m. This value corresponds to a typical 'downstand' height in the local building fire code (Buildings Department 1996). The second case is t_{op} at 150 s, when the

51

smoke layer temperature is heated up to 68°C. This is a common actuation temperature for sprinkler head. However, a 68°C-rated sprinkler head might not be actuated even if the smoke layer temperature reaches 68°C. The response time index (Heskestad and Smith 1982) has to be considered. Otherwise, the smoke extraction system might be operated first if both systems are installed.

Results of the smoke layer temperature and smoke layer interface height with the extraction system operated at the two operation times are shown in Figures 5-2 and 5-3. It is observed that small extraction rates would not have any effect on the smoke layer temperature and smoke layer interface height, unless the value is increased to 40 ACH. In this way, the smoke layer can be kept at a higher position if the extraction rate is sufficiently high.

The time to operate the system is important. For earlier operation of the extraction system at 37 s when the smoke layer fell by 0.45 m, the smoke layer at the early time, say within 500 s, could be kept at a higher level. But if the system was operated at a later time at 150 s, the smoke layer would fall by 1.3 m before the operation of the system. Because of this thick smoke layer, only very high extraction rates can keep the smoke layer at a higher level at the early stage of the fire. For example, 180 ACH would move the smoke up to 2.8 m before 500 s. Effects of extraction rates less than 60 ACH are not obvious.

5-3-3   Thermal sensitivity of sprinkler heads

Sprinkler systems are also installed in a cabin for controlling the fire. Basically, there are at least four mechanisms (Chow and Fong 1991) by which a sprinkler water spray interacts with a fire:

• Direct cooling of the burning object.

• Prewetting the walls, floors and objects not yet ignited.

• Cooling of the smoke layer.

• Displacing oxygen from the burning object.

The first two mechanisms are very important in controlling a fire. Before discharging water, the sprinkler heads must be activated first. The thermal sensitivity of sprinkler head is very important and response time index is one of the parameters to specify how fast a sprinkler head would operate. The time for the sprinkler to operate might be quite long as it takes time to transfer heat from the surrounding hot smoke.

For a sprinkler head with response time index RTI and temperature rating T_s (68°C for common design) subjected to hot gas at temperature T_g moving towards it with speed V_g, the time constant τ' of the sprinkler head is given by (Alpert 1972, Heskestad and Smith 1982, Chow and Ho 1990):

$$\tau' = RTI \, V_g^{-1/2} \qquad\qquad (5\text{-}2)$$

The time t_{op} taken for the sprinkler head to operate, i.e. rising temperature from an initial value of T_0 to T_s (say 68°C), is:

$$(T_s - T_0) = (T_g - T_0)(1 - e^{-t_{op}/\tau'}) \qquad\qquad (5\text{-}3)$$

For smoke with T_g of 100°C, V_g of 1 ms^{-1}, and initial temperature T_0 at 20°C, putting these numerical values to equation (5-2) gives:

$$t_{op} = 0.916 \, RTI \qquad\qquad (5\text{-}4)$$

RTI for a normal sprinkler head is about 400 m$^{1/2}$s$^{1/2}$, and for an Early Suppression Fast Response (ESFR) sprinkler head is about 70 m$^{1/2}$s$^{1/2}$. Putting RTI in equation (5-4), t_{op} for a normal sprinkler head is about 366 s and for an ESFR sprinkler head is 64 s. That means, even if the smoke temperature is increased to 200°C (took more than 400 s for the cabin example shown in the above section as simulated by FIREWIND (FMC 1997)), another 64 to 366 s would be required for heating up the sprinkler head before discharging water.

Therefore, it is likely that the smoke extraction system would be operated first if it is controlled by smoke detectors. It should be noted that if thermal sensing element is used for smoke extraction system, its RTI has to be considered. For a

smoke extraction system operated before sprinkler, some quantity of the hot smoke would be removed. This together with the air movement induced by the ventilation system might not give a favourable condition for heating up the sprinkler head. As a result, the sprinkler system cannot be activated.

Even if a sprinkler head is activated to discharge water, there might be adverse effects:

- Production of hot steam.
- Loss of buoyancy of smoke layer due to cooling.

The first point would do harm to the occupants trapped inside. The second point might give rise to smoke logging down to lower levels, and also affect the performance of the smoke extraction system. Therefore, the sprinkler systems must be designed carefully when smoke extraction system is provided at the same time.

5-4   Simulations for case 2

Cabins with length L up to 10 m, width W up to 8 m and height H up to 5 m are studied. Different openings with height H_v up to 2.5 m and width W_v up to the width of the cabin are considered. The number of openings is varied from 1 to 4. A fire of size 1 m by 1 m is located at the centre of the cabin floor. The heat release rate curves follow all the four sets of NFPA slow, medium, fast, and

ultra-fast t^2-fires (NFPA 92B 1995 & 2001) with a cut-off value of 5 MW. The geometrical picture of a cabin is shown in Figure 5-4.

It is important to study the performance of smoke extraction system in a cabin and FIREWIND (FMC 1997) is used for this purpose. In each cabin, extraction rates of 40, 80, 120 and 180 air changes per hour (ACH) are simulated.

The system is operated at time t_{op} under two different conditions:

- t_{op} at $t_{0.45}$ when the smoke layer thickness is 0.45 m, corresponding to a typical 'downstand' height in the local building fire code (Buildings Department 1996a).

- t_{op} at t_{68} when the smoke layer temperature is heated up to 68°C. This is a common actuation temperature for sprinkler head. Note that a 68°C-rated sprinkler head might not be actuated when the smoke layer temperature reaches 68°C, depending on its response time index. Fast response type sprinkler head is assumed in this analysis so that the sprinkler head would be activated once the temperature reaches 68°C. This point is very important as the smoke extraction system might be operated first before a slower response type sprinkler head, if both systems are installed.

Nine cases are simulated, each of 40 configurations, two different operation times of the smoke extraction system and four exhaust rates, giving a total of 14,400 [$4 \times 9 \times 40 \times (1 + 4) \times 2$] simulations.

The initial temperature is taken to be 20°C. Flashover in the enclosure is said to occur when the upper layer gas temperature reaches 500°C as listed in the User's Manual of FIREWIND (FMC 1997).

5-5   Results

Typical results of the smoke layer temperature and smoke layer interface height with the extraction system operated at the two operation times in the cabin of 4 m long, 4 m wide and 5 m high, and with a vertical opening of width 2 m and height 2.5 m, are shown in Figures 5-5 to 5-12 for the four sets of t^2-fires.

For the slow and medium t^2-fires, it is observed that extraction rates less than 40 ACH would not have any significant effect on the smoke layer temperature and smoke layer interface height. The smoke layer can be kept at a higher position only when the extraction rate is higher than 40 ACH.

The time to operate the extraction system is important. Values of $t_{0.45}$ and t_{68} of the corresponding smoke layer temperature and smoke layer interface height for the four sets of t^2-fires are shown in Table 5-2. For earlier operation of the extraction system at $t_{0.45}$ (i.e. 14 s for both slow t^2-fire and medium t^2-fire), the

smoke layer at the early stage of the fire, say within 500 s, can be kept at a higher level when the extraction rate is high. However, if the system is operated at a later time, say at $t_{68} = 179$ s for a slow t^2-fire, the smoke layer would fall by 1.6 m before turning on the system. For a medium t^2-fire, t_{68} is 116 s and so the smoke layer would fall by 1.48 m before operating the system. Since a thick smoke layer is developed, only very high extraction rates (say 180 ACH) can keep the smoke layer at a higher level up to 3.5 m before 500 s. Extraction rates less than 40 ACH are not able to keep the smoke layer at higher level.

For the fast and ultra-fast t^2-fire, it is observed that the smoke layer would fall to low level quickly. Even though the extraction system is operated at an earlier time, the smoke layer cannot be kept at higher positions. Therefore, it can be concluded from the simulated results shown in Figures 5-10 and 5-11 that the extraction system has no effect on the fire environment, apart from reducing the temperature slightly, say by 10%. However, this is critical in determining flashover for cases where the maximum smoke temperature is very close to the flashover temperature, which is set to be 500°C in this chapter.

5-6   Time to flashover

Results on time to flashover t_f for the two operating times t_{op} of the smoke extraction system under a slow, medium, fast, and ultra-fast t^2-fire are shown in Table 5-3.

Under the same cabin geometry, ventilation condition and heat release rate, t_f would be longer when the smoke extraction rate is increased. For some cases, flashover would not occur if the smoke extraction rate is sufficiently high.

For extraction rates of 40 ACH and 80 ACH, the smoke layer interface height curves predicted are almost the same. Values of t_f are extended to a later stage when the smoke extraction system is operated earlier at $t_{0.45}$ when the extraction rate is 120 ACH. Values of t_f are the same for the two values of t_{op} when the extraction rate is 180 ACH.

As stated previously, for fast and ultra-fast t^2-fires, smoke extraction rates would not have any significant effect on the smoke temperature and smoke layer interface height. The time to flashover is short. Operating the smoke extraction system with higher extraction rate would extend t_f, or even give no flashover if the maximum smoke temperature is very close to the flashover temperature for a bare cabin fire without operating the smoke extraction system.

5-7   Conclusion

Case 1 is on simulation of time to flashover under different natural ventilation conditions. Relationship between the flashover time and geometry of the cabin (H and A_f) was found. The effects of smoke extraction system operation on the smoke layer temperature and smoke layer height, and its effects on the operation of sprinkler heads are also preliminarily discussed. Case 2 is on simulation of

time to flashover under different forced ventilation conditions, for studying the performance of smoke extraction system under different operation conditions with different size of fire. Case 1 and Case 2 are two steps of numerical study.

In case 1

The time to flashover in 'bare cabins' under NFPA t^2-fires in cabins of different sizes is studied using a two-layer zone model FIREWIND (Thomas 1995). Flashover might occur quickly, say within 210 s, for cabins with a NFPA fast t^2-fire. Correlation equations are fitted between the flashover time with the cabin floor area and ceiling height. The equations are useful for the Authority to inspect new projects of this kind, especially for those who are not experienced in using fire models while implementing engineering performance-based fire codes (Chow 1999a).

Fire protection systems including fire detection system, sprinkler system and local smoke extraction system should be provided (Bressington 1999b) in each cabin. The effects of smoke extraction are studied. However, the performance of the systems integrated together is also important. For example, whether the sprinkler system or smoke extraction system should be operated first had been debated in many projects. The time for detecting a fire, operating the sprinkler to discharge water, turning on the smoke extraction system and the time for people staying inside to escape must be considered carefully. Further, whether the cabin should be enclosed completely in case of a fire is a question, as some occupants

60

might not be able to leave it in time. Exposure of occupants to the steam generated by the sprinkler water is of great concern.

In case 2

The time to flashover in 'cabins' with only the smoke extraction system operating is simulated with the two-layer zone model FIREWIND (FMC 1997). The design fire is a NFPA t^2-fire of cut-off value 5 MW. Cabins of different sizes are studied.

It is found that for fast growing fires, such as the fast and ultra-fast t^2-fires, the smoke extraction system would not have any significant effect on the development of smoke temperature and smoke layer thickness. As shown in Table 5-3, the time to flashover would be extended slightly for larger extraction rates.

The design fire is important for flashover to occur. A 5 MW fire is likely to occur in shops selling alcohol, or in shops storing lots of combustibles. A detailed fire load survey and the heat release rate of a design fire should be worked out.

Three works of added value have been done in this chapter, which can be summarized as:

- Relationship between time to flashover and geometry of cabin (H and A_f) was found. It is useful in understanding the possibility of flashover and the time required to achieve it.

- The performance of smoke extraction system under different operation conditions with different size of fire was evaluated.

- The effects of smoke extraction system operation on the smoke layer temperature and the smoke layer height were analyzed.

Chapter 6 TWO-LAYER FIRE ZONE MODELS WITH SYMBOLIC MATHEMATICS

In the study of cabin fire, mathematical fire models are the essential approach popularly used in fire hazard assessment. The equations on the two-layer fire zone model ASET for a chamber with air supplied through leakage are solved by the symbolic mathematics programme MATLAB (1997) and MAPLE V (1998). Two key equations are considered. A total number of 12 simulations were carried out on two design fires in six compartments with floor area varying from 10 to 100 m². The results are compared with those simulated by the ASET itself and another software FIREWIND (FMC 1997).

Fire scientists and fire engineers need to solve problems by calculations, such as fluid dynamics problems. Normally, there are three ways to solve ode problems: integral by hand, numerical equations solutions and fire element equations (by Fortran or Basic). Before 1960's, fire engineers calculated experimental equations with the help of charts on coefficients. With the development of computer in 1970's, engineers began to solve equations by using Fortran program with main-frame computers. In 1980's, BASIC program was popularly used in solving equations on PC. And after 1990's, updated software has appeared in the market, such as MATLAB, it is very convenient to check integral algebra and calculations such as ode solver. With the help of symbolic mathematics, fire scientists and engineers no long solve complex problems from basic equations.

The use of symbolic mathematics (Christensen 1996, Holmes et al. 1995) is now very popular. How this technique can be applied for fire modeling is studied in this chapter. The software developed for handling matrices MATLAB (1997) and MAPLE V (1998) are selected. This is a high-performance language for technical computing, integrating computation, visualization, and programming in an easy-to-use environment. Typical uses include mathematical analysis, computational process, modeling, simulation, data analysis and visualization with scientific graphics. A good graphical processor is available for presenting the results.

Two-layer zone models are developed (Cooper 1982a, Birk 1991, Rehm and Forney 1992, Law 1990) for simulating building fire by taking into account an upper hot smoke layer, a lower cool layer and a plume. There should be 11 variables on the properties of the two layers and the compartment pressure with 11 equations for solving them (Rehm and Forney 1992). But since there are seven physical constraints, the maximum number of ordinary differential equations required to be solved is only four. With intelligent use of assumptions, the number of different equations to be solved can be less than four.

Available Safe Egress Time (ASET) is one of the earliest zone models (Cooper 1982a) for calculating the temperature and interface height of the hot smoke layer in a single room with doors and windows closed. Available Safe Egress Time - BASIC (ASET-B) is a compact and easy-to-run program which solves the same equations as ASET but in BASIC (Birk 1991). Input data like the

geometry of the room such as floor area and ceiling height; heat loss fraction; the height and heat release rate of the fire; and the maximum time for the simulation are required for predicting the transient smoke layer temperature and interface height.

In this chapter, the equations for ASET (Cooper 1982a) are put into MATLAB and MAPLE V to simulate a typical room fire. The results are compared with those by FIREWIND version 3.4 (FMC 1997), which is a user-friendly tool for fire engineers to carry out fire hazard assessment.

6-1   The model ASET

ASET is a two-layer zone model for closed chambers (Cooper 1982a). There are no openings assigned in the room with air supplied through leakage. In this way, the equations for vent flow need not be solved.

The following assumptions are made (Cooper 1982a, Brani and Black 1992):

- Room pressure is independent of height when the conservation of mass and energy equations are applied to both zones.

- The specific heat capacities of the gases in the room are assumed to be constant and estimated from the initial room temperature.

- The model may not be reliable for enclosures with a large length to width aspect ratio; or height to minimum horizontal dimension ratio (Quintiere 1995).

- The enclosure is assumed to be divided into two layers with heat and mass transfer through the plume. There might be problems when the upper layer temperature increases to give strong enough radiative heat flux to cause flashover.

6-2   Key equations

A fire with heat release rate $\dot{Q}(t)$ in a room of height H and cross-sectional area as shown in Figure 6-1 is considered. A smoke layer is formed with interface height Z_i above the floor. The derivation of equations for smoke layer interface height and smoke layer temperature is shown in Appendix C. The set of ordinary differential equations for such a two-layer zone model ASET for Z_i higher than the height of the fire are summarized as:

$$dZ_N / dt_N = -C_1 q - C_2 q^{1/3} Z_N^{5/3} \tag{6-1}$$

$$dT_N / dt_N = T_N [C_1 q + (1 - T_N / T_g) C_2 q^{1/3} Z_N^{5/3}] / (H - Z_N) \tag{6-2}$$

where C_1 and C_2 are constants and the following dimensionless quantities are defined as:

$$C_1 = \frac{(1 - L_c)}{\rho_L C_p T_g A_f} \tag{6-3}$$

$$C_2 = \frac{0.21}{A_f} \left[\frac{(1 - L_C)g}{\rho_L C_p T_g} \right]^{1/3} \qquad (6\text{-}4)$$

$$Z_N = \frac{Z_i}{l_c} \qquad l_c \sim 1 \text{ m} \qquad (6\text{-}5)$$

$$t_N = \frac{t}{t_c} \qquad t_c \sim 1 \text{ s} \qquad (6\text{-}6)$$

$$T_g \sim 300 \text{ K} \qquad (6\text{-}7)$$

$$q = \dot{Q}(t) \qquad (6\text{-}8)$$

The equations are put into MATLAB and MAPLE V for predicting the smoke layer temperature and interface height.

6-3   Numerical analysis

In this chapter, equation (6-1) is solved by the Runge-Kutta (RK) method. There are many versions of the RK method but the choice of the time step is important. Rewriting the equation as:

$$\frac{dZ_N}{dt_N} = f(Z_N, t_N) \qquad (6\text{-}9)$$

with

$$Z_N(t_0) = Z_0 \qquad (6\text{-}10)$$

Advancing from the nth time step to the $(n+1)^{th}$ time step:

$$t_{n+1} = t_n + h_s \qquad (6\text{-}11)$$

$$Z_{n+1} = Z_n + (\frac{h_s}{6})(p_n + 2 \times q_n + 2 \times r_n + s_n) \qquad (6\text{-}12)$$

$$p_n = f(t_n, Z_n) \qquad (6\text{-}13)$$

$$q_n = f(t_n + \frac{h_s}{2}, Z_n + \frac{h_s}{2} \times p_n) \qquad (6\text{-}14)$$

$$r_n = f(t_n + \frac{h_s}{2}, Z_n + \frac{h_s}{2} \times q_n) \qquad (6\text{-}15)$$

$$s_n = f(t_n + h_s, Z_n + h_s \times r_n) \qquad (6\text{-}16)$$

In solving an ordinary differential equation (ODE), the rate of convergence, the accuracy (or even validity) of the predicted results, and the completeness of the response should be considered. Particularly, convergence must be judged by some global criteria.

"ODE45" in MATLAB for solving non-stiff differential equations is used in this chapter to solve the two ODEs (MATLAB 1997). This is an explicit Runge-Kutta (4,5) pair of Dormand and Prince method with a "free" interpolate of order

four communicated privately by Dormand and Prince (Dormand and Prince 1980, Dormand 1996). Local extrapolation is done.

The expression in MATLAB is:

```
[t,Z] = ode45('asetsub',[1:1:te],[3.5;300],[],Tg,Lc,Lr,A,pcl,Cp,Qt,Q0)

tout = t

yout = Z

o3,o4,o5,o6 = null

odefile = asetsub, asetsub2

tspan = 1:1:620

y0 = 3.5 ; 300

options = null

varargin = Tg,Lc,Lr,A,pcl,Cp,Q0,Q,k


function [tout,yout,o3,o4,o5,o6] = ode45(odefile,tspan,y0,options,varargin)
```

Non-stiff differential equations would be solved by ODE45 by the medium order method.

[T,Y] = ODE45('F',TSPAN,Y0) with

TSPAN = [T0 TFINAL] integrates the system of differential equations $y' = F(t,y)$ from time T0 to TFINAL with initial conditions Y0.

'F' is a string containing the name of an ODE file. The function F(T,Y) must return a column vector. Each row in solution array Y corresponds to a time returned in column vector T. To obtain solutions at specific times T0, T1, ..., TFINAL (all increasing or all decreasing), use TSPAN = [T0 T1 ... TFINAL].

As an example, the commands

options = odeset('RelTol',1e-4,'AbsTol',[1e-4 1e-4 1e-5]);

ode45('asetsub',[1:1:te],[3.5; 300],options);

solve the system y' = rigidode(t,y) with relative error tolerance 1e-4 and absolute tolerances of 1e-4 for the first two components and 1e-5 for the third. When called with no output arguments, as in this example, ODE45 calls the default output function ODEPLOT to plot the solution as it is computed.

6-4   Stiff ODE

A stiff ODE means an ODE in which the solution function exhibits rapid and extreme changes in the dependent variable with small variations in the independent variable (Oxford 1992, Dormand 1996). As a result, a plot of the solution function over long time frames (since time is taken as the independent variable in this study) will look quite different from a plot over short time frames.

A set of differential equations is called "stiff" (Oxford 1992, Dormand 1996) when the maximum eigenvalue in its jacobian matrix is several orders of

magnitude larger than the minimum eigenvalue. In such case, the step size of integration is determined by the largest eigenvalue, while the final time of integration usually depends on the smallest eigenvalue. There are easier, but less precise, definitions on stiff differential equations:

- A set of differential equations is "stiff" when an excessively small step is needed to obtain correct integration.
- A set of differential equations is "stiff" when it contains at least two "time constants" (where "time" is supposed to be the joint independent variable) that differ by several orders of magnitude.

Integrating such equations using traditional explicit (Runge Kutta) methods may take very long computing time: implicit methods should be used to reduce computation time. However, implicit methods are not very efficient for solving normal and non-stiff equations.

A non-stiff ODE means an ODE in which the solution function exhibits slow and smooth changes in the dependent variable with small variations. As a result, plotting the solution function over long time frames (time is the independent variable) will look quite the same as plotting over shorter time frames.

6-5 Numerical experiments

A fire is placed at the center of six rooms of different areas but of the same height of 3.5 m. Two sets of heat release rate $\dot{Q}(t)$ are considered:

- Fire F1: Steady burning with constant heat release rate of 0.8 MW
- Fire F2: NFPA slow t^2-fire (NFPA 92B 1995 & 2001), with cut-off value of 0.8 MW

Considering the fast changes in fire environment, excessively small step is needed to obtain correct integration to ensure convergence and accuracy of the predicted results. Stiff ODE is selected to solve the above equations by a series of testing calculations.

The fraction of heat lost by conduction and radiation L_C is taken to be 0.35, the specific heat capacity of air C_p is 1004 $Jkg^{-1}K^{-1}$ and the cool layer temperature T_L is 300 K.

The floor areas of the six rooms are:

- Room 1: 10 m^2
- Room 2: 20 m^2
- Room 3: 30 m^2
- Room 4: 40 m^2
- Room 5: 50 m^2

• Room 6: 100 m^2

Typical example of a MAPLE V program listing and a MATLAB program listing are shown in Appendix D.

The results predicted are compared with those by the FIREWIND – HotLayer (FMC 1997) and the ASET (Cooper 1982a & 1982b) itself as shown in Figures 6-2 to 6-7. There are differences in the results predicted by the three models.

Floor area of the compartment is a key factor. It is expected that the results of using MATLAB, i.e. curve A in all figures, should be similar to those simulated by the ASET itself as given by curves C. However, there are many cases where the two do not agree. Results of FIREWIND (i.e. curves B) are used for comparison which agree in some cases.

6-6   Conclusion

The following conclusion can be drawn from this study:

• Symbolic mathematics is now a powerful tool for doing mathematics with a computer. It can be applied to simulate a building fire with a two-layer model. A relatively simple model like ASET can be put into the computer easily. Graphics outputs can be achieved easily.

- It is easier to change the equations and parameters concerned on describing the physics concerned in comparing to traditional computer programming.

- The software is under active development, both on the numerical schemes and graphical presentation.

From the simulations, floor area should be watched carefully in using two-layer zone models. Symbolic mathematics should be put into the teaching curriculum of engineering degree programmes.

Chapter 7   CFD STUDIES ON 'BARE CABIN' FIRES WITH OPERATION OF SMOKE EXTRACTION SYSTEM

'Cabins' for fire protection (Law 1990, Beever 1991 & 1995; Bressington 1995 & 1999b) are commonly used in the big halls in Hong Kong, such as the new airport and railway stations. This is a kind of design that uses the hall spaces effectively without installing big smoke extraction systems.   However, the likelihood of flashover in a cabin and its consequences of occurrence should be considered, bearing in mind that the sprinkler systems are not so reliable as experienced locally, and the requirements on the sizing of smoke extraction fans are not spelled out clearly in the local design guides (Fire Services Department 1994a).   Fires occurring in a cabin where the sprinkler system and smoke extraction system did not work, or 'bare cabin fires' (Chow 1995d, Chow 1997a, 1997b, 1998b, 1998c & 1999b), had been studied before.   In case of the sprinkler system in a cabin does not work, a 'small' cabin might become a big hot object, in particular for shops selling alcohol where spillage fires might happen.

To evaluate the performance of fire protection systems in enclosures like cabin, CFD field models are studied and used. The commercial package PHOENICS version 3.1 1 (PHOENICS 2000) is used in simulation. PHOENICS use k-ε type of turbulence model with the flair post-processor manual. It is a less costly shareware, which offers inexpensive method for studying the compartmental

fires under forced ventilation conditions. A cabin of 4 m × 4 m × 3 m with ventilation conditions is considered as an example. Zone model FIREWIND 3.4 (FMC 1997) is used as a tool for results comparison.

7-1   A brief overview of Computational Fluid Dynamics (CFD)

The physical aspects of any fluid flow are governed by three fundamental principles: conservation of mass; Newton's second law and conservation of energy. These fundamental principles can be expressed in terms of mathematical equations, which in their most general form are usually partial differential equations. CFD is the science of determining a numerical solution to the governing equations of fluid flow whilst advancing the solution through space or time to obtain a numerical description of the complete flow field of interest (Webster 2001).

The governing equations for Newtonian fluid dynamics, the unsteady Navier-Stokes equations, have been known for over a century. However, the analytical investigation of reduced forms of these equations is still an active area of research, as is the problem of turbulent closure for the Reynolds averaged form of the equations. For non-Newtonian fluid dynamics, chemically reacting flows and multiphase flows theoretical developments are at a less advanced stage. Derivation of Navier-Stokes equations is shown in Appendix E (Currie 1974).

The role of CFD in engineering predictions has become so strong that today it may be viewed as a new developing way of fluid dynamics, besides classical cases of pure experiment and pure theory.

The development of more powerful computers has furthered the advances being made in the field of CFD. Consequently, CFD is now the preferred means of testing alternative designs in many engineering, building and consulting companies before experiments are carried out.

On the discretized mesh, the Navier-Stokes equations take the form of a large system of non-linear equations. Going from the continuum to the discrete set of equations is a problem that combines both physics and numerical analysis, for example, it is important to maintain conservation of mass in the discrete equations. At each node in the mesh, between 3 to 20 variables are associated: the pressure, the three velocity components, density, temperature, etc. Furthermore, capturing physically important phenomena such as turbulence requires extremely fine meshes in parts of the physical domain. Currently, meshes with 20,000 to 2,000,000 nodes are common.

Once the solution is found, analyzing, validating, and presenting it calls into play visualization and graphics techniques. Those techniques are useful for understanding the nature of the problem, the interaction of algorithms with the computer architecture, and performance analysis of the code (Webster 2001).

7-2   Simulations

A cabin with length of 4 m, width of 4 m and height of 3 m, divided into 25, 15 and 15 parts along the x, y and z directions as shown in Figure 7-1 is studied. The dimensions studied are: length of 8 m, width of 4 m and height of 3 m, divided into 25, 15 and 30 parts along the x, y and z directions respectively. The grid size is smaller in the regions close to the fire and door. There is one opening with height H_v of 2.5 m and width W_v of 2 m.

An NFPA slow-t^2 fire (NFPA 92B 1995 & 2001) of size 1 m by 1 m is located at the center with cut-off value 1 MW.

Two simulations are presented (other simulation details are listed in Table 7-1) for a better comparison:

- Case A: Cabin without exhaust system installed.
- Case B: Cabin with exhaust system installed on the top.

It is important to study the performance of smoke extraction system in a cabin and PHOENICS is used for this purpose. Extraction rates of 40 air changes per hour (ACH) are simulated.

It is assumed that all the walls are adiabatic. Ambient temperature was set to 27 °C (300 K), air pressure was set to 1.01 x 10^5 Pa, initial values for k and ε were 1

x 10^{-3} Jkg^{-1} and 1 x 10^{-2} Jkg^{-1}s^{-1} respectively. Calculation loops up to 2000 times. The results are believed to be a constant situation.

7-3   Results

The results of vector velocity across the central plane (x = 2 m) are shown in Figure 7-3. There are little changes in the maximum vector velocity from 4.56 to 3.87 ms^{-1} after the operation of exhaust system. The predicted temperature field ranged from 30 to 120 °C in the same center plane (x = 2 m) as shown in Figure 7-4. It is shown that temperature distributions move towards the fire after the operation of exhaust system, temperature inside the cabin dropped obviously. This is useful to verify if the forced ventilation system functions properly, and also can be used to evaluate the performance of fire protection systems. Pressure distributions close to the neutral line are shown in Figure 7-5. A comparison of the vertical temperature profiles computed by two models (PHOENICS CFD model and FIREWIND zone model) is shown in Figure 7-6. In order to make clear of the layer in the CFD model, temperature was measured at three selected positions. It is clearly shown that, the zone model result is very close to the CFD simulation results in the division of temperature zone. The closer to the doorway opening, the more changes of the vertical temperature profiles.

7-4   Flux calculation

Mass balance: $\sum \rho_1 v_1' A_1 = \sum \rho_2 v_2' A_2$ (7-1)

Energy balance: $\quad\quad\quad \sum \rho_1 v_1' A_1 C_{p1} T_1 = \sum \rho_2 v_2' A_2 C_{p2} T_2$ $\quad\quad\quad\quad\quad$ (7-2)

$$\dot{Q}(t) = E_2 - E_1 \quad\quad\quad\quad\quad\quad\quad\quad (7\text{-}3)$$

No ventilation:

Mass balance $\quad\quad\quad M_1 = 2.82 \text{ kgs}^{-1}$

$\quad\quad\quad\quad\quad\quad\quad\quad M_2 = 2.78 \text{ kgs}^{-1}$

Energy balance $\quad\quad\quad \dot{Q}(t) = E_2 - E_1$

$\quad\quad\quad\quad\quad\quad\quad\quad 800 \text{ kW} = 966 \text{ kW} - 165 \text{ kW}$

Forced ventilation:

Mass balance $\quad\quad\quad M_1 = 3.03 \text{ kg s}^{-1}$

$\quad\quad\quad\quad\quad\quad\quad\quad M_2 = 2.44 + 0.5 = 2.94 \text{ kg s}^{-1}$

Energy balance $\quad\quad\quad \dot{Q}(t) = E_2 - E_1$

$\quad\quad\quad\quad\quad\quad\quad\quad 800 \text{ kW} = 947 \text{ kW} - 165 \text{ kW}$

7-5   Conclusion

'Bare cabins' of different sizes with only the smoke extraction system operating under a 1 MW NFPA slow-t^2 fire (NFPA 92B 1995 & 2001) are studied. The CFD model PHOENICS is used.

From the results, it can be concluded that, when the exhaust system was operating, there were few changes in the temperature from 30 to 120 °C. The pressure around the neutral line had small changes, but the neutral area changed.

From the comparison of the relationship between temperature and hot layer height in CFD and zone model as shown in Figure 7-6, the hot layer and cool layer are clearly seen in the CFD simulation. The temperature dropped after the exhaust system operation.

The relationships between the average room temperature and hot layer height in CFD and zone model are shown in Figure 7-7.

From the CFD simulation results, it is clearly shown that, temperature distributions moved towards the fire after the operation of exhaust system, temperature inside of the cabin dropped obviously. Laminar pressure distribution is broken after the operation of exhaust system. Pressure difference showed clearly that ambient air moved from outside into the cabin, and then moved out through the exhaust system on the top ceiling. Flux calculation showed the balance of mass and energy. The hot layer and cool layer are shown in the CFD average temperature distribution. The result is useful to verify if the forced ventilation system functions properly, and also can be used to evaluate the performance of fire protection systems.

Chapter 8 NUMERICAL STUDIES ON THERMALLY-INDUCED INDOOR AERODYNAMICS IN A COMPARTMENT WITH NATURAL VENTILATION

Mechanical ventilation system is usually installed at the inlet and outlet openings of an enclosed chamber. To optimize building safety in enclosures by improving the design of natural ventilation systems, air movement at the inlet and outlet opening, as well as the situation inside enclosure are very important. Air flow induced by a point heat source in a natural ventilated compartment is studied in this chapter. Three models, fully-mixed model, water-filling box model and emptying air-filling box model, on air flow in a chamber reported in the literature are reviewed. With a point heat source located at the center of the compartment, two different cases with and without walls are considered. A two-layer zone modeling approach with an upper hot air layer and a lower cool air layer is assumed. Two such zone models, Model 1 and Model 2, are developed. Model 1 is for a compartment without any walls. Model 2 is for an enclosed compartment with adiabatic walls, but with two openings, one at the top and the other at the bottom. Air flow induced by a point heat source in the natural ventilated compartments is solved. Volume flow rate equations and two-layer temperature difference equations are derived. Equations in the developed zone models are solved by the symbolic mathematics. The relationship between the neutral plane height and the outlet area is drawn. Results are compared with

those predicted by CFD. It is found that the two new models give results agreed fairly well with CFD.

8-1   Introduction

Indoor air movement induced by thermal heat sources is studied to provide better ventilation design and more efficient smoke management systems (Etheridge 1990). There are numerous studies reported (Andersen 1995, Baines 1990, Chow 1997c, Cooper 1996, Davies 1992, Li 2000, Linden 1990 & 1996) in the literature. But only a few of these models are applicable to study air flow induced by a point heat source in a compartment. These included the water-filling box model by Linden (1990), the fully-mixed model by Andersen (1995), and emptying air-filling model by Li (2000). On the other hand, a two-layer model is commonly used for simulating fire (Thomas 1995). In this chapter, indoor air flow induced by a point heat source is studied by a two-layer zone model. There is an upper hot air layer and a lower cool air layer with the plume serving as the vehicle to transfer heat and mass.

Two different cases with a point heat source located at the center of a compartment, with and without walls are considered. Model 1 is a compartment without any walls. Model 2 is an enclosed compartment with adiabatic walls, and two openings with one at the top and the other at the bottom.

With those models, air flow induced by a point heat source in a compartment can be studied. Equations in the developed zone models are solved by the symbolic mathematical packages (MATLAB 1997, MAPLE V 1998) with MATLAB selected for the calculation. Results are compared with those by the CFD package PHOENICS (2000).

8-2 A brief review of indoor air flow models

There are many models developed for studying indoor air movement in a compartment with natural ventilation (Andersen 1995, Baines 1990, Chow 1997c, Cooper 1996, Davies 1992, Etheridge 1990, Li 2000, Linden 1990 & 1996). Three suitable models are selected with their key fluid dynamics equations (Rouse 1954, Yih 1977) briefly reviewed:

8-2-1 Fully-mixed model

In the fully-mixed model with a heat source in the chamber by Andersen (1995), indoor air is assumed to be fully-mixed, the indoor air temperature is uniform, and all the walls are adiabatic. Air inside is warmer than air outside.

A two-layer model is assumed due to the thermal source of power Q with the lower cool air of density ρ_1, temperature T_1; upper hot air of density ρ_2, temperature T_2; lower and upper parts of flow areas are A_c and A_{c1} as in Figures

84

8-1 and 8-2. The volume flow rate V is given in terms of the flow coefficient C_d, and the separation height h' as in Figure 8-1 (Anderson 1995):

$$V = C_d \sqrt{\frac{2A_1^2 A_2^2}{A_1^2 + A_2^2} \frac{\rho_2 - \rho_1}{\rho} gh'} \qquad (8\text{-}1)$$

Defining A as the effective opening area of the building:

$$A = \sqrt{2} A_1 A_2 / (\sqrt{A_1^2 + A_2^2}) \qquad (8\text{-}2)$$

The volume flow rate V is then:

$$V = C_d A \sqrt{\frac{T_1 - T_2}{T_2} gh'} \qquad (8\text{-}3)$$

Heat balance gives:

$$Q = \rho C_p V (T_1 - T_2) \qquad (8\text{-}4)$$

Putting in equations (8-1) and (8-3):

$$T_1 - T_2 = \left(\frac{Q}{\rho_0 C_p C_d A} \right)^{2/3} \left(\frac{T_0}{gh'} \right)^{1/3} \qquad (8\text{-}5)$$

Defining the buoyancy flux B:

$$B = \frac{Qg}{C_p \rho_0 T_0} \tag{8-6}$$

V can be further simplified as:

$$V = (C_d A)^{2/3} (Bh')^{1/3} \tag{8-7}$$

Putting in the flow rate V_P calculated by the plume equation through a constant C, and the neutral plane height h_c:

$$V_P = C(Bh')^{1/3} h_c^{5/3} \tag{8-8}$$

Defining

$$\xi = (h_c / h') \tag{8-9}$$

Equating the air entrainment rate to the plane V_P to ventilation flow rate V gives:

$$\frac{C_d A}{h'^2} = C^{3/2} \sqrt{\xi^5} \tag{8-10}$$

8-2-2 Water-filling box model

For the water-filling box model by Linden (1990), the compartment is also divided into two zones. The upper zone is of lower density ρ_2 and higher temperature T_2 and the lower zone is of higher density ρ_1 which is the same as ambient and temperature T_1.

The volume flow rate equation V is also given by:

$$V = C_d A \sqrt{\frac{T_1 - T_2}{T_2} g(h' - h_c)} \qquad (8\text{-}11)$$

Heat balance gives:

$$T_1 - T_2 = \left(\frac{Q}{\rho_0 C_p C_d A}\right)^{2/3} \left(\frac{T_0}{g(h' - h_c)}\right)^{1/3} \qquad (8\text{-}12)$$

Putting equation (8-12) into (8-11):

$$V = (C_d A)^{2/3} (B(h' - h_c))^{1/3} \qquad (8\text{-}13)$$

After introducing the plume equation and equating the flow rate into the plume with the ventilation rate,

$$\frac{C_d A}{h'^2} = C^{3/2} \sqrt{\frac{\xi^5}{1-\xi}} \qquad (8\text{-}14)$$

8-2-3 Emptying air-filling box model

Surface thermal radiation effect in the building is included in the emptying air-filling box model by Li (2000). A constant temperature profile is assumed with the air temperature T_1 at the lower cool layer to be the same as the near-floor air temperature. Air temperature T_2 at the upper layer is the same as the air temperature next to the ceiling. This gives:

$$T_2 = \frac{Q}{\rho C_p V} + T_0 \qquad (8\text{-}15)$$

$$T_1 = \lambda(T_2 - T_0) + T_0 \qquad (8\text{-}16)$$

Note that λ is the temperature coefficient given in terms of the convective heat transfer coefficient α_f at the floor; the radiative heat transfer coefficient α_r at the ceiling; and the convective heat transfer coefficient α_c at the ceiling:

$$\lambda = \left[\frac{\rho C_p V}{A_{floor}} \left(\frac{1}{\alpha_f} + \frac{1}{\alpha_r} + \frac{1}{\alpha_c} \right) + 1 \right]^{-1}$$

The volume flow rate V is:

$$V = C_d A \sqrt{\frac{T_1 - T_0}{T_0} g h_c + \frac{T_2 - T_0}{T_0} g(h' - h_c)} \qquad (8\text{-}17)$$

Again, heat balance gives:

$$V = (C_d A)^{2/3} (B(h' - h_c + \lambda h_c))^{1/3} \qquad (8\text{-}18)$$

and

$$\frac{C_d A}{h'^2} = C^{3/2} \sqrt{\frac{\xi^5}{1 - (1 - \lambda)\xi}} \qquad (8\text{-}19)$$

8-3   Two proposed zone models

Two zone models, Models 1 and 2, have been developed to study the phenomena of air movement in both an area of open boundary condition and an enclosed area.

8-3-1   Model 1

A compartment without walls in the perimeter as in Figure 8-1 is considered. The dimensions of the room are of length L, width W and height H. A point heat source is located at the center of the chamber. A thermally-driven plume would rise to the ceiling, form a ceiling jet and then a hot air layer. The lower part is considered as the cool air layer. Eventually, ambient air would be drawn into the chamber, moving into the cool air layer, being heated up

and rise to the hot air layer, and then flow out of the chamber through the hot layer. The vertical distance between the upper and lower openings h' in Model 1 is specified as certain half height of the cabin. A constant smoke layer thickness is assumed under a steady condition when the mass of outflow equals to the inflow entrainment and mass generated by the plume.

8-3-2   Model 2

This is a compartment of the same size as in Model 1, but surrounded by adiabatic walls. There are two openings, one at the top and one at the bottom. A point heat source is located at the center of the chamber as in Figure 8-2. Again, a two-layer zone model is assumed. Ambient air would flow into the chamber through the lower opening, heated up, rise to the ceiling, and then flow out through the upper opening.

The equations for volume flow rates inflow V_1 and outflow V_2 are derived in Appendix F and summarized as follows:

$$V_1 = C_{d1}A_1\sqrt{\frac{2\Delta Tgh_c}{T_2}} \tag{8-20}$$

$$V_2 = C_{d2}A_2\sqrt{\frac{2\Delta Tg(h'-h_c)}{T_0}} \tag{8-21}$$

The buoyancy flux B is given by:

$$B = \frac{Qg}{C_P \rho_0 T_0}$$

Equations (8-20) and (8-21) become:

$$V_1 = (C_{d1} A_1)^{2/3} (2Bh_c)^{1/3} \tag{8-22}$$

$$V_2 = (C_{d2} A_2)^{2/3} (2B(h' - h_c))^{1/3} \tag{8-23}$$

The temperature difference between the upper layer and the lower layer is:

$$\Delta T = (\frac{Q}{\rho_0 C_p C_{d2} A_2})^{2/3} (\frac{T_0}{2g(h' - h_c)})^{1/3} \tag{8-24}$$

The neutral level h_c is defined as the height where the pressure difference across

the opening is zero and is given by:

$$h_c = \frac{h'}{n+1} \tag{8-25}$$

where

$$n = \frac{T_2}{T_0} (\frac{C_{d1} A_1}{C_{d2} A_2})^2$$

The relationship between the neutral level height h_c and the outlet area A_2 is:

$$\frac{A_2}{h'^2} = 0.042318/C_{d2}\sqrt{\frac{(\frac{h_c}{h'})^5}{(1-\frac{h_c}{h'})}}$$

(8-26)

8-4   Zone modeling results

Results predicted by the two developed zone models are solved by MATLAB (1997) with listing shown in Appendix F.

Ventilation flow rates predicted by Model 1 and Model 2 are compared with the emptying air-filling box model by Li (2000) given by equation (8-18). Results are shown in Figure 8-3 and compared with equation (8-23) in Model 2. The relationship between the outlet area A_2, the distance between the inlet and outlet opening h' and the outlet volume ventilation flow rate V_2 is shown the figure. It can be seen that the outlet flow rate would increase when A_2/h'^2 is increased. A very small difference between the results of the two models was found for A_2/h'^2 less than 0.02.

The neutral plane heights of Model 1 and Model 2 are plotted in Figure 8-4 for comparison with the emptying air-filling box model ($\gamma = 0.2$). There is an equation on h_c in the emptying air-filling box model given by:

$$h_c = \gamma h' + (1 - \lambda)(1 - \gamma)h_1 \qquad (8\text{-}27)$$

The above equation is compared with equation (8-26) in Model 2. Note that γ is the vertical temperature gradient. The relationship between the neutral zone height h_c, the distance between the inlet and outlet opening h', and the outlet area A_2 is shown in Figure 8-4. The result showed that the height of the neutral plane would increase when A_2 / h'^2 is increased. For A_2 / h'^2 less than 0.02, the neutral plane height increased. There are large differences between the results of the two models. But for A_2 / h'^2 greater than 0.02, neutral plane heights predicted by the two models agreed better.

For interest, the neutral plane heights predicted by Model 1 and 2 are compared with the hot air layer height of the emptying air-filling box model in Figure 8-5 to show the similarities of the two parameters in the two models. The following equation in the emptying air-filling box model is compared with equation (8-26):

$$\frac{C_d A_2}{h'^2} = C^{3/2} \sqrt{\frac{(\frac{h_1}{h'})^5}{(1 - (1 - \lambda)\frac{h_1}{h'})}} \qquad (8\text{-}28)$$

where C is a constant used in the plume flow rate calculation.

The result showed that the neutral plane height h_c in Model 1 and Model 2 agrees well with the hot air layer height in the emptying air-filling box model when the temperature coefficient λ is 0.2.

Comparisons are also made in the following conditions to study the inflow and outflow rates in the zone model separately. The height of the chamber H is taken as 6 m with both the upper and lower openings in Model 2 to be 1 m^2. A point heat source is located at the center of the control volume, with a constant heat release rate of 500 W. The ambient temperature T_0 is 300 K. To simplify the calculation, C_d is 0.6, C_p is 1010 Jkg^{-1}K^{-1}, and p_0 is 101300 Pa.

A comparison of the inlet airflow rate in Model 1 and Model 2 with Andersen's model is shown in Figure 8-6. The following equation in Anderson's model is compared with equation (8-22):

$$V_1 = 0.037(Qh_c)^{1/3}(C_{d1}A_1)^{1/2} \tag{8-29}$$

Result showed that the inflow rate V_1 increased when the neutral plane height h_c increased.

A comparison of the outlet airflow rate in Model 1 and Model 2 with Andersen's model is shown in Figure 8-7. The following equation in Andersen's model is compared with equation (8-23):

94

$$V_2 = 0.038(Q(h' - h_c))^{1/3}(C_{d2}A_2)^{1/2} \qquad (8\text{-}30)$$

The result showed that when the neutral plane height h_c increased, the outflow rate V_2 decreased.

Finally, a comparison of the temperature difference in Model 1 and Model 2 with Anderson's model is made in Figure 8-8. The equation in Anderson's model is compared with equation (8-24):

$$\Delta T = 7.5 \cdot 10^{-5} T_0 (\frac{Q}{C_{d2}A_2})^{2/3} (\frac{1}{h' - h_c})^{1/3} \qquad (8\text{-}31)$$

It is found that before the neutral plane height $h_c / h' = 0.8$, there are less changes in the temperature difference ΔT of the two layers, but after that point, there is an obvious increase in the temperature difference of the two layers with the increase of h_c / h'.

The relationship between the neutral zone height h_c, height of inlet and outlet opening h' and the outlet area A_2 is shown by equation (8-26). But usually, the area and position of the openings are known first, and the neutral zone height needs to be solved. That could be a very complex equation but can be fitted by:

$$\frac{h_c}{h'} = 1.7276(\frac{A_2}{h'^2})^{0.3187} \qquad (8\text{-}32)$$

Results are plotted in Figure 8-9 with the correlation coefficient being 0.9899.

8-5   Simulation with Computational Fluid Dynamics

CFD was used for comparing the zone modeling results. The commercial software PHOENICS (2000) was taken as the simulator. A compartment with L of 10 m, W of 10 m and H of 6 m was taken for comparison of the two models. The grid and geometry of CFD simulation are shown in Figure 8-10.

Airflow vectors predicted are shown in Figure 8-11 to show the air movement pattern. Maximum air speed changed from 0.187 ms^{-1} in the open boundary condition to 0.2 m s^{-1} in the enclosed condition. The inflow rate and outflow rate were calculated from the results of CFD simulation.

The simulation results of pressure distribution are shown in Figure 8-12. The height of neutral plane is clearly shown. The result of CFD simulation and the result of the zone models are compared in Table 8-1.

The results showed that the inflow rate and outflow rate in CFD simulation are very close, but the results in the theoretical zone model simulation are quite different. In Model 1, the outflow ventilation rate is limited by the small cross-sectional area of outflow air. In Model 2, the outlet area and the inlet area are the same, but the neutral plane has changed a little, and the outflow rate is still limited by the zone model equation. The inflow and outflow results in Model 2

in CFD simulation are quite different from the zone model result. That is because only the air flowing in the control volume through A_1 and flowing out through A_2 was considered. It is assumed that each zone is fully mixed. The turbulence inside the chamber was not considered. But from Figure 8-11, it is obvious to see that most of the air would rise to the ceiling and create turbulence inside the chamber, so that the inflow rate and outflow rate are significantly reduced to a lower level.

8-6   Conclusion

Two zone models are developed to study air flow problems induced by a point heat source in a natural ventilated chamber. The difference in the results of CFD simulation and zone model simulation was discussed. Model 1 could be considered as a special situation of Model 2, when the area of the upper opening and the lower opening in Model 2 is exactly equal to the opening area of upper layer and lower layer in Model 1 respectively.

Volume flow rate equations and two-layer temperature difference equations were derived. The relationship between the neutral level height and the outlet area was drawn. The neutral plane h_c equation was defined by curve-fitting, which made the solution easy to use.

In comparing with CFD results, results of the new models give fairly good predictions on the neutral plane height. The results can be widely used in the fire

engineering field which has a lot of needs to calculate the volume flow rates in both the inlet and outlet, and the temperature difference between the upper layer and the lower layer. Further, dynamics of plume is driven by pressure difference, the neutral plane equation can help engineers to predict the neutral plane just by the height of the inlet and outlet opening h′ and the outlet area A_2, which is important to control the airflow and study the dynamics of plume inside the enclosures. The results simplified the profound aerodynamics equations, making it easy to use in engineering applications.

Chapter 9 A STUDY ON PLUME EQUATION IN A CHAMBER WITH FORCED VENTILATION

Fire control under forced ventilation in enclosure is very important in fire safety aspects. To optimize the safety in enclosures with mechanical ventilation by improving the design of forced ventilation systems, the form of plume equation under forced ventilation must be solved. Thermally-induced plume in a chamber under forced ventilation are studied in this chapter. Plume equations derived under natural ventilation available in the literature are reviewed first (Rouse 1954, Yip 1997, Morton 1956). Computational Fluid Dynamics are then applied to study two 'models' induced by a heat source in a chamber with forced ventilation. They are the parallel flow model and the jet flow model. Based on the plume expression in a chamber with natural ventilation, two plume equations under forced ventilation are then derived from seven sets of CFD simulations. There are four cases on different thermal power of the point heat source; and three cases on the plume in a chamber with forced ventilation under three different air speeds. Symbolic mathematics are used for solving some equations concerned.

9-1   Introduction

Plume induced by a thermal source such as a fire in a chamber under forced ventilation condition is very complicated. Most of the plume equations in the literature (Beyler 1986, Chow 1998a, Drysdale 1985, Rouse 1954, Heskestad 1984, Hinkley 1971, Morton 1956, Morgan 1987, Thomas 1963, Yih 1977, Yu

1992, Zukoski 1981) were derived under natural ventilation condition with free boundary conditions. However, the equations concerned might not be applicable in a chamber with forced ventilation. The following questions are raised:

- Can those equations be applied under forced ventilation conditions?
- How is the situation under forced ventilation conditions?

To answer the above questions, equations under forced ventilation condition in a chamber will be studied in this chamber. The plume equation under forced ventilation can be described by two flow models as in Figure 9-1:

- A parallel flow model

  The fluid is assumed to be incompressible flow through two horizontal parallel planes with constant pressure difference. The direction of flow is taken along the horizontal axis, with velocities in other directions taken as zero. Velocity distribution is laminar and plane parallel (Yu 1992), an indent mixing of forced ventilation (Galea 2001) in a chamber.

- A jet flow model

  Incompressible fluid flow is assumed through a fine nozzle, and then diffused in a free boundary space (Kong 1979). The resultant plume is then induced by a point heat source on the floor.

These two models are studied by Computational Fluid Dynamics. Associated plume equations are then discussed in this Chapter.

9-2   Jet flow model

A chamber of length 4 m, width 4 m, and height 3 m as shown in Figure 9-2 was considered. A point heat source with radius 0.1 m and height 0.1 m is located at the center of the chamber as shown in the figure. There are no walls in the perimeter, just a floor and a ceiling. This is labeled as the 'fire case with an open lid' by Galea et al. (2001).

Air flow induced by the thermal source was simulated with the following assumptions (Rouse 1954):

• The rate of entrainment at the plume edge is proportional to some characteristic velocity at that height.

• The profiles of mean vertical velocity and mean buoyancy in horizontal sections are of similar form at all heights.

• The largest local variations of density in the field of motion are small in comparison with some chosen reference of density, this reference being taken as the density of the ambient fluid at the level of the source.

• The scale of the initial laminar zone is small compared with the subsequent zone of turbulent convection.

• Pressure is distributed uniformly throughout the field of motion.

- Transverse forces are ignored in comparison with those in the vertical direction.

- Turbulent mixing in the vertical direction is ignored in comparison with that in the horizontal.

- Notation for either two-dimensional flow over a line source or axially symmetric flow over a point source may be reduced to that shown in Figure 9-3.

- No mixing mechanics between the plume and ambient air flow.

- Floor, ceiling and walls of the chamber are made of adiabatic materials.

- No viscosity between horizontal sections.

- The form of the plume border is like a cone, which can be considered as a source point extended to a circle with the rise of the plume.

A typical plume model is shown in Figure 9-3. Under the above assumptions and taking the point heat source on the floor, four cases with different thermal pressure are simulated for studying the plume equation:

- Case 1: 1 kW

- Case 2: 3 kW

- Case 3: 5 kW

- Case 4: 8 kW

The CFD package PHOENICS was used for simulating the thermally-induced air flow. The results of velocity distribution, pressure distribution and temperature

distribution are shown in Figures 9-4 to 9-6 respectively. The results of vertical velocity of the plume v are plotted in Figure 9-7. Derivation of plume model equations is listed in Appendix G.

As a result, for the condition of axial symmetry model, the vertical velocity v has the following relationship with x and h (Rouse 1954):

$$\frac{v}{(B/h)^{1/3}} = f\left(\frac{x}{h}\right) \tag{9-1}$$

Suppose the velocity distribution is uniform, according to both the simulation above and the experimental results (Beyler 1986, Drysdale 1985, Rouse 1954, Heskestad 1984, Hinkley 1971, Morton 1956, Morgan 1987, Thomas 1963, Yih 1977, Yu 1992, Zukoski 1981), the velocity distribution could be expressed as Gaussian distribution.

$$v = v_{max} \exp\left(-\frac{x^2}{R^2}\right) \tag{9-2}$$

where R is the specified plume radius.

Then, key results related to the plume equations are:

- Velocity distribution

$$v = \alpha \left(\frac{B}{h} \right)^{1/3} \exp\left(-65 \frac{x^2}{h^2} \right) \tag{9-3}$$

where α is a coefficient related to height h in Figure 9-8, expressed in terms of a characteristic length l_c (taken as 1 m) as:

$$\alpha = -1.379 \, (h / l_c)^3 + 8.032 \, (h / l_c)^2 - 16.427 \, (h / l_c) + 17.029 \tag{9-4}$$

The buoyancy flux B is defined as:

$$B = \frac{Qg}{C_p \rho T} \tag{9-5}$$

where Q is the heat release rate, g is the gravitational acceleration, C_p is the specific heat capacity of air, ρ is the air density and T is the absolute temperature.

- Volume flux

$$V = 0.0483 \alpha B^{1/3} h^{5/3} \tag{9-6}$$

- Momentum flux

$$M = 0.02415\alpha^2 \rho B^{2/3} h^{4/3} \qquad (9\text{-}7)$$

- Energy flux

$$E = 0.00805\alpha^3 \rho Bh \qquad (9\text{-}8)$$

From the result of this simulation, it is found that in the main part of the plume, normally $\alpha = 4.0$.

- Velocity distribution

$$v = 4.0 \left(\frac{B}{h}\right)^{1/3} \exp\left(-65\frac{x^2}{h^2}\right) \qquad (9\text{-}9)$$

- Volume flux

$$V = 0.1932 B^{1/3} h^{5/3} \qquad (9\text{-}10)$$

- Momentum flux

$$M = 0.3864 \rho B^{2/3} h^{4/3} \qquad (9\text{-}11)$$

• Energy flux

$$E = 0.5152\rho Bh \qquad (9\text{-}12)$$

The plume equation by Rouse (1954) takes the following form:

$$v = 4.7\left(\frac{B}{h}\right)^{1/3} \exp\left(-96\frac{r^2}{h^2}\right) \qquad (9\text{-}13)$$

$$V = 0.154B^{1/3}h^{5/3} \qquad (9\text{-}14)$$

$$M = 0.361\rho B^{2/3}h^{4/3} \qquad (9\text{-}15)$$

$$E = 0.566\rho Bh \qquad (9\text{-}16)$$

The simulation results are compared with those by Rouse's equation as shown in Figure 9-9. Better results are obtained by using the equation here than using the equation by Rouse, because of the introduced height coefficient α.

The maximum velocity v_{max} in each horizontal level could be expressed as:

$$v_{max} = 4.0\left(\frac{B}{h}\right)^{1/3} \qquad (9\text{-}17)$$

9-3   Horizontal velocity at the plume edge

From the definition of jet plume and the calculations above, on the central axis, the horizontal velocity at the plume edge is assumed to be proportional to v_{max}.

$$t = \frac{h}{v_{max}} = \frac{R}{u}$$

$$\frac{u}{v_{max}} = \frac{R}{h} = \tan 15°$$

$$u = v_{max} \tan 15° \qquad\qquad (9\text{-}18)$$

Putting equation (9-3) into equation (9-18), in the central axis, $x = 0$, the horizontal velocity distribution of the plume edge is:

$$u = \alpha \tan 15° \left(\frac{B}{h}\right)^{1/3} \qquad\qquad (9\text{-}19)$$

The speed in the position of $h_0 = 0.1$ m above the floor is selected as the initial plume velocity.

Finally, the relationship between u and buoyancy flux B is obtained, the maximum velocity of the plume in horizontal direction is:

$$u = 0.5773 \, \alpha B^{1/3} \qquad\qquad (9\text{-}20)$$

The velocity at the plume edge u when expressed in ms^{-1} is:

$$u = 0.238 \left(\frac{Q}{1000} \right)^{1/3} \qquad\qquad (9\text{-}21)$$

The relationship between horizontal velocity of plume edge u and heat release rate is shown in Figure 9-10. The correlation coefficient r^2 is 0.9998.

9-4   Plane parallel flow

The plane flow model is quite well known in fluid mechanics (Kong 1979). The chamber for CFD simulation is of length 4 m, width 4 m and height 3 m as in Figure 9-11. There are two adiabatic walls built along two opposite sides in the perimeter, making the chamber look like a corridor.

The following assumptions are made:

- The air flow is constant, and incompressible.

- A flow with pressure difference only.

- A flow through two parallel planes.

- Turbulent mixing in the vertical direction is ignored.

- Floor, ceiling and walls of the chamber are made of adiabatic materials.

According to the above assumptions, velocity distribution can be solved by N-S equation:

$$\begin{cases} -\dfrac{1}{\rho}\dfrac{\partial P}{\partial x} + v\dfrac{\partial w^2}{\partial y^2} = 0 \\[4mm] -\dfrac{1}{\rho}\dfrac{\partial P}{\partial y} = 0 \end{cases} \qquad (9\text{-}22)$$

Taking the assumption that air flow is incompressible and $\dfrac{\partial w}{\partial x} = 0$, expressing in terms of the building length scale L, equation (9-22) gives:

$$\frac{d^2 w}{dy^2} = \frac{\Delta P}{\mu L} \qquad (9\text{-}23)$$

where μ is the dynamical viscidity coefficient.

$$\Delta P = P_1 - P_2, \qquad (9\text{-}24)$$

P_1 is the air pressure on one side of the control volume and P_2 is the air pressure on the other side of the control volume (Kong 1979).

$$\Delta P = \frac{8\mu L w_{max}}{H^2} \qquad (9\text{-}25)$$

Integrating equation (9-23) twice by the use of the following boundary conditions:

$$\begin{cases} y = H, w = U \\ \\ y = 0, w = 0 \end{cases}$$

where U is the moving speed of ceiling.

The velocity distribution can be solved as:

$$w = \frac{\Delta P}{2\mu L}(Hh - h^2) + \frac{Uh}{H} \tag{9-26}$$

The moving speed of the ceiling is 0, the flow could be considered as a pure pressure difference flow. The velocity distribution is:

$$w = \frac{\Delta P}{2\mu L}(Hh - h^2) \tag{9-27}$$

Putting equation (9-25) into equation (9-27):

$$w = \frac{4w_{max}}{H^2}(H - h)h \tag{9-28}$$

- Flux of the parallel flow

Area of the control surface is taken as $W \cdot dy$, multiplying it with w would give the flow flux $w \cdot W \cdot dy$. Integrating the height from 0 to H:

$$V = \int_0^H wWdy \qquad (9\text{-}29)$$

Putting in equation (9-26):

$$V = W \int_0^H [\frac{\Delta P}{2\mu L}(Hh - h^2) + \frac{Uh}{H}]dz = W(\frac{\Delta PH^3}{12\mu L} + \frac{UH}{2}) = \frac{WH}{2}(\frac{\Delta PH^2}{6\mu L} + U)$$

$$(9\text{-}30)$$

The upper ceiling moving speed is 0, the flow could be considered as a pure pressure difference flow, and $\Delta P > 0$. The flux of the parallel flow is:

$$V = \frac{W\Delta PH^3}{12\mu L} \qquad (9\text{-}31)$$

Putting in equation (9-25):

$$V = \frac{2HWw_{max}}{3} \qquad (9\text{-}32)$$

9-5   Derived plume equation under forced ventilation condition

After studying the jet plume flow and the plane parallel flow individually, the plume equations for the two models under forced ventilation in that chamber are discussed. The plume can be described as a jet flow, and forced ventilation in a chamber can be described as a plane parallel flow. The plume equation under forced ventilation can be described as a jet flow in a parallel flow model as in Figure 9-1, i.e. combining the two models together.

The chamber studied is of length 4 m, width 4 m and height 3 m. There are two adiabatic walls built along two opposite sides in the perimeter. A point heat source with radius 0.1 m and height 0.1 m is located at the center of the chamber, as in Figure 9-1.

Three simulations with different air flow speeds were carried out for studying the plume situation under forced ventilation condition. The results are shown in Figure 9-12.

Assuming that the parallel flow has no effect on the vertical velocity of the plume, there would be no mixing and energy exchange between the plume and ambient air flow. The equations for volume, momentum flux and energy flux of the plume have the same format as those of natural ventilation. Only the position of the plume central axis would be changed by forced ventilation of the ambient air flow.

112

If the dynamical viscosity coefficient between the floor and ceiling is not considered, the parallel flow speed w is a constant, there would be four different situations.

When the speed of parallel flow w is zero, it means that the plume would rise without any forced ventilation. The situation of the plume without any forced ventilation is shown in Figure 9-13.

The situations of the plume when the speed of parallel flow w is less than, equal to and greater than the horizontal velocity of plume edge u are shown in Figures 9-14 to 9-16 respectively.

The plume central axis equation can be written as (derivation in Appendix G):

$$x = wt + \frac{C_p \Delta T \rho_0 w^2}{4Q} t^2$$

$$h = vt + \frac{(1 - \frac{T_0}{T})\rho_0 HgC_p \Delta T}{2Q} t^2 \qquad (9\text{-}33)$$

An example calculation was carried out with different velocity of parallel flow as 1 ms^{-1}, 2 ms^{-1}, 3 ms^{-1} and 10 ms^{-1}.

The heat release rate of fire Q was set to be 5 kW, T as 600K, T_0 as 300K, g as 9.8 ms^{-2}, H as 3 m, C_p as 1010 J kg^{-1}K^{-1}, α in v as 4.0 (v_{max} is 1.58 ms^{-1}). The

comparison of the plume central axis position with different velocity of parallel flow is shown in Figure 9-17. The result showed that, the higher velocity of parallel flow, the more the plume central axis is deviated from the vertical.

Another example calculation was carried out with different heat release rate of fire of 1 kW, 3 kW, 5 kW and 8 kW. The comparison of the plume central axis position with different heat release rate of fire is shown in Figure 9-18. The result showed that, the bigger the heat release rate of a fire, the less the plume central axis is deviated from the vertical.

Further, in a special case, as assumed above, when the velocity of parallel flow w is constant and the plume has no effects on the forced ventilation from ambient air, and the temperature inside the plume is uniform, the above equation can be simplified as:

$$x = \frac{w}{v} h \qquad\qquad (9\text{-}34)$$

Following the settings above, with velocity of parallel flow of 1 ms^{-1}, the comparison of the plume central axis position in the example calculation is shown in Figure 9-19. The result showed that, the simplified equation has a good fitting of the plume central axis equation, so that the simplified equation can be used in some engineering area to predict the form of a plume in a chamber.

9-6   Conclusion

The plume equation under forced ventilation condition in a chamber is studied. CFD PHOENICS (2000) simulations were carried out for creating plume equations under natural ventilation condition with free boundary. A comparison of the new plume equation with Rouse's plume equation is made. The simulation results can be better described by the new plume equation after the height coefficient α is introduced. Therefore, the results of the new plume equation are more precise.

The plane parallel flow is studied as an easy forced ventilation condition. Two different situations are discussed. If the dynamical viscosity coefficient between the floor and ceiling is not considered, the parallel flow speed w is constant, then there would be another four different situations: $w = 0$, $w < u$, $w = u$, $w > u$. If the dynamical viscosity coefficient between the floor and ceiling is considered, then the parallel speed w is not a constant, but has a distribution like plane parallel flow.

Since the parallel flow is assumed to have no effect on the vertical velocity of the plume, there would be no mixing and energy exchange between the plume and the ambient air flow. The equations for volume flux, momentum flux and energy flux of the plume have the same format as those of natural ventilation. Only the position of the plume central axis would be changed by forced ventilation of the

ambient air flow. The position of plume central axis equation is drawn by calculation under each different condition.

The result solved the two questions raised in the beginning of the chapter. It is very useful in fire engineering field, where plume equations are needed to calculate the volume flux, momentum flux and energy flux of the plume under forced-ventilation condition in enclosures. The result can also be used to predict the plume position for protecting occupants and property when fires occur under forced-ventilation condition in enclosures like cabins under atrium, duty-free shops, mini-banks or convenience stores.

Chapter 10   CONCLUSION

Fire hazard, particularly smoke aspect in forced ventilated compartment should be studied carefully. This would help the Authority to draft workable fire codes on those buildings with forced ventilation, and mechanical smoke extraction system. Smoke has been recognized as the major problem of fire safety to human lives. Fire codes should be improved and applied thoroughly to protect people against accidental fires. Mechanical ventilation system should be designed properly to make better control of smoke by studying the hazard scenarios on the occupants, the building and its contents under forced ventilation condition. Part of the above had been carried out in this thesis with the following stages.

Stage 1 is on studying principles of forced ventilation systems. The fire codes in respect to fire safety and both natural ventilation system and forced ventilation design as well as the fire codes applied in Hong Kong and Mainland China are reviewed and evaluated. The performance-based fire codes are also studied fundamentally. The application of engineering performance-based fire code to carparks in China is discussed.

Stage 2 is on applying the symbolic mathematics program MATLAB to solve the equations on the two-layer fire zone model ASET for a chamber with air supplied through leakage. Two key ordinary differential equations on smoke layer height and temperature are considered. A total number of 12 simulations were carried out on two design fires in six compartments with floor area varying

from 10 m^2 to 100 m^2. The results are compared with those simulated by the ASET itself and another software FIREWIND version 3.4.

Stage 3 is on applying CFD model for studying 'bare cabin' fires with the operation of smoke extraction system. The effect of operating only the smoke extraction system in a 'bare cabin' fire without sprinkler operating is studied. The CFD software PHOENICS 3.1 capable of studying the effect of smoke extraction operation was used for fire simulation. Cabins with and without exhaust system installed were simulated. Relationship between temperature and hot layer height has been drawn out. Further, more than 14,400 simulations were made for studying 'bare cabin' fires numerically. The fire environments due to all the four sets of slow, medium, fast, and ultra-fast t^2-fires including four smoke exhaust rates each are tested. The time to flashover in 'bare cabins' under NFPA t^2-fires in cabins of different sizes is studied using a two-layer zone model FIREWIND (FMC 1997). Correlation equations were fitted between the flashover time with the cabin floor area and ceiling height. The equations are useful for the Authority to inspect new projects of this kind, especially for those who are not experienced in using fire models while implementing engineering performance-based fire codes.

Stage 4 is on studying thermally-induced indoor aerodynamics in a compartment with natural ventilation. A theoretical zone model equation is developed. The results are compared with different former works. CFD simulation is applied to the two models. The results are compared with the theoretical model. The

neutral plane h_c equation is defined by curve fitting, which makes the solution easy to use. The difference in the solution of CFD simulation and zone model simulation is discussed.

Finally, plume equations are studied, and plume equations under different forced ventilation conditions are developed. Both zone model and CFD model are developed for simulating air movement and plume. PHOENICS is used as the simulation tool. This software has been successfully applied in the simulations of air movement in both natural ventilation and forced ventilation condition. The new plume equation can describe more precisely the plume under both natural ventilation and forced ventilation conditions. It is believed to be a significant work for further studying of plume and ventilation.

The main results and conclusions of the study can be summarized as:

- Forced ventilation is further studied from two main areas, the zone model and CFD field model. Two-layer fire zone models with symbolic mathematics have the following features: Symbolic mathematics is now a powerful tool for doing mathematics with a computer. It can be applied to simulate a building fire with a two-layer model. A relatively simple model like ASET can be put into the computer easily. Graphics outputs can be achieved easily. It is easier to change the equations and parameters concerned on describing the physics concerned in comparing to traditional computer programming.

The software is under active development, both on the numerical schemes and graphical presentation.

• From the simulations, floor area should be watched carefully in using two-layer zone models. Symbolic mathematics should be put into the teaching curriculum for engineering degree programs.

• In the CFD model of studies on 'bare cabin' fires with the operation of smoke extraction system, there are few changes in the temperature area from 30 to 120 °C. The pressure around the neutral line has moved only slightly, but the neutral area has changed. Hot layer and cool layer are clearly shown in CFD simulation in the comparison of the relationship between temperature and hot layer height in CFD and zone model. The temperature dropped after operating the exhaust system.

• Numerical studies on 'bare cabin' fires indicated that flashover might occur quickly, say within 210 s, for cabins with a NFPA fast t^2-fires. Correlation equations were fitted between the flashover time with the cabin floor area and ceiling height.

• Fire protection systems should be provided (Bressington 1999b) in each cabin. The time for detecting a fire, operating the sprinkler to discharge water, turning on the smoke extraction system and the time for people staying inside to escape must be considered carefully. It will be a big

problem if the cabin is enclosed completely in case of a fire, since some occupants might not be able to leave it in time and they would be exposed to the steam generated by the sprinkler water.

- For fast-growing fires, such as the fast and ultra-fast t^2-fires, the mechanical ventilation system would have little effect on the development of smoke temperature and smoke layer thickness. The time to flashover would be extended slightly under larger air change rates.

- For the study of thermally-induced indoor aerodynamics in a compartment with natural ventilation, it is found that the results of the new theoretical zone model developed are more accurate than the three models when compared with CFD experimental results.

- A new plume equation given by equation (9-3) under natural ventilation condition with free boundaries was derived. This is compared with Rouse's plume equation. The new plume equation can better describe the simulation results than the old one after introducing the height coefficient α. So, the result of the new plume equation is more precise.

- For the study in a chamber with forced ventilation, since it is assumed that the parallel flow has no effect on the vertical velocity of the plume, there is no mixing and no energy exchange between the plume and ambient air flow. It can be said that the volume, momentum flux and energy flux of the plume

have the same format as that of the natural ventilation. Forced ventilation of ambient air flow would just change the position of the plume central axis. The position of the plume central axis equation is drawn by calculation under each different condition.

- New developed air flow models can be widely used in compartment fire assessment particularly under forced ventilation conditions, such as for cabin design, and the design of airport terminals and railway stations.

The originality and contribution to fire science, engineering and industry can be summarized into three points:

The first part is on attempting to apply concept behind performance-based fire code into the Chinese fire code by taking a carpark as an example.

The second part is on selecting suitable zone and CFD field models as simulation tools for fire hazard assessment and performance evaluation of fire protection system. Correlation relationships between time to flashover and geometry of the building; and between smoke layer temperature and smoke layer height were derived. Assumptions made in zone model were verified by CFD simulations.

The last part is on developing new zone models for studying aerodynamics in chambers induced by a thermal source. Plume equations under forced ventilation were developed for building services engineering system design. Inlet and outlet

volume flow rates across the enclosure boundaries were derived in terms of the temperature difference. The relationship between neutral plane height, outlet volume flow rate and geometry of the building was found. These equations are not so complicated as traditional aerodynamic equation and plume equation under forced ventilation condition, making it easier to use in practice.

Based on the above studies, the fundamentals and application of enclosure fires with mechanical ventilation system are studied and developed. Both theoretical model and computational simulations are successfully performed.

NOMENCLATURE

A   effective opening area of building, m^2

A_c area of window, m^2

A_f floor area of building, m^2

a   variable

B   buoyancy flux, $m^4 s^{-3}$

C   constant used in plume flow rate calculation

C_1, C_2 constants

C_c contraction coefficient

C_d discharge coefficient

C_{in} carbon monoxide concentration in an enclosed space

C_m mixing coefficient

C_p specific heat capacity of air, $J\ kg^{-1}\ K^{-1}$

C_t carbon monoxide concentration

$C(t)$ instantaneous carbon monoxide concentration

d_l thickness of the air layer around the plume, m

E   energy flux, $kJ\ s^{-1}$

g   gravity acceleration, $9.8\ m\ s^{-2}$

g' effective acceleration of gravity, $m\ s^{-2}$

H   height of building, m

H_V height of opening, m

h   vertical distance above the floor, m

h_l height of smoke zone, m

h_c height of neutral zone interface, m

h_s approximation step used in Runge-Kutta (RK) method

h' vertical distance between upper and lower openings, m

I_w width index

K coefficient used in plume calculation

K' doorway orifice coefficient

L length scale of building, m

L_C coefficient of heat loss by conduction and radiation

M momentum flux, $kg\ s^{-1}$

m mass flow, $kg\ s^{-1}$

m_C mass in control volume, kg

m_e mass flow rate through leakage, $kg\ s^{-1}$

M_f mass flow in the plume, $kg\ s^{-1}$

N_{per} number of persons

n unit

P air pressure, Pa

p_n, q_n, r_n, s_n variables used in Runge-Kutta (RK) method

P_S surface vector

Q heat release rate, W

$\dot{Q}(t)$ heat release rate of fire source, kW

q heat flow rate, kW

R radius of plume in a specified height of h, m

R' gas constant, $kJ\ kg^{-1}\ K^{-1}$

R_0 radius of the pool, m

r^2 correlation coefficient

S surface component

S_0 vertical distance from the floor to the point heat source, m

S_t emitting rate, kg s^{-1}

T absolute temperature, K

T_0 ambient air absolute temperature, K

T_s temperature of sprinkler activation, K

t time, s

t_f predicted flashover time, s

t_{op} time to operate the smoke extraction system, s

U move speed of ceiling, m s^{-1}

U^i velocity of inviscid flow, m s^{-1}

u horizontal velocity of plume edge, m s^{-1}

u', v' velocity component, m s^{-1}

V volume flow rate, m^3 s^{-1}

V_C volume of control volume, m^3

V_g moving speed of gas, m s^{-1}

V_h volume of hot smoke layer, m^3

V_m mixing flow rate, m^3 s^{-1}

V_n net flow rate, m^3 s^{-1}

V_{Room} volume of building, m^3

V^i volume flow rate of inviscid flow, m^3 s^{-1}

v vertical velocity of plume, m s^{-1}

v_{max} maximum velocity of the plume in vertical direction, m s^{-1}

W   width of building, m

W_e width of exit, m

W_V width of opening, m

w   velocity distribution of plane flow, m s^{-1}

w_{max} maximum velocity of plane flow, m s^{-1}

x, y   direction components

Z_i interface height above the floor, m

Z_N interface height above the floor in a specified time, m

α coefficient

α_c convective heat transfer coefficient at the ceiling

α_f convective heat transfer coefficient at the floor

α_r radiative heat transfer coefficient at the ceiling

Δ difference

ΔB unit buoyant force

ΔT difference in temperature

γ vertical temperature gradient

λ temperature coefficient

μ dynamical viscosity coefficient

ρ air density, kg m^{-3}

ρ_a average density, kg m^{-3}

ρ_e effective density, kg m^{-3}

ρ_0 ambient air density, kg m^{-3}

σ	stress tensor
τ	vertical shear stress
τ'	time constant
ξ	h_c / h'
ζ	resistance coefficient

Subscripts

0	initial values
1	inflow, inlet
2	outflow, outlet
c	contracted
d	discharge
e	effective
f	floor
g	gas
h	hot layer
i,j,k,l	tensor notations
L	lower cool layer
m	mixing
N	value at specified time
n	step number
P	plume
V	ventilation

LIST OF FIGURES

Figure 9-19   Comparison of the plume central axis position in the example calculation

Chapter 1   An introduction including a brief literature review.

Chapter 2   An advanced study of fire codes in China.

Chapter 3   A review of forced ventilation design.

Chapter 4   A study of applying performance-based fire codes to China.

Chapter 5   Application of numerical studies of forced ventilation to cabin.

Chapter 6   A study and evaluation of two-layer zone model.

Chapter 7   CFD simulation, including introduction to theory and application to cabin.

Chapter 8   Application of air flow model on thermally-induced indoor aerodynamics in a compartment with natural ventilation.

Chapter 9   A further study on plume equation under forced ventilation.

Chapter 10   Conclusion.

Figure 1-1: Outline of thesis
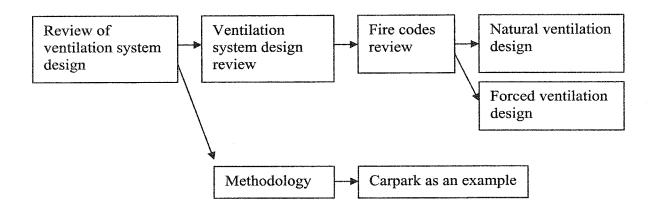
Figure 3-1: Outline of Chapter 3
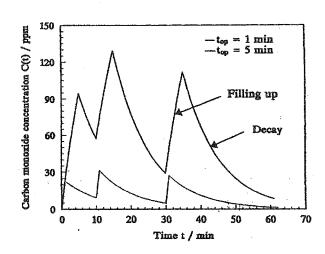
Figure 3-2: Transient carbon monoxide level (Chow 1995b)
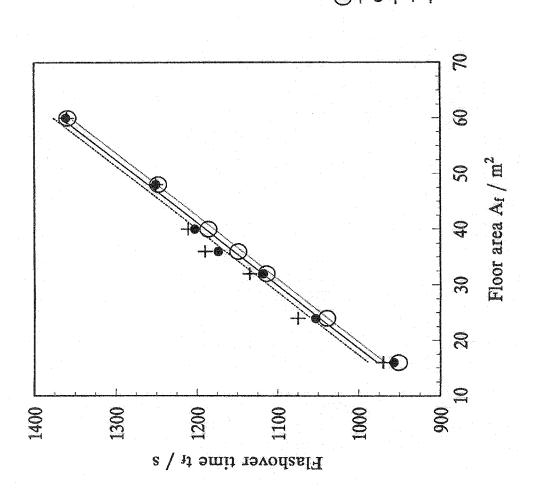
Figure 5-1: Flashover time for slow-t^2 fire

F-8

(a) Smoke layer temperature

(b) Smoke layer interface height

— No extraction
O 40 ACH
✳ 80 ACH
+ 120 ACH
● 180 ACH
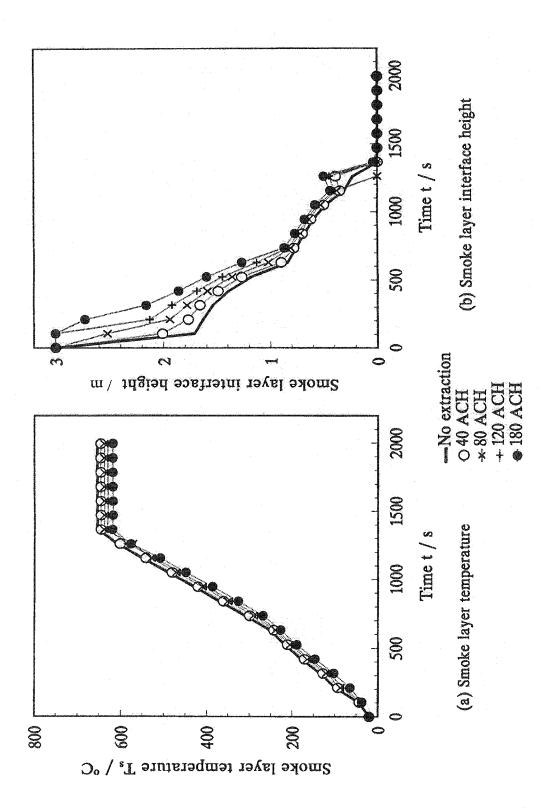
Figure 5-2: Extraction system operated at 37 s

F-9

(a) Smoke layer temperature

(b) Smoke layer interface height

Legend:
— No extraction
O 40 ACH
✳ 80 ACH
+ 120 ACH
● 180 ACH
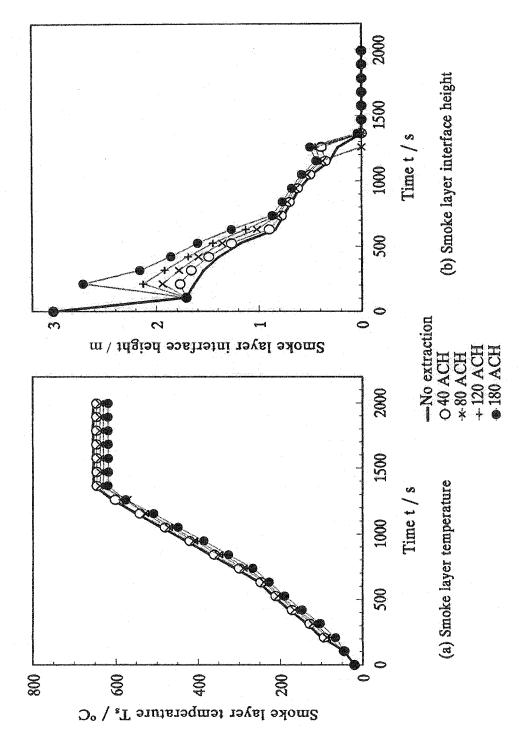
Figure 5-3: Extraction system operated at 150 s

F-10
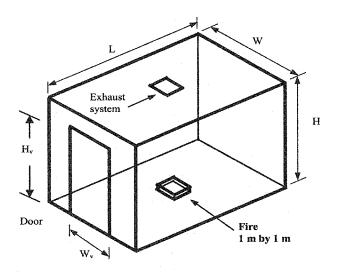
Figure 5-4: Geometry of cabin
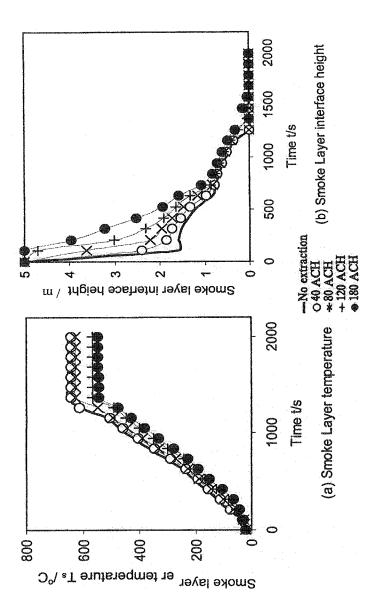
Figure 5-5: Extraction system operated at $t_{0.45}$ under a slow t^2-fire

(a) Smoke Layer temperature   (b) Smoke Layer interface height
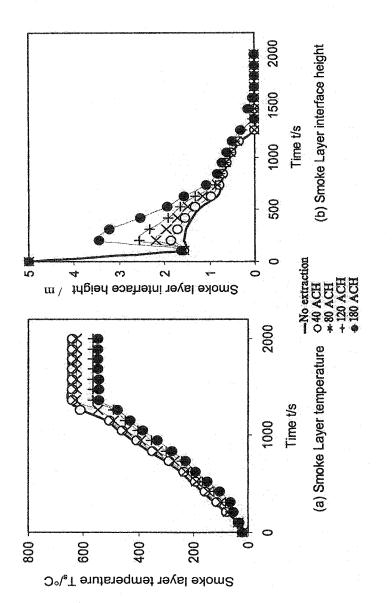
Figure 5-6: Extraction system operated at t_{68} under a slow t^2-fire

(a) Smoke Layer temperature

(b) Smoke Layer interface height

— No extraction
○ 40 ACH
✳ 80 ACH
+ 120 ACH
● 180 ACH
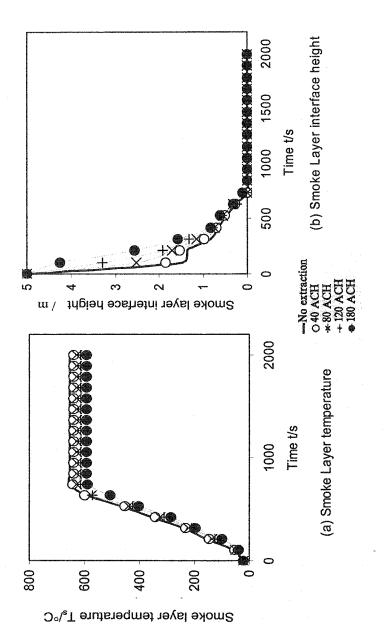
Figure 5-7: Extraction system operated at $t_{0.45}$ under a medium t^2-fire

F-14
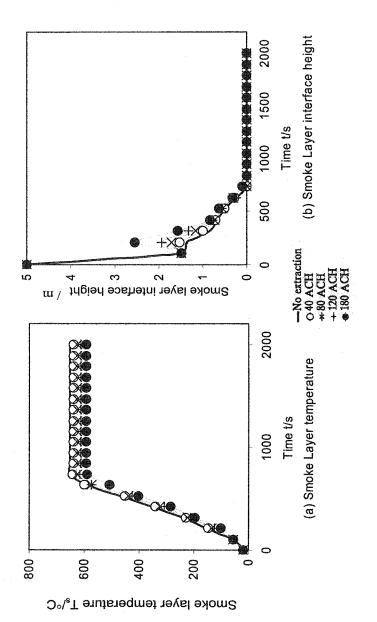
Figure 5-8: Extraction system operated at t_{68} under a medium t^2-fire

(a) Smoke Layer temperature

(b) Smoke Layer interface height

Legend:
— No extraction
○ 40 ACH
✳ 80 ACH
+ 120 ACH
● 180 ACH
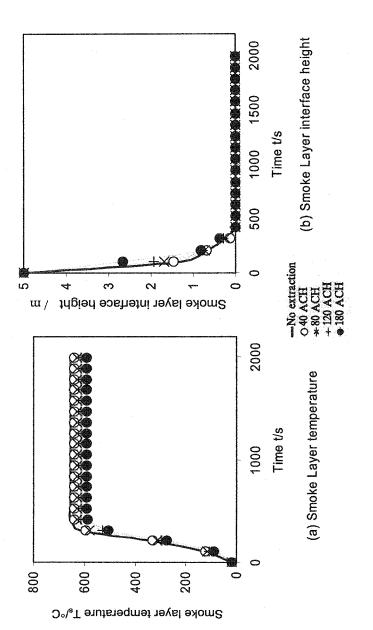
Figure 5-9: Extraction system operated at $t_{0.45}$ under a fast t^2-fire

(a) Smoke Layer temperature

(b) Smoke Layer interface height

Legend:
— No extraction
○ 40 ACH
✳ 80 ACH
+ 120 ACH
● 180 ACH
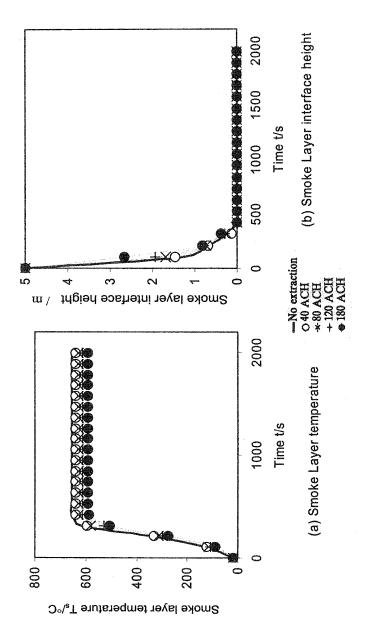
Figure 5-10: Extraction system operated at t_{68} under a fast t^2-fire
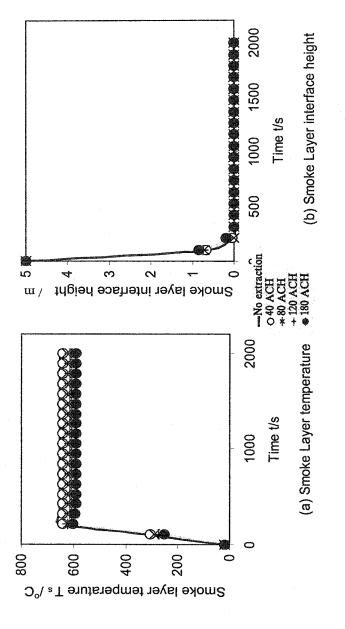
Figure 5-11: Extraction system operated at $t_{0.45}$ under an ultra-fast t^2-fire

(a) Smoke Layer temperature

(b) Smoke Layer interface height
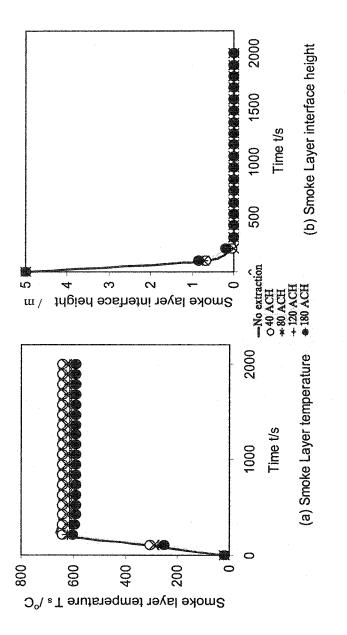
Figure 5-12: Extraction system operated at t_{68} under an ultra-fast t^2-fire
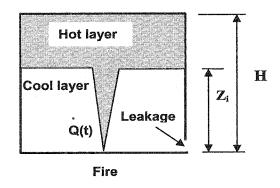
Figure 6-1: ASET zone model

(iii) Smoke layer interface height

(iv) Smoke layer temperature

(b) F2

(i) Smoke layer interface height

(ii) Smoke layer temperature

(a) F1
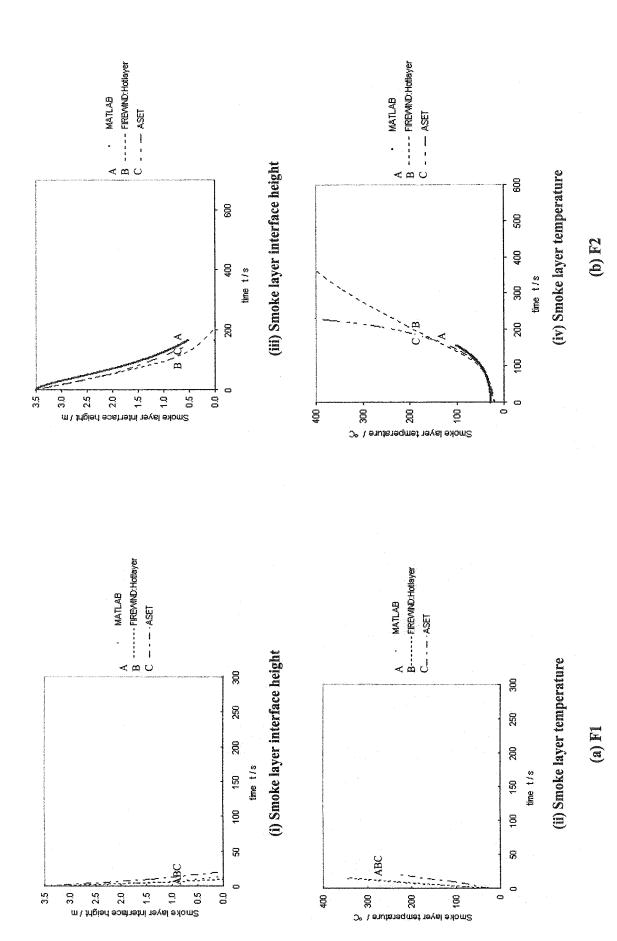
Figure 6-2: Results for room 1
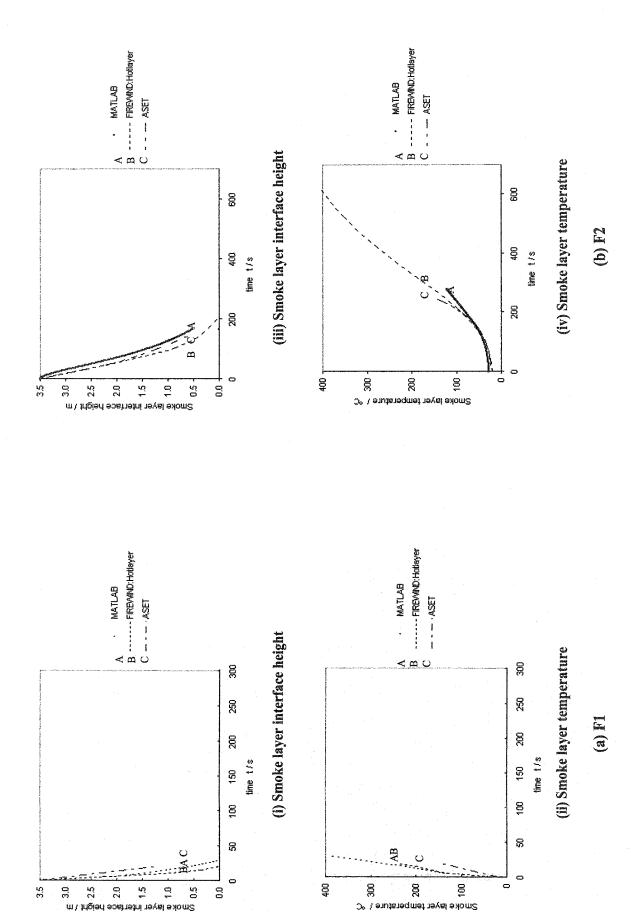
Figure 6-3: Results for room 2

(iii) Smoke layer interface height

(iv) Smoke layer temperature

(b) F2

(i) Smoke layer interface height

(ii) Smoke layer temperature

(a) F1
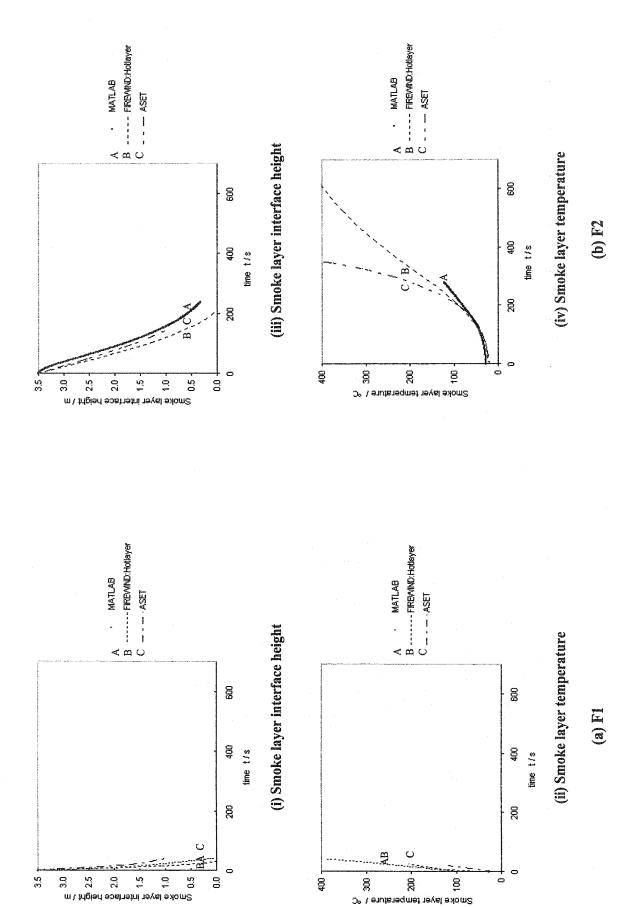
Figure 6-4: Results for room 3

F-23

(iii) Smoke layer interface height

Legend:
A — MATLAB
B — FIREWIND:Hotlayer
C — ASET

Y-axis: Smoke layer interface height / m
X-axis: time t / s

(iv) Smoke layer temperature

Legend:
A — MATLAB
B — FIREWIND:Hotlayer
C — ASET

Y-axis: Smoke layer temperature / °C
X-axis: time t / s

(b) F2

(i) Smoke layer interface height

Legend:
A — MATLAB
B — FIREWIND:Hotlayer
C — ASET

Y-axis: Smoke layer interface height / m
X-axis: time t / s

(ii) Smoke layer temperature

Legend:
A — MATLAB
B — FIREWIND:Hotlayer
C — ASET

Y-axis: Smoke layer temperature / °C
X-axis: time t / s

(a) F1

Figure 6-5: Results for room 4

F-24

(iii) Smoke layer interface height

(iv) Smoke layer temperature

(b) F2

(i) Smoke layer interface height

(ii) Smoke layer temperature

(a) F1
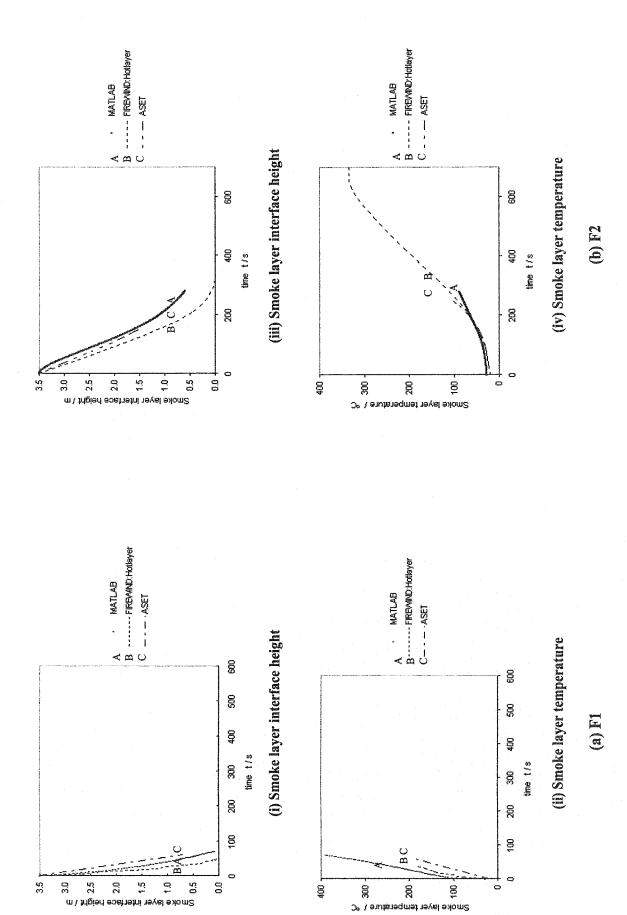
Figure 6-6: Results for room 5

F-25

(iii) Smoke layer interface height

(iv) Smoke layer temperature

(b) F2

(i) Smoke layer interface height

(ii) Smoke layer temperature

(a) F1
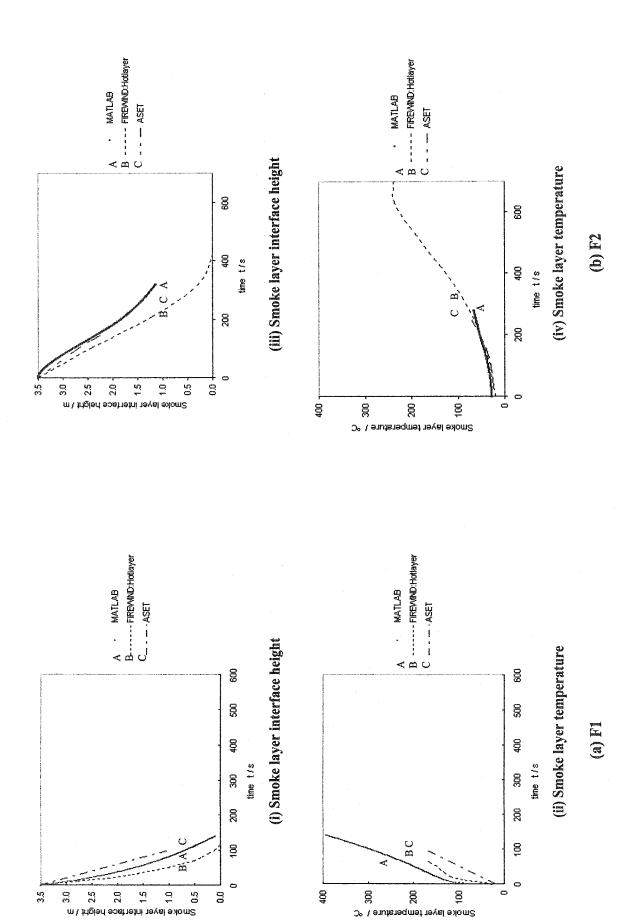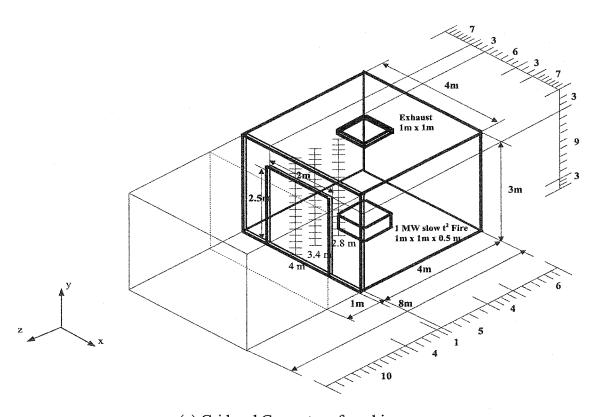
Figure 6-7: Results for room 6

F-26

(a) Grid and Geometry of a cabin

(b) Side view of a cabin
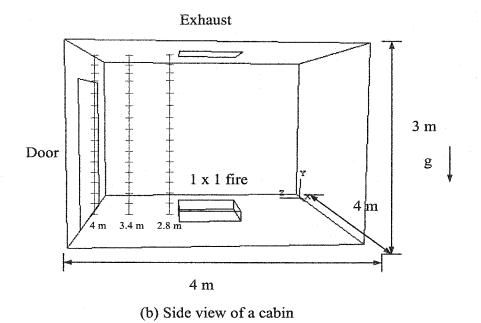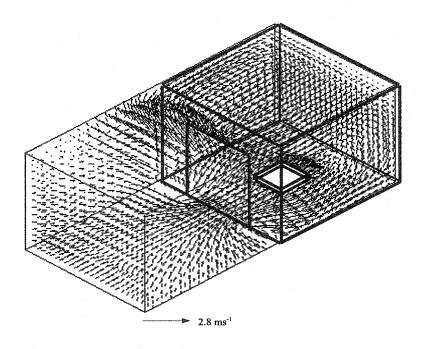
Figure 7-1: Geometry of a cabin

(a) Simulation A

(b) Simulation B
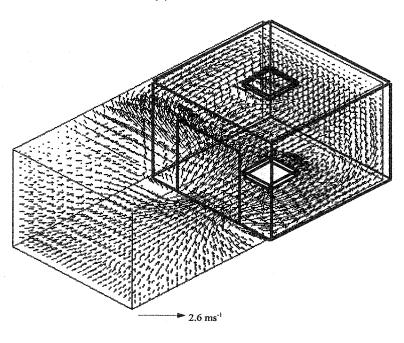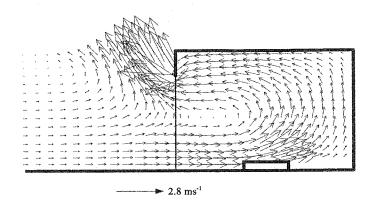
Figure 7-2: Geometry of cabin and vector velocity

(a) Simulation A

(b) Simulation B
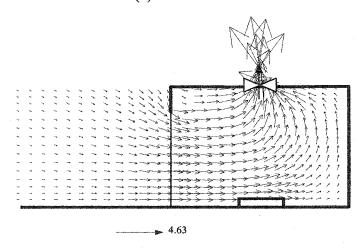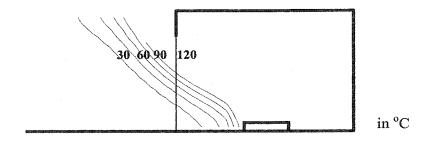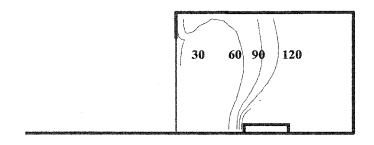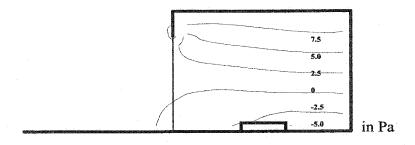
Figure 7-3: Velocity vector across the central plane at x = 2 m

(a) Simulation A

(b) Simulation B

Figure 7-4: Temperature distributions across the central plane at x = 2 m

(a) Simulation A

(b) Simulation B
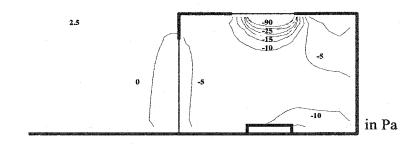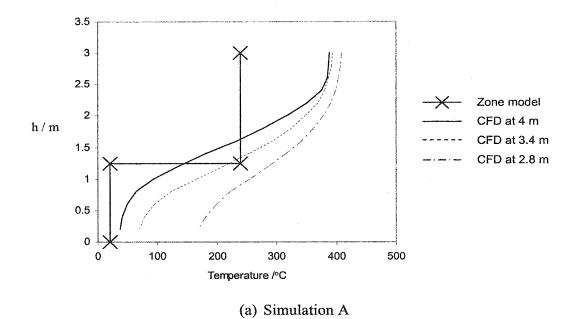
Figure 7-5: Pressure distribution across the central plane at x = 2 m

(a) Simulation A

(b) Simulation B
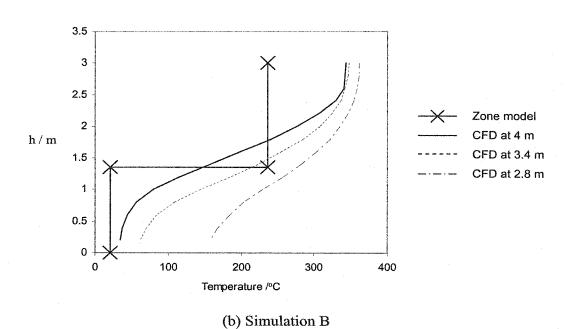
Figure 7-6: Air temperature and hot layer height in CFD and zone model

(a) Simulation A

(b) Simulation B
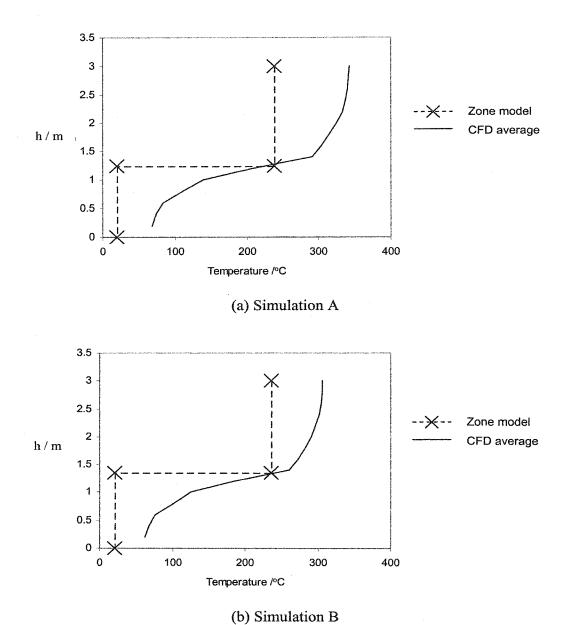
Figure 7-7: Average ventilation temperature profile of CFD modeling
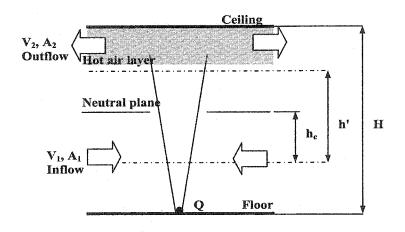
Figure 8-1: Geometry of model 1
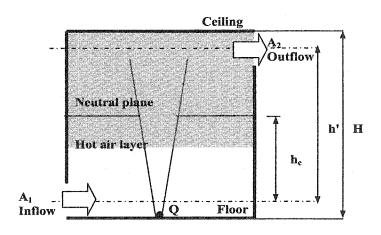
Figure 8-2: Geometry of model 2
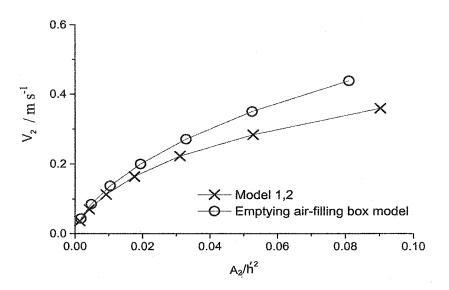
Figure 8-3: Outlet ventilation flow rates
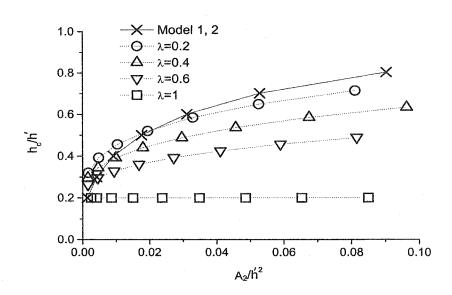
Figure 8-4: Neutral plane height for $\gamma = 0.2$
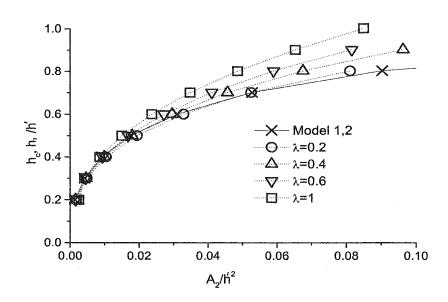
Figure 8-5: Neutral plane height (h_c/h') of model 1 and model 2 with the hot air layer height (h_1/h') of emptying air-filling box model
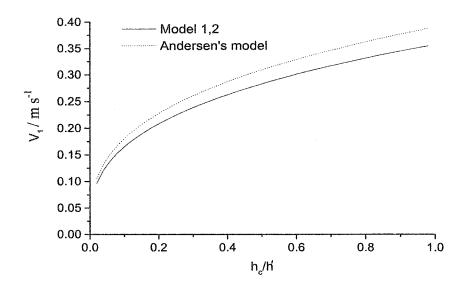
Figure 8-6: Inlet airflow rates
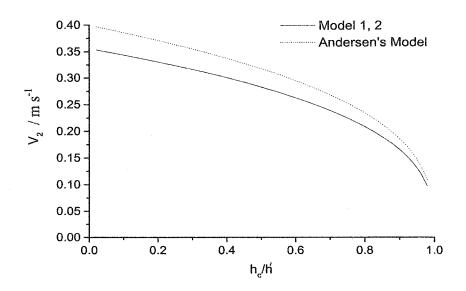
Figure 8-7: Outlet airflow rates
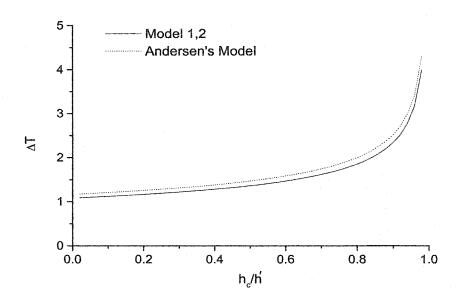
Figure 8-8: Temperature difference
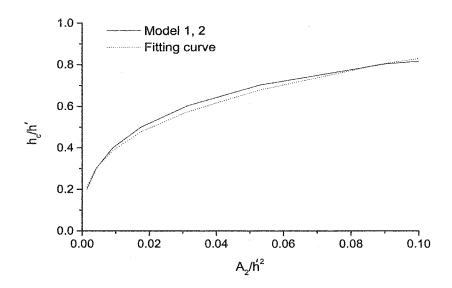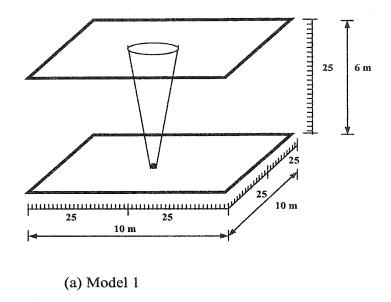
Figure 8-9: Fitting of the neutral plane equation

(a) Model 1

(b) Model 2
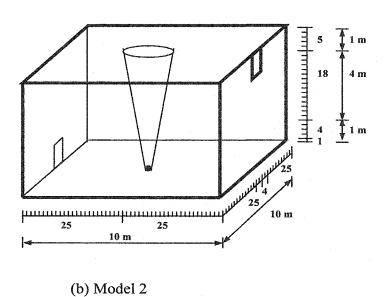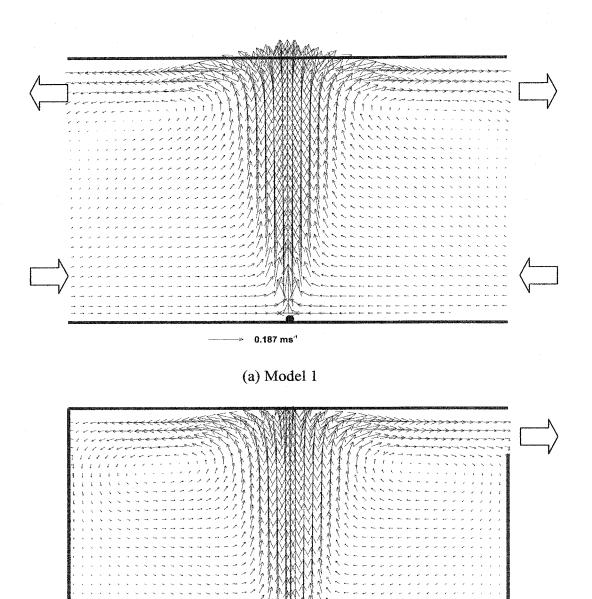
Figure 8-10: Geometry and grid of the CFD simulation

(a) Model 1

(b) Model 2

Figure 8-11: Vector results in CFD simulation

0.14

0.7

0.035

0

-0.035

in Pa

-0.07

(a) Model 1

0.15

0.07

0

-0.07

-0.15

(b) Model 2
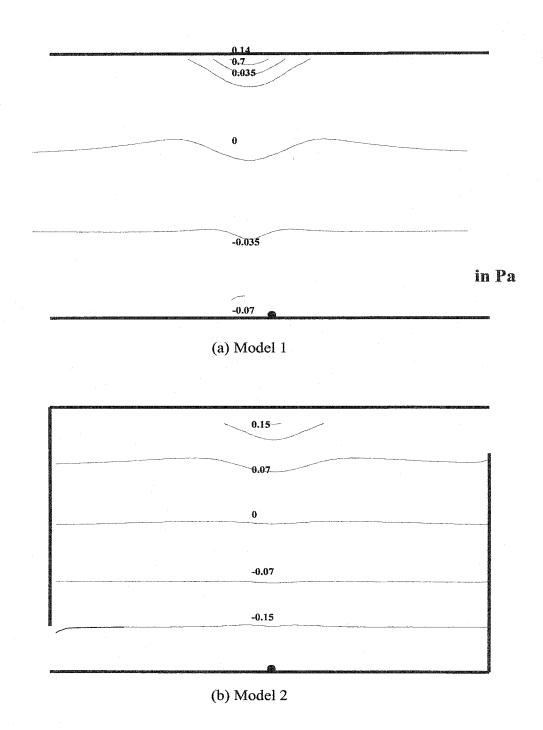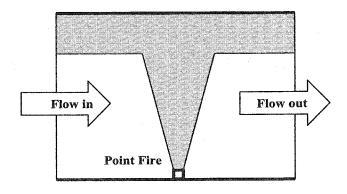
Figure 8-12: Pressure distribution results in CFD simulation

(a) Parallel flow model

(b) Jet flow model
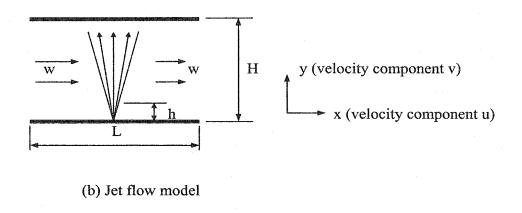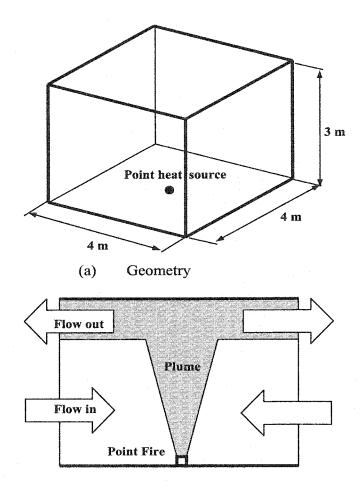
Figure 9-1: The two flow models in a chamber

(a)   Geometry

(b)   Thermally-induced flow under natural ventilation

Figure 9-2: Chamber under natural ventilation
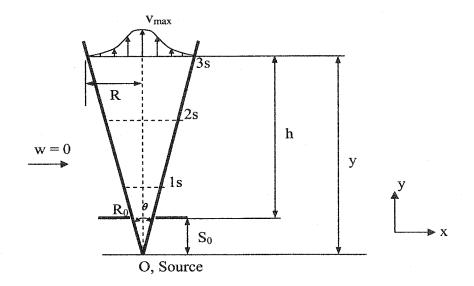
Figure 9-3: Typical plume model

(a) Case 1

(b) Case 2

(c) Case 3

(d) Case 4
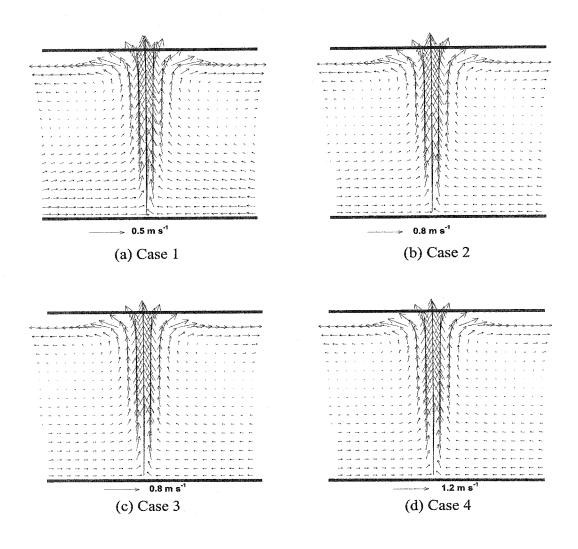
Figure 9-4: Velocity distribution in central plane

(a) Case 1

(b) Case 2

(c) Case 3

(d) Case 4
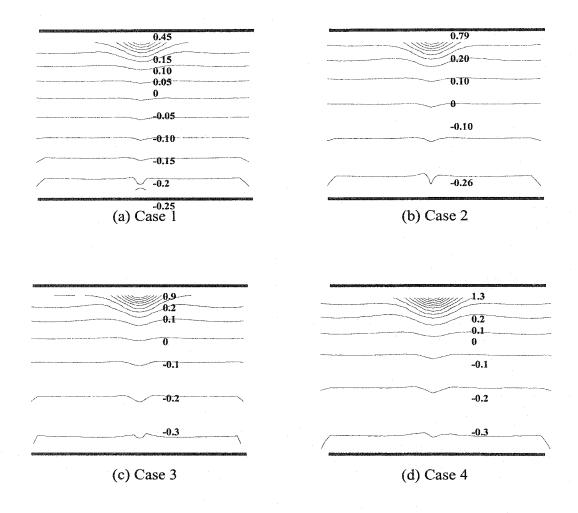
Figure 9-5: Pressure distribution in central plane (in Pa)

(a) Case 1

(b) Case 2

(c) Case 3

(d) Case 4
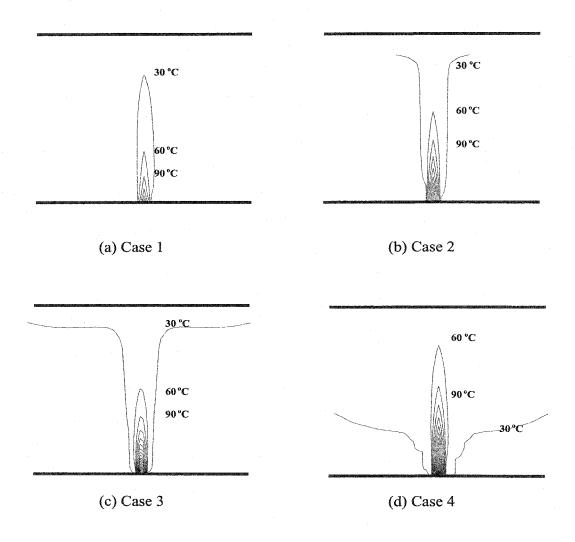
Figure 9-6: Temperature distribution in central plane
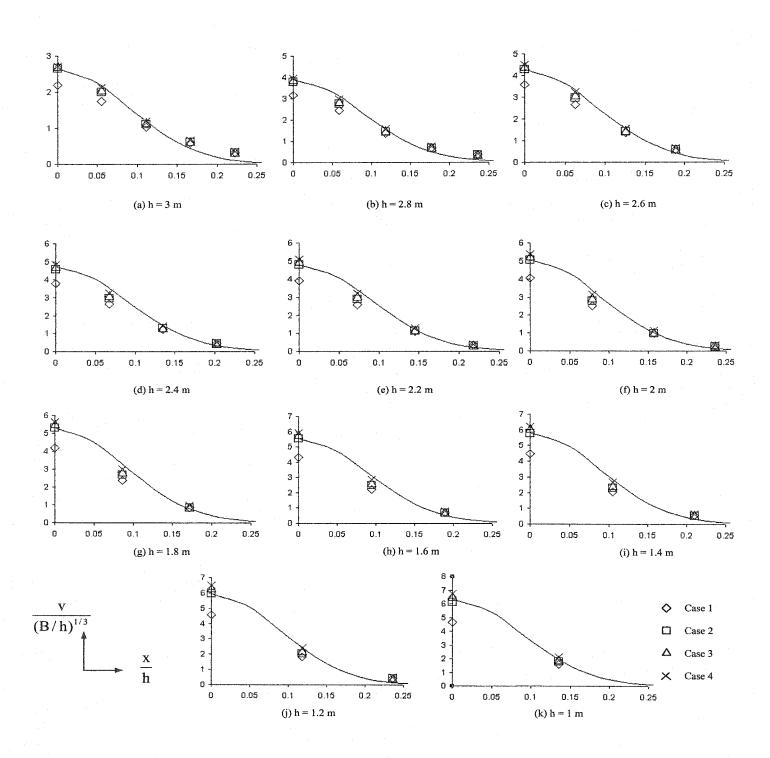
Figure 9-7: Relationship between vertical velocity of plume v and plume radius in each layer of different height
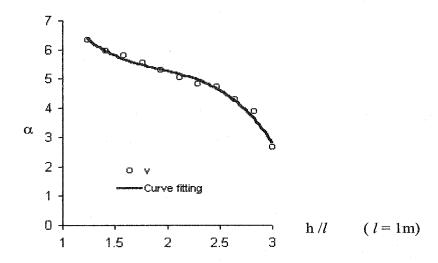
Figure 9-8: Probability distribution of height coefficient α, correlation coefficient r² = 0.9859
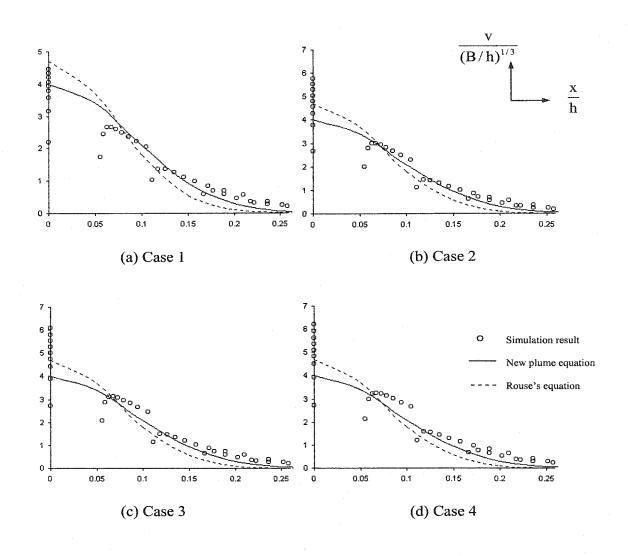
Figure 9-9: Comparison of plume equations with Rouse's equation
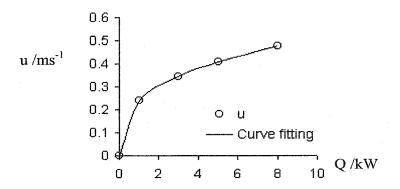
Figure 9-10: Relationship between horizontal velocity of plume edge u and heat release rate Q
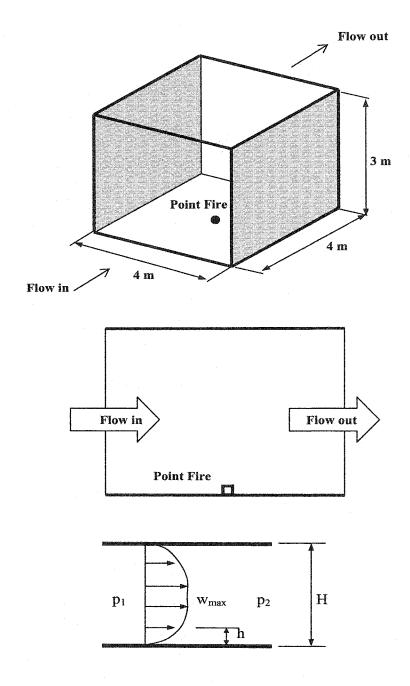
Figure 9-11: Parallel flow model

(a) w = 0.05 m s^{-1}

(b) w = 0.1 m s^{-1}

(c) w = 0.5 m s^{-1}
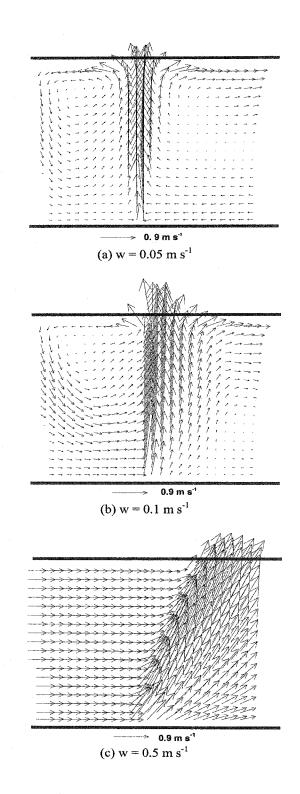
Figure 9-12: Air flow under forced ventilation with three different air flow speeds for 5 kW fire
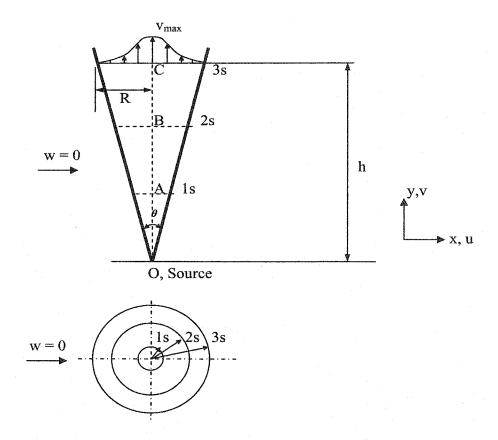
Figure 9-13: Situation of plume without any forced ventilation (the speed of parallel flow w is zero)
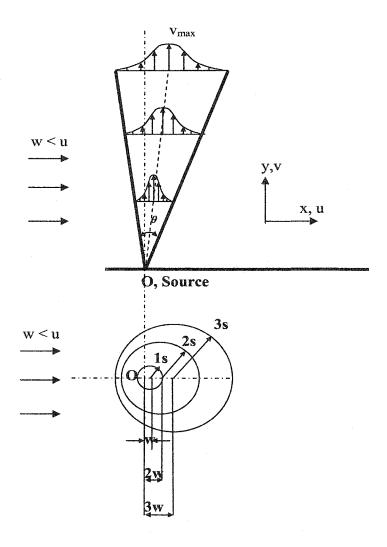
Figure 9-14: Situation of plume when the speed of parallel flow w is less than the horizontal velocity of plume edge u
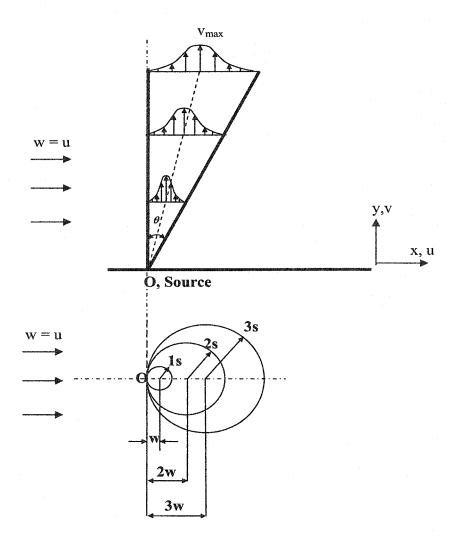
Figure 9-15: Situation of plume when the speed of parallel flow w is equal to the horizontal velocity of plume edge u
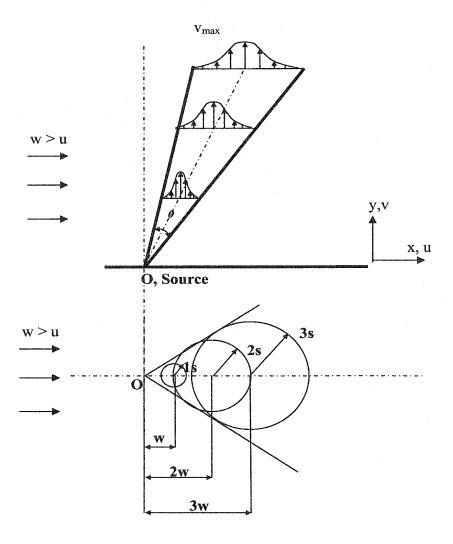
Figure 9-16: Situation of plume when the speed of parallel flow w is greater than the horizontal velocity of plume edge u
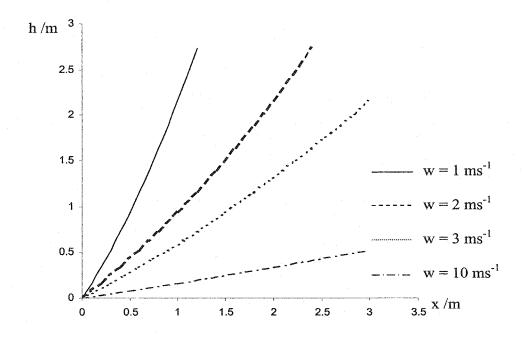
Figure 9-17: Comparison of the plume central axis position with different velocity of parallel flow
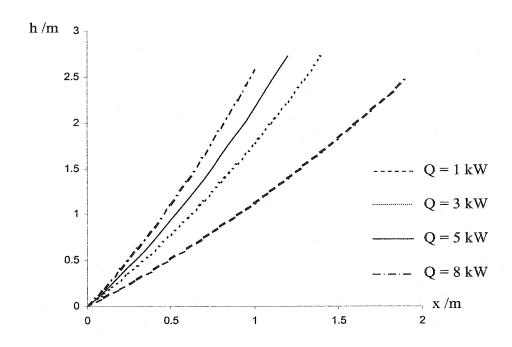
Figure 9-18: Comparison of the plume central axis position with different heat release rate of fire
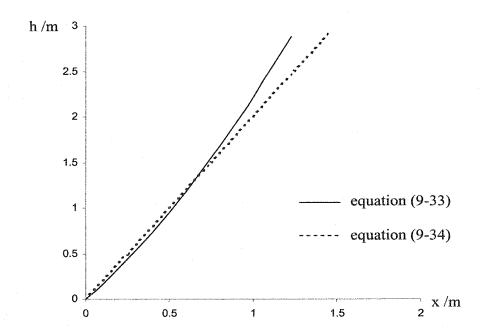
Figure 9-19: Comparison of the plume central axis position in the example calculation

LIST OF TABLES

Issued by	Classified by legal effects	Classified by contents
National People's Congress	Legislative Fire Code	Administrative Fire Code
	• Fire Law of China • Penal Law of China • Punishment Regulation • Administrative Procedural Law • City Planning Law, etc.	
• State Council • Ministry of Public Security • Other Ministries (e.g. Ministry of Construction) • Local governments	Administrative Fire Code	Fire Code of Management and Administration
	• Building Fire Administrative Regulation, etc.	
• Ministry of Public Security • Ministry of Construction • Local governments	Local Fire Code	Technical Law
	• City Planning Regulations • Design code for residential buildings • Code for fire protection design of buildings, etc.	

Table 2-1: Classification of fire codes in China

NFPA code		China code	
Classification	Notes	Fireproof class	Notes
Low hazard	Low combustibility that no self-propagation fire therein can occur.	I, II	Reinforced concrete floor, roof and wall, or steel structure frame.
Ordinary hazard	Those likely to burn with moderate rapidity or to give off a considerable volume of smoke.	III	Wood roof, reinforced concrete floor and brick wall.
High hazard	Likely to burn with extreme rapidity or from which explosions are likely.	IV	Noncombustible firewall only, with difficult combustible or combustible components.

Table 2-2: Classification of fire hazard (GBJ-16-87, 1995)

China Code			
	Capacity requirements (m/100person) (cm/person)		
Fireproof class	I, II	III	IV
Stories 1, 2	0.65	0.75	1.00
Stories 3	0.75	1.00	-
Stories 4	1.00	1.25	-

Table 2-3: Egress capacity for approved components of means of egress in China Code (GBJ-16-87, 1995)

NFPA Code		
Use	Stairways (cm/person)	Level components and ramps (cm/person)
Board and care	1.0	0.5
Health care sprinkled	0.8	0.5
Health care nonsprinkled	1.5	1.3
High hazard contents	1.8	1.0
All others	0.8	0.5

Table 2-4: Egress capacity for approved components of means of egress in NFPA Code

Table 2-5: Comparison of travel distance limits

NFPA Code

Type of occupancy		Travel Distance Limit	
		Unsprinkled (m)	Sprinkled (m)
Educational		45	60
Health care		45	60
Assembly		45	60
Detention and correctional		45	60
Residential		53	99
Mercantile		30	60
Business		60	91
Industrial		60	75
Storage	Low hazard	N.R.	N.R.
	Ordinary hazard	60	122
	High hazard	23	23

China Code

Type of occupancy	Maximum distance from room door to exit or stairs					
	Rooms between two Exits/Stairs			Rooms on the side/End of a U type corridor		
	Fireproof Class			Fireproof Class		
	I, II	III	IV	I, II	III	IV
School	35	30	-	22	20	-
Hospital, sanatorium	35	30	20	15	-	-
Child-care, nursery	25	20	-	20	15	-
Others	40	35	25	22	20	15

Hong Kong Code

Type of occupancy	Type of exit route	Max. travel distance	Max. sum of the direct distance and travel distance
Offices, schools and shops	A	36 m	45 m
	B	24 m	36 m
	C	30 m	30 m
All other cases	A	30 m	36 m
	B	24 m	36 m
	C	30 m	30 m

Notes:
(A) exit route along balcony approach or internal corridor with ventilation and complying

(B) exit route along internal corridor without ventilation and complying

(C) story partitioned into rooms but exit route is not along balcony approach or internal corridor which complies with the requirements of the code of Practice for Fire Resisting Construction.

NFPA Code				China Code					
No. of seats	Flow time (sec)	Clear width per seat served (cm)		Type of building	Width index (m/100 person)				
		Stairs	Passageways, ramps, Doorways		No. of seats	Fireproof class	Doors and corridors		Stairs
							Ramp	Stairs	
≤1200				Theater	≤1200	III	0.85	1.00	1.00
2,000	200	0.762 AB	0.5588 C	Cinema	≤2500	I, II	0.65	0.75	0.75
5,000	260	0.508 AB	0.381 C		3000-5000	I, II	0.43	0.50	0.50
10,000	360	0.3302 AB	0.254 C		5001-10000	I, II	0.37	0.43	0.43
15,000	460	0.24384 AB	0.1778 C	Gymnasium	10001-20000	I, II	0.50	0.43	0.37
20,000	560	0.19304 AB	0.14224 C		-	-	-	-	-
25,000 / more	660	0.1542 AB	0.11176 C						

A=1+(riser height − 17.78cm) / 5 cm
B=3.175 cm
C=2.794

Table 2-6: Comparison of width requirements on assembly occupancies

NFPA Code

Type of occupancy	Width requirements (m)	Exit number (No.)
Educational	1.8	2
Health care	1.22	2
Hotel	1.12	2
Apartment	1.12	2
Lodging	0.71	2
Family	1	1
Mercantile	1.5	2
Business	1.12	

China Code

Type of occupancy	Minimum width requirements (m)	Exit number (No.)
School	1~1.1	2
Hospital	1~1.1	2
Others	1	2

Hong Kong Code

Capacity of room or story	Min. no. of exit doors	Min. Total Width of		Min. width of each	
		Exit doors (m)	Exit routes (m)	Exit door (m)	Exit route (m)
4-30	1			0.75	1.05
31-200	2	1.75	2.10	0.85	1.05
201-300	2	2.50	2.50	1.05	1.05
301-500	2	3.00	3.00	1.05	1.05
501-750	3	4.50	4.50	1.20	1.20
751-1000	4	6.00	6.00	1.20	1.20
1001-1250	5	7.50	7.50	1.35	1.35
1251-1500	6	9.00	9.00	1.35	1.35
Over 1500	7 or greater	0.3 m per 50 persons		1.50	1.50

Table 2-7: Comparison of requirements of width and exit of common buildings

China code		US code	
Class	Feature of danger	Class	Note
A	Use or Product 1. Liquids, flash point <28°C. 2. Gas, lower limits < 10%. 3. Self-resolve under normal temperature, combustion or explosion when exposed to the air. 4. Matters product combustible or explosive gases when meet water or vapor under normal temperature. 5. Combustible minerals when accept acid heating, hitting, rubbing, catalyzed or organic compounds. Strong oxidants. 6. Combustible or explosive matters when accept hitting, rubbing, oxidant or organic compounds. 7. Operative temperature equals or exceeds self-ignite point in airtight can.	High hazard industrial occupancy	Occupancies where gasoline and other flammable liquids are handled, used or stored under such conditions as to involve possible release of flammable vapors; where grain, dust, wood flour or plastic dusts, aluminum or magnesium dust or other explosive dusts may be produced; where hazardous chemicals or explosives are manufactured, stored or handled; where cotton or other combustible fibers are processed or handled under conditions such as to produce flammable flings; and other similar hazard.
B	Use or Product 1. Liquids, flash point between 28 °C and 60 °C 2. Gas, lower limits over 10%. 3. Oxidants not included in type A. 4. Chemical combustible solids not included in type A. 5. Combust-supporting gases. 6. Pelagic powder, textile and mist drops with flash point equal or over 60 °C which become explosive when mixed with air.		
C	Use or Product 1.Liquids, flash point at 20 °C 2.Combustible solid	Special purpose industrial occupancy	Ordinary and low hazard industrial operations in buildings designed for and suitable only for particular types of operations, characterized by a relatively low density of employee population with much of the area occupied by machinery or equipment

Table 2-8: Comparison of hazard classification of industrial buildings

	Use or Product	
D	1.Machining noncombustible matter under heat or melt condition with radiant heat, spark or flame appears during production. 2.Productions need combustible gas, liquid or solid as fuel. 3. Machining hard-combustion matter under normal temperature.	General industrial occupancy	Ordinary and low hazard industrial operations conducted in buildings of conventional design suitable for various types of industrial processes. Included are multistory buildings where floors are occupied by different tenants or buildings suitable for such occupancy and, therefore, subject to possible use for types of industrial processes with a high density of employee population.
E	Using or machining noncombustible matter under normal temperature.		

Table 2-8 (Cont'd): Comparison of hazard classification of industrial buildings

T-11

Type	Class	Maximum story	Maximum occupied area limited			
			1 floor	2 floor	Multi-floor	Basement
A	1	1 floor except special requirements	4000	3000	-	-
	2		3000	2000	-	-
B	1	No limit	5000	4000	2000	-
	2	6	4000	3000	1500	-
C	1	No limit	No limit	6000	3000	500
	2	No limit	8000	4000	2000	500
	3	2	3000	2000	-	-
Omit	-	-	-	-	-	-

Table 2-9: The requirements on fire class, story number and occupied area for industrial buildings in China code

Fireproof space (m)			
Fireproof class	I, II	III	IV
I,II	6	7	9
III	7	8	10
IV	9	10	12

Table 2-10: Fireproof space between buildings (GBJ-16-87, 1995)

Components of building		Combustion performance and minimum fireproof time (Hours)			
Fireproof class		I	II	III	IV
Wall	Fire wall	NC 4.00	NC 4.00	NC 4.00	NC 4.00
	Supporting wall	NC 2.50	NC 2.50	NC 2.50	DC 2.50
	Non-supporting wall	NC 1.00	NC 1.00	NC 0.50	DC 0.25
	Separate wall	NC 0.75	NC 0.50	NC 0.50	DC 0.25
Column	Multi-story supporting column	NC 3.00	NC 2.50	NC 2.50	DC 0.50
	One story supporting column	NC 2.50	NC 2.00	NC 2.00	C
Roof beam		NC 2.00	NC 1.50	NC 1.00	DC 0.50
Floor		NC 1.50	NC 1.00	NC 0.50	DC 0.25
Roof supporting		NC 1.50	NC 0.50	C	C
Fire stairs		NC 1.50	NC 1.00	NC 1.00	C
Drop roof		NC 0.25	DC 0.025	DC 0.15	C

C- Combustible components
NC-Non-combustible components
DC-Difficult combustible components

Table 2-11: The performance of combustion and the minimum fireproof time (GBJ-16-87, 1995)

Fireproof class	Maximum Stories	Maximum length (m)	Maximum area/story (m^2)	Notes
I, II	9	150	2500	1. The limited length and width on gymnasium and theater can be broadened 2. Playing room in child-care and nursery schools should not higher than 4th floor.
III	5	100	1200	1. Playing rooms in child-care and nursery schools shoulds not higher than 3rd floor. 2. Cinemas, theaters, auditoriums and canteens should not be higher than 2 stories. 3. Hospitals, sanatoriums should not be higher than 3 stories.
IV	2	60	600	Schools, canteens, food markets, hospitals, child-care and nursery schools should not be higher than 1 story.

Table 2-12: The relationships between fireproof class and the area, length and stories of the building (GBJ-16-87, 1995)

Name	Maximum distance from room door to exit or stairs (m)					
	Rooms between two exits/stairs			Rooms on the side/end of a U type corridor		
	Fireproof Class			Fireproof Class		
	I, II	III	IV	I, II	III	IV
Child-care, Nursery	25	20	-	20	15	-
Hospital, Sanatorium	35	30	20	15	-	-
School	35	30	-	22	20	-
Others	40	35	25	22	20	15

Table 2-13: Travel distance requirements on buildings (GBJ-16-87, 1995)

Fireproof Class	No. of stories	Area (m^2)	Number of people
I, II	2-3	400	≤ 100
III	2-3	200	≤ 50
IV	2	200	30

Table 2-14: Requirements of exit permitted to install one stair (GBJ-16-87, 1995)

		Width index (m/100 person)	
Seats (No.)		≤ 2500	≤ 1200
Fireproof class		I, II	III
Doors and corridors	Ramp	0.65	0.85
	Stair	0.75	1.00
Stairs		0.75	1.00

Table 2-15: Width index of theater, cinema, auditorium (GBJ-16-87, 1995)

	Width index (m/100 person)		
Seats (No.)	3000-5000	5001-10000	10001-20000
Fireproof class	I, II	I, II	I, II
Doors and corridors — Ramp	0.43	0.37	0.32
Doors and corridors — Stair	0.50	0.43	0.37
Stairs	0.50	0.43	0.37

Table 2-16: Width index of gymnasium (GBJ-16-87, 1995)

	Width index (m/100 person)		
Fireproof class	I, II	III	IV
1, 2 floor	0.65	0.75	1.00
3 floor	0.75	1.00	-
4 floor	1.00	1.25	-

Table 2-17: Width index of school, shopping mall, office, lounge (GBJ-16-87, 1995)

Classification	Height, stories, volume	Water supply (l/s)	Number of hydrant	Minimum flow rates per hydrant (l/s)
Academic occupations	height≤24m, volume≤10000m^3	10	2	5
	height≤24m, volume>10000m^3	15	3	5
Shopping mall, Educational occupations Nursing room	5001~10000m^3	5	2	2.5
	10001~25000m^3	10	2	5
	>25000m^3	15	3	5
Residential occupations	7~9 stories	5	2	2.5

Table 2-18: The requirements of water supply system indoor (GBJ-16-87, 1995)

	China Code	Hong Kong SAR Code
Type of room	A_c/A_f	
Kitchen, livingroom, bedroom	1/7, and no less than 0.6 m^2 in kitchen, at least 2% of the area of floor for less than 60 m^2.	1/10 floor of room at most 2 m above the floor and no less than 4.5 m wide
Stair case	1/12	

(The window area A_c in a room corresponds with the room floor area A_f)

Table 3-1: Minimum requirements of windows for residential buildings in China design code (GB 50096-1999) and in Hong Kong Buildings Ordinance

China design code for residential buildings		
Type of door	Width of door (m)	Height of door (m)
Corridor	1.2	2.0
Room	0.9	2.0
Living room	0.9	2.0
Bedroom	0.9	2.0
Kitchen	0.8	2.0
Bathroom	0.7	2.0
Balcony	0.7	2.0

Hong Kong Buildings Ordinance		
Type of door	Width of door (m)	Height of door (m)
Corridor	1.05-1.5	2.0
Room	0.75	2.0
Living room	0.75	2.0
Bedroom	0.75	2.0
Kitchen	0.75	2.0
Bathroom	0.75	2.0
Balcony	0.75	2.0

Table 3-2: The requirements on doors for residential buildings in China design code (GB 50096-1999) and in Hong Kong Buildings Ordinance

	Hong Kong SAR Code	China Mainland Code	
	Min. extraction rate	Extraction rate	
Hotel	10 ACH	4-6 ACH	60 m^3/h for each smoke proof zone
Industrial	8 ACH	15-20 ACH	
Basement	8 ACH	8 ACH	
Commercial buildings	8 ACH	8.5 m^3/h per person	

ACH = air changes per hour

Table 3-3: A comparison of minimum forced ventilation requirements for residential buildings in Hong Kong code (Building Department 1997, Fire Services Department 1994) and China code (Ministry of Public Security 1995, GBJ-16-87, 1995)

Type of parking	Type of fire proof (by the number of cars)			
	I	II	III	IV
Enclosure parking	>200	101~200	26~100	≤ 25
Maintain garage	>15	6~15	3~5	≤ 2
Opening parking	>300	201~300	101~200	≤ 100

Table 4-1: Types of fireproof, classified by the number of cars

Components of building		Combustion performance and the Minimum fireproof time (Hours)		
Fire resistant class		A	B	C
Wall	Fire wall	NC 4.00	NC 4.00	NC 4.00
	Supporting wall	NC 3.00	NC 2.50	NC 2.50
	Fire separate wall	NC 2.00	NC 2.00	NC 2.00
	Separate wall	NC 1.00	NC 0.50	NC 0.50
Column	Multi-story supporting column	NC 3.00	NC 2.50	NC 2.50
	One story supporting column	NC 2.50	NC 2.00	NC 2.00
Roof beam		NC 2.00	NC 1.50	NC 1.00
Floor		NC 1.50	NC 1.00	NC 0.50
Fire stairs		NC 1.50	NC 1.00	NC 1.00
Drop roof		NC 0.25	DC 0.25	DC 0.15
Roof supporting		NC 1.50	NC 0.50	C

C-Combustible components, NC-Non-combustible components, DC-Difficult combustible components

Table 4-2: The performance of combustion and the minimum fireproof time for carpark and garage

Type	Fireproof class	Maximum area permitted in carpark(m²)							
		Single story		Ground floor		Multi-story		Underground	
		Area	Fire space	Area	Fire space	Area	Fire space	Area	Fire space
I, II, III	A	N/L	1500	6000	1000	6000	1500	6000	1000
	B	N/L	1000	4000	500	4000	1000	-	-
IV	A	N/L	1500	3000	1000	-	-	3000	1000
	B	N/L	1000	2000	500	-	-	-	-
	C	N/L	200	-	-	-	-	-	-

Table 4-3: Maximum occupied area and fireproof area of carpark

Table 5-1: Flashover time t_f

Cut-off value = 5 MW

Cabin		Openings			Slow t^2-Fire				Medium t^2-Fire				Fast t^2-Fire				Ultra fast t^2-Fire			
					Height of cabin /m				Height of cabin /m				Height of cabin /m				Height of cabin /m			
Length L/m	Width W/m	Number	W_V/m	H_V/m	2 m t_f/s	3 m t_f/s	4 m t_f/s	5 m t_f/s	2 m t_f/s	3 m t_f/s	4 m t_f/s	5 m t_f/s	2 m t_f/s	3 m t_f/s	4 m t_f/s	5 m t_f/s	2 m t_f/s	3 m t_f/s	4 m t_f/s	5 m t_f/s
4	4	4	4x4	1.5	1384	1316	1337	N/F	637	1041	771	N/F	544	490	375	412	188	199	202	209
4	6	4	2x(4+6)	1.5	1771	N/F	N/F	N/F	941	N/F	N/F	N/F	1460	N/F	N/F	N/F	931	N/F	N/F	N/F
4	4	3	3x4	1.5	1199	1217	1230	1264	598	608	616	636	299	305	309	330	211	186	190	196
4	6	3	4+6+4	1.5	1328	1357	N/F	N/F	697	727	N/F	N/F	382	413	N/F	N/F	205	209	N/F	N/F
4	4	2	2x4	1.5	1103	1121	1129	1161	553	562	569	584	277	282	287	295	513	168	174	180
4	6	2	4+6	1.5	1237	1258	1280	1322	618	629	651	693	309	316	342	383	190	194	199	205
4	4	1	4	1.5	952	966	975	997	478	486	491	504	244	251	253	257	283	145	142	148
4	6		4	1.5	1044	1060	1070	1103	524	532	537	547	269	273	277	288	141	156	159	371
4	8		4	1.5	1130	1146	1162	1196	566	575	585	601	289	294	300	308	173	175	178	182
4	10		4	1.5	1206	1222	1245	1283	603	611	624	657	306	311	328	368	185	189	192	202
6	6		6	1.5	1245	1266	1294	1333	622	635	665	705	316	349	376	412	192	196	202	207
4	4		2	2.5	-	1067	1074	1117	-	538	541	552	-	267	270	284	-	156	159	161
4	6		2	2.5	-	1149	1169	1185	-	573	576	581	-	288	288	294	-	173	176	178
4	8		2	2.5	-	1216	1222	1254	-	608	613	646	-	306	314	334	-	187	188	193
4	10		2	2.5	-	1294	1310	1321	-	660	678	693	-	350	370	381	-	199	201	201
6	6		2	2.5	-	1248	1280	1298	-	627	652	667	-	314	339	358	-	193	195	198
6	8		2	2.5	-	1360	1364	1362	-	730	731	733	-	413	499	419	-	210	394	309
4	4	2	2	2.5	-	1346	N/F	N/F	-	717	N/F	N/F	-	1043	N/F	N/F	-	207	N/F	N/F
4	4	1	2	2	-	951	957	970	-	476	478	499	-	241	243	245	-	135	139	143
4	6		2	2	-	1039	1053	1075	-	522	528	540	-	262	264	267	-	152	156	161
4	8		2	2	-	1114	1118	1135	-	559	565	574	-	281	283	284	-	168	172	177
4	10		2	2	-	1186	1203	1211	-	593	596	599	-	298	299	308	-	183	186	189

Table 5-1 (cont'd): Flashover time t_f

Cabin		Openings			Slow t^2-Fire				Medium t^2-Fire				Fast t^2-Fire				Ultra fast t^2-Fire			
					Height of cabin /m				Height of cabin /m				Height of cabin /m				Height of cabin /m			
Length L/m	Width W/m	Number	W_V/m	H_V/m	2 m t_f/s	3 m t_f/s	4 m t_f/s	5 m t_f/s	2 m t_f/s	3 m t_f/s	4 m t_f/s	5 m t_f/s	2 m t_f/s	3 m t_f/s	4 m t_f/s	5 m t_f/s	2 m t_f/s	3 m t_f/s	4 m t_f/s	5 m t_f/s
6	6	1	2	2	-	1149	1174	1190	-	576	579	585	-	290	291	293	-	176	180	184
6	8		2	2	-	1248	1251	1251	-	624	624	625	-	314	343	360	-	194	197	199
6	10		2	2	-	1359	1361	1360	-	728	732	732	-	414	420	451	-	210	210	210
4	4		1.5	2	-	880	884	889	-	442	446	451	-	224	228	231	-	121	126	131
4	6		1.5	2	-	970	977	990	-	486	489	490	-	246	249	252	-	140	145	152
4	8	1	1.5	2	-	1043	1045	1045	-	524	526	548	-	266	268	271	-	157	162	169
4	10		1.5	2	-	1119	1125	1131	-	563	568	575	-	283	285	288	-	172	177	182
6	6		1.5	2	-	1080	1082	1107	-	546	553	562	-	275	278	280	-	164	170	176
6	8		1.5	2	-	1184	1186	1210	-	595	598	602	-	299	301	302	-	184	189	192
6	10		1.5	2	-	1283	1285	1285	-	653	656	681	-	344	369	380	-	201	203	204
8	8		1.5	2	-	1321	1321	1342	-	691	700	712	-	384	394	399	-	205	206	209
4	4	2	2	2.5	-	1146	1155	1187	-	574	582	596	-	288	293	301	-	309	178	184
4	6		2	2.5	-	1225	1242	1277	-	613	622	649	-	307	312	343	-	188	194	199
4	8		2	2.5	-	1309	1338	N/F	-	678	708	N/F	-	365	395	N/F	-	202	207	N/F

* N/F: No flashover.

Table 5-1 (cont'd): Flashover time t_f

Cut-off value = 7.5 MW

Cabin		Openings			Slow t²-Fire Height of cabin /m				Medium t²-Fire Height of cabin /m				Fast t²-Fire Height of cabin /m				Ultra fast t²-Fire Height of cabin /m			
Length L/m	Width W/m	Number	W_V/m	H_V/m	2 m t_f/s	3 m t_f/s	4 m t_f/s	5 m t_f/s	2 m t_f/s	3 m t_f/s	4 m t_f/s	5 m t_f/s	2 m t_f/s	3 m t_f/s	4 m t_f/s	5 m t_f/s	2 m t_f/s	3 m t_f/s	4 m t_f/s	5 m t_f/s
4	4		4x4	1.5	1350	1278	1301	1337	633	644	655	672	493	565	456	341	165	256	171	175
4	6		2x(4+6)	1.5	1403	1419	1448	1482	698	712	727	747	351	363	370	380	179	183	187	192
4	8	4	2x(4+8)	1.5	1503	1540	1573	1624	1025	780	799	818	383	394	402	411	192	198	202	207
4	10		2x(4+10)	1.5	1615	N/F	N/F	N/F	815	N/F	N/F	N/F	409	N/F	N/F	N/F	205	N/F	N/F	N/F
6	6		4x6	1.5	1536	1578	1629	N/F	777	802	820	839	392	404	411	420	196	202	207	211
4	4	4	4x4	2	1605	N/F	N/F	N/F	830	N/F	N/F	N/F	416	N/F	N/F	N/F	207	N/F	N/F	N/F

* N/F: No flashover.

Table 5-2: Operation time of the smoke extraction system

t^2-fire	Range of $t_{0.45}$/s	Range of corresponding smoke layer temperature/°C	Range of corresponding smoke layer interface height/m	Range of t_{68}/s	Corresponding smoke layer temperature/°C	Range of corresponding smoke layer interface height/m
Slow	12 to 76	21 to 49	1.55 to 4.55, giving a smoke layer thickness of 0.45 m	112 to 267	68	0.75 to 1.92
Medium	9 to 74	18 to 83		51 to 161	68	1.0 to 4.30
Fast	11 to 68	26 to 131		25 to 104	68	1.18 to 4.02
Ultra-fast	10 to 49	35 to 159		12 to 31	68	1.80 to 4.44

Table 5-3: Flashover time t_f with smoke extraction system

Length L/m	Width W/m	Number	W_v/m	H_v/m	t²-fire	No smoke extraction (2 m)	\$t_{0.45}\$ 40	80	120	180	\$t_{68}\$ 40	80	120	180	No smoke extraction (3 m)	\$t_{0.45}\$ 40	80	120	180	\$t_{68}\$ 40	80	120	180
4	4	4	4x4	1.5	Slow	1384	1281	1309	1382	1311	1281	1309	1382	1311	1316	1297	1304	1334	1350	1297	1304	1334	1350
					Medium	637	667	694	655	664	667	694	655	664	1041	666	678	691	719	666	678	691	719
					Fast	544	317	354	559	710	317	354	559	710	490	483	369	383	403	483	369	383	403
					Ultrafast	188	190	196	196	199	190	196	196	199	199	200	202	204	207	200	202	204	207
6	4	4	2x(4+6)	1.5	Slow	1771	N/F	N/F	N/F	N/F	N/F	N/F	N/F	N/F	N/F	N/F	N/F	N/F	N/F	N/F	N/F	N/F	N/F
					Medium	941	N/F	N/F	N/F	N/F	N/F	N/F	N/F	N/F	N/F	N/F	N/F	N/F	N/F	N/F	N/F	N/F	N/F
					Fast	1460	N/F	N/F	N/F	N/F	N/F	N/F	N/F	N/F	N/F	N/F	N/F	N/F	N/F	N/F	N/F	N/F	N/F
					Ultrafast	931	N/F	N/F	N/F	N/F	N/F	N/F	N/F	N/F	N/F	N/F	N/F	N/F	N/F	N/F	N/F	N/F	N/F
4	4	3	3x4	1.5	Slow	1199	1205	1213	1219	1230	1205	1213	1219	1230	1217	1228	1239	1249	1267	1228	1239	1249	1267
					Medium	598	602	606	609	614	602	606	609	614	608	614	619	624	636	614	619	624	636
					Fast	299	301	303	305	307	301	303	305	307	305	307	310	313	324	307	310	313	324
					Ultrafast	211	194	191	189	129	194	191	189	129	186	188	190	192	195	188	190	192	195
6	4	3	4+6+4	1.5	Slow	1328	1340	1352	1364	N/F	1340	1352	1364	N/F	1357	N/F	N/F	N/F	N/F	N/F	N/F	N/F	N/F
					Medium	697	709	722	734	N/F	709	722	734	N/F	727	N/F	N/F	N/F	N/F	N/F	N/F	N/F	N/F
					Fast	382	394	407	419	N/F	394	407	419	N/F	413	N/F	N/F	N/F	N/F	N/F	N/F	N/F	N/F
					Ultrafast	205	206	208	210	N/F	206	208	210	N/F	209	N/F	N/F	N/F	N/F	N/F	N/F	N/F	N/F
4	4	2	2x4	1.5	Slow	1103	1111	1120	1129	1141	1111	1120	1129	1141	1121	1133	1146	1159	1178	1133	1146	1159	1178
					Medium	553	557	561	565	572	557	561	565	572	562	568	574	581	590	568	574	581	590
					Fast	277	279	281	283	286	279	281	283	286	282	285	288	291	296	285	288	291	296
					Ultrafast	513	433	149	158	173	433	149	158	173	168	171	173	175	179	171	173	175	179
6	4	2	4+6	1.5	Slow	1237	1247	1258	1271	1292	1247	1258	1271	1292	1258	1278	1299	1320	1351	1278	1299	1320	1351
					Medium	618	623	628	638	660	623	628	638	660	629	648	669	690	721	648	669	690	721
					Fast	309	311	314	323	345	311	314	323	345	316	336	356	376	406	336	356	376	406
					Ultrafast	190	192	194	196	199	192	194	196	199	194	197	200	203	208	197	200	203	208
4	4	1	4	1.5	Slow	952	962	973	984	1000	962	973	984	1000	966	982	998	1014	1038	982	998	1014	1038
					Medium	478	484	489	494	502	484	489	494	502	486	494	502	510	521	494	502	510	521
					Fast	244	250	247	252	255	250	247	252	255	251	250	254	257	263	250	254	257	263
					Ultrafast	283	145	157	255	138	145	157	255	138	145	474	142	232	153	474	142	232	153
6	4	1	4	1.5	Slow	1044	1059	1074	1088	1111	1059	1074	1088	1111	1060	1082	1104	1126	1155	1082	1104	1126	1155
					Medium	524	531	539	546	557	531	539	546	557	532	543	554	565	581	543	554	565	581
					Fast	269	268	271	275	280	268	271	275	280	273	274	279	285	293	274	279	285	293

Note: The "2 m" and "3 m" super-headers each contain "No smoke extraction", "Smoke extraction operated at \$t_{0.45}\$" (40, 80, 120, 180) and "Smoke extraction operated at \$t_{68}\$" (40, 80, 120, 180).

Table 5-3 (cont'd): Flashover time t_f with smoke extraction system

Cabin Length L/m	Width W/m	Openings Number	Wv/m	Hv/m	t²-fire	2 m No smoke extr.	2 m t0.45 40	80	120	180	2 m t48 40	80	120	180	3 m No smoke extr.	3 m t0.45 40	80	120	180	3 m t48 40	80	120	180
					Ultrafast	141	145	162	170	167	145	162	170	167	156	162	168	172	177	162	168	172	177
8	4	1	4	1.5	Slow	1130	1147	1165	1183	1209	1147	1165	1183	1209	1146	1172	1199	1225	1267	1172	1199	1225	1267
					Medium	566	575	583	592	605	575	583	592	605	575	588	600	613	636	588	600	613	636
					Fast	289	289	293	297	303	289	293	297	303	294	296	302	308	325	296	302	308	325
					Ultrafast	173	175	178	181	188	175	178	181	188	175	180	185	190	197	180	185	190	197
10	4	1	4	1.5	Slow	1206	1226	1246	1268	1309	1226	1246	1268	1309	1222	1252	1290	1330	N/F	1252	1290	1330	N/F
					Medium	603	613	622	636	678	613	622	636	678	611	626	660	700	733	626	660	700	733
					Fast	306	307	311	321	363	307	311	321	363	311	314	349	387	418	314	349	387	418
					Ultrafast	185	189	193	197	203	189	193	197	203	189	195	201	206	210	195	201	206	210
6	6		6	1.5	Slow	1245	1262	1284	1306	1339	1262	1284	1306	1339	1266	1298	1331	1363	N/F	1298	1331	1363	N/F
					Medium	622	630	652	674	708	630	652	674	708	635	668	701	733	N/F	668	701	733	N/F
					Fast	316	315	337	359	393	315	337	359	393	349	356	387	418	N/F	356	387	418	N/F
					Ultrafast	192	195	198	202	206	195	198	202	206	196	201	205	210	N/F	201	205	210	N/F
4	4		2	2.5	Slow	-	-	-	-	-	-	-	-	-	1067	1082	1101	1117	1140	1082	1101	1117	1140
					Medium	-	-	-	-	-	-	-	-	-	538	550	548	560	570	550	548	560	570
					Fast	-	-	-	-	-	-	-	-	-	267	273	276	279	285	273	276	279	285
					Ultrafast	-	-	-	-	-	-	-	-	-	156	159	163	165	172	159	163	165	172
6	4		2	2.5	Slow	-	-	-	-	-	-	-	-	-	1149	1170	1190	1210	1246	1170	1190	1210	1246
					Medium	-	-	-	-	-	-	-	-	-	573	584	594	604	622	584	594	604	622
					Fast	-	-	-	-	-	-	-	-	-	288	293	298	304	312	293	298	304	312
					Ultrafast	-	-	-	-	-	-	-	-	-	173	178	183	187	192	178	183	187	192
8	4		2	2.5	Slow	-	-	-	-	-	-	-	-	-	1216	1241	1280	1309	1356	1241	1280	1309	1356
					Medium	-	-	-	-	-	-	-	-	-	608	624	645	677	726	624	645	677	726
					Fast	-	-	-	-	-	-	-	-	-	306	313	335	364	412	313	335	364	412
					Ultrafast	-	-	-	-	-	-	-	-	-	187	192	197	202	211	192	197	202	211
10	4		2	2.5	Slow	-	-	-	-	-	-	-	-	-	1294	1326	1365	N/F	N/F	1326	1365	N/F	N/F
					Medium	-	-	-	-	-	-	-	-	-	660	697	734	N/F	N/F	697	734	N/F	N/F
					Fast	-	-	-	-	-	-	-	-	-	350	384	706	N/F	N/F	384	706	N/F	N/F
					Ultrafast	-	-	-	-	-	-	-	-	-	199	205	323	N/F	N/F	205	323	N/F	N/F
6	6		2	2.5	Slow	-	-	-	-	-	-	-	-	-	1248	1289	1322	1356	N/F	1289	1322	1356	N/F
					Medium	-	-	-	-	-	-	-	-	-	627	656	692	727	N/F	656	692	727	N/F
					Fast	-	-	-	-	-	-	-	-	-	314	346	381	413	N/F	346	381	413	N/F
					Ultrafast	-	-	-	-	-	-	-	-	-	193	198	204	252	N/F	198	204	252	N/F
8	6		2	2.5	Slow	-	-	-	-	-	-	-	-	-	1360	N/F	N/F	N/F	N/F	N/F	N/F	N/F	N/F
					Medium	-	-	-	-	-	-	-	-	-	730	N/F	N/F	N/F	N/F	N/F	N/F	N/F	N/F

Table 5-3 (cont'd): Flashover time t_f with smoke extraction system

Cabin Length L/m	Cabin Width W/m	Number	W_v/m	H_v/m	t²-fire	No smoke extraction	2 m — No smoke extraction	2 m — t_0.45 (40)	(80)	(120)	(180)	2 m — t_68 (40)	(80)	(120)	(180)	No smoke extraction	3 m — t_0.45 (40)	(80)	(120)	(180)	3 m — t_68 (40)	(80)	(120)	(180)
4	4	1	1.5	2	Fast	-	-	-	-	-	-	-	-	-	-	413	N/F	N/F	N/F	N/F	N/F	N/F	N/F	N/F
					Ultrafast	-	-	-	-	-	-	-	-	-	-	210	N/F	N/F	N/F	N/F	N/F	N/F	N/F	N/F
4	4	2	2	2.5	Slow	-	-	-	-	-	-	-	-	-	-	1346	1362	N/F	N/F	N/F	1362	N/F	N/F	N/F
					Medium	-	-	-	-	-	-	-	-	-	-	717	732	N/F	N/F	N/F	732	N/F	N/F	N/F
					Fast	-	-	-	-	-	-	-	-	-	-	1043	417	N/F	N/F	N/F	417	N/F	N/F	N/F
					Ultrafast	-	-	-	-	-	-	-	-	-	-	207	N/F	N/F	N/F	N/F	N/F	N/F	N/F	N/F
4	4	1	2	2	Slow	-	-	-	-	-	-	-	-	-	-	951	966	983	1003	1028	966	983	1003	1028
					Medium	-	-	-	-	-	-	-	-	-	-	476	484	496	504	517	484	496	504	517
					Fast	-	-	-	-	-	-	-	-	-	-	241	243	249	253	258	243	249	253	258
					Ultrafast	-	-	-	-	-	-	-	-	-	-	135	139	142	145	150	139	142	145	150
6	4		2	2	Slow	-	-	-	-	-	-	-	-	-	-	1039	1061	1084	1107	1147	1061	1084	1107	1147
					Medium	-	-	-	-	-	-	-	-	-	-	522	533	545	556	573	533	545	556	573
					Fast	-	-	-	-	-	-	-	-	-	-	262	268	274	279	288	268	274	279	288
					Ultrafast	-	-	-	-	-	-	-	-	-	-	152	157	162	167	175	157	162	167	175
8	4		2	2	Slow	-	-	-	-	-	-	-	-	-	-	1114	1142	1176	1203	1244	1142	1176	1203	1244
					Medium	-	-	-	-	-	-	-	-	-	-	559	573	587	601	626	573	587	601	626
					Fast	-	-	-	-	-	-	-	-	-	-	281	288	295	302	313	288	295	302	313
					Ultrafast	-	-	-	-	-	-	-	-	-	-	168	174	181	186	194	174	181	186	194
10	4		2	2	Slow	-	-	-	-	-	-	-	-	-	-	1186	1219	1252	1300	1360	1219	1252	1300	1360
					Medium	-	-	-	-	-	-	-	-	-	-	593	609	627	670	730	609	627	670	730
					Fast	-	-	-	-	-	-	-	-	-	-	298	306	319	358	415	306	319	358	415
					Ultrafast	-	-	-	-	-	-	-	-	-	-	183	189	195	201	279	189	195	201	279
6	6		2	2	Slow	-	-	-	-	-	-	-	-	-	-	1149	1184	1214	1245	1306	1184	1214	1245	1306
					Medium	-	-	-	-	-	-	-	-	-	-	576	592	607	624	675	592	607	624	675
					Fast	-	-	-	-	-	-	-	-	-	-	290	297	305	314	363	297	305	314	363
					Ultrafast	-	-	-	-	-	-	-	-	-	-	176	182	188	194	202	182	188	194	202
8	6		2	2	Slow	-	-	-	-	-	-	-	-	-	-	1248	1292	1346	N/F	N/F	1292	1346	N/F	N/F
					Medium	-	-	-	-	-	-	-	-	-	-	624	672	715	N/F	N/F	672	715	N/F	N/F
					Fast	-	-	-	-	-	-	-	-	-	-	314	360	401	N/F	N/F	360	401	N/F	N/F
					Ultrafast	-	-	-	-	-	-	-	-	-	-	194	191	198	N/F	N/F	191	198	N/F	N/F
10	6		2	2	Slow	-	-	-	-	-	-	-	-	-	-	1359	N/F	N/F	N/F	N/F	N/F	N/F	N/F	N/F
					Medium	-	-	-	-	-	-	-	-	-	-	728	N/F	N/F	N/F	N/F	N/F	N/F	N/F	N/F
					Fast	-	-	-	-	-	-	-	-	-	-	414	N/F	N/F	N/F	N/F	N/F	N/F	N/F	N/F
					Ultrafast	-	-	-	-	-	-	-	-	-	-	210	N/F	N/F	N/F	N/F	N/F	N/F	N/F	N/F
4	4		1.5	2	Slow	-	-	-	-	-	-	-	-	-	-	880	897	914	940	965	897	914	940	965

Table 5-3 (cont'd): Flashover time t_f with smoke extraction system

Cabin L/m	Cabin W/m	Openings Number	Wv/m	Hv/m	t^2-fire	2m No smoke extr.	2m $t_{0,45}$ 40	2m $t_{0,45}$ 80	2m $t_{0,45}$ 120	2m $t_{0,45}$ 180	2m t_{68} 40	2m t_{68} 80	2m t_{68} 120	2m t_{68} 180	3m No smoke extr.	3m $t_{0,45}$ 40	3m $t_{0,45}$ 80	3m $t_{0,45}$ 120	3m $t_{0,45}$ 180	3m t_{68} 40	3m t_{68} 80	3m t_{68} 120	3m t_{68} 180
4	4	1	1.5	2	Medium	-	-	-	-	-	-	-	-	-	442	452	462	470	483	452	462	470	483
					Fast	-	-	-	-	-	-	-	-	-	224	229	233	238	245	229	233	238	245
					Ultrafast	-	-	-	-	-	-	-	-	-	121	126	130	134	140	126	130	134	140
6	4		1.5	2	Slow	-	-	-	-	-	-	-	-	-	970	994	1017	1041	1085	994	1017	1041	1085
					Medium	-	-	-	-	-	-	-	-	-	486	498	511	526	545	498	511	526	545
					Fast	-	-	-	-	-	-	-	-	-	246	252	259	265	274	252	259	265	274
					Ultrafast	-	-	-	-	-	-	-	-	-	140	146	151	156	164	146	151	156	164
8	4		1.5	2	Slow	-	-	-	-	-	-	-	-	-	1043	1075	1111	1141	1188	1075	1111	1141	1188
					Medium	-	-	-	-	-	-	-	-	-	524	544	559	574	596	544	559	574	596
					Fast	-	-	-	-	-	-	-	-	-	266	273	281	288	300	273	281	288	300
					Ultrafast	-	-	-	-	-	-	-	-	-	157	169	170	176	185	169	170	176	185
10	4		1.5	2	Slow	-	-	-	-	-	-	-	-	-	1119	1154	1191	1230	1291	1154	1191	1230	1291
					Medium	-	-	-	-	-	-	-	-	-	563	581	598	615	663	581	598	615	663
					Fast	-	-	-	-	-	-	-	-	-	283	292	301	309	358	292	301	309	358
					Ultrafast	-	-	-	-	-	-	-	-	-	172	179	186	193	201	179	186	193	201
6	6	1	1.5	2	Slow	-	-	-	-	-	-	-	-	-	1080	1118	1151	1185	1238	1118	1151	1185	1238
					Medium	-	-	-	-	-	-	-	-	-	546	563	579	595	619	563	579	595	619
					Fast	-	-	-	-	-	-	-	-	-	275	283	291	299	311	283	291	299	311
					Ultrafast	-	-	-	-	-	-	-	-	-	164	171	178	185	194	171	178	185	194
8	6		1.5	2	Slow	-	-	-	-	-	-	-	-	-	1184	1227	1269	1325	N/F	1227	1269	1325	N/F
					Medium	-	-	-	-	-	-	-	-	-	595	614	640	700	N/F	614	640	700	N/F
					Fast	-	-	-	-	-	-	-	-	-	299	309	340	387	N/F	309	340	387	N/F
					Ultrafast	-	-	-	-	-	-	-	-	-	184	192	199	206	N/F	192	199	206	N/F
10	6		1.5	2	Slow	-	-	-	-	-	-	-	-	-	1283	1345	N/F	N/F	N/F	1345	N/F	N/F	N/F
					Medium	-	-	-	-	-	-	-	-	-	653	717	N/F	N/F	N/F	717	N/F	N/F	N/F
					Fast	-	-	-	-	-	-	-	-	-	344	405	N/F	N/F	N/F	405	N/F	N/F	N/F
					Ultrafast	-	-	-	-	-	-	-	-	-	201	208	N/F	N/F	N/F	208	N/F	N/F	N/F
8	8		1.5	2	Slow	-	-	-	-	-	-	-	-	-	1321	1362	N/F	N/F	N/F	1362	N/F	N/F	N/F
					Medium	-	-	-	-	-	-	-	-	-	691	732	N/F	N/F	N/F	732	N/F	N/F	N/F
					Fast	-	-	-	-	-	-	-	-	-	384	417	N/F	N/F	N/F	417	N/F	N/F	N/F
					Ultrafast	-	-	-	-	-	-	-	-	-	205	210	N/F	N/F	N/F	210	N/F	N/F	N/F
4	4	2	2	2.5	Slow	-	-	-	-	-	-	-	-	-	1146	N/F	N/F	N/F	N/F	N/F	N/F	N/F	N/F
					Medium	-	-	-	-	-	-	-	-	-	574	N/F	N/F	N/F	N/F	N/F	N/F	N/F	N/F
					Fast	-	-	-	-	-	-	-	-	-	288	N/F	N/F	N/F	N/F	N/F	N/F	N/F	N/F
					Ultrafast	-	-	-	-	-	-	-	-	-	309	N/F	N/F	N/F	N/F	N/F	N/F	N/F	N/F

Table 5-3 (cont'd): Flashover time t_f with smoke extraction system

Cabin		Openings			t^2-fire	2 m									No smoke extraction	3 m								
Length L/m	Width W/m	Number	W_V/m	H_V/m		No smoke extraction	Smoke extraction operated at $t_{0.45}$				Smoke extraction operated at t_{68}					Smoke extraction operated at $t_{0.45}$				Smoke extraction operated at t_{68}			
							40	80	120	180	40	80	120	180		40	80	120	180	40	80	120	180
6	4	2	2	2.5	Slow	-	-	-	-	-	-	-	-	-	1225	N/F	N/F	N/F	N/F	N/F	N/F	N/F	N/F
					Medium	-	-	-	-	-	-	-	-	-	613	N/F	N/F	N/F	N/F	N/F	N/F	N/F	N/F
					Fast	-	-	-	-	-	-	-	-	-	307	N/F	N/F	N/F	N/F	N/F	N/F	N/F	N/F
					Ultrafast	-	-	-	-	-	-	-	-	-	188	N/F	N/F	N/F	N/F	N/F	N/F	N/F	N/F
8	4	2	2	2.5	Slow	-	-	-	-	-	-	-	-	-	1309	N/F	N/F	N/F	N/F	N/F	N/F	N/F	N/F
					Medium	-	-	-	-	-	-	-	-	-	678	N/F	N/F	N/F	N/F	N/F	N/F	N/F	N/F
					Fast	-	-	-	-	-	-	-	-	-	365	N/F	N/F	N/F	N/F	N/F	N/F	N/F	N/F
					Ultrafast	-	-	-	-	-	-	-	-	-	202	N/F	N/F	N/F	N/F	N/F	N/F	N/F	N/F

* N/F: No flashover.

Table 5-3 (Cont'd): Flashover time t_f with smoke extraction system

Cabin		Openings				4 m									5 m								
						No smoke extraction	Smoke extraction operated at $t_{0.45}$				Smoke extraction operated at t_{68}				No smoke extraction	Smoke extraction operated at $t_{0.45}$				Smoke extraction operated at t_{68}			
Length L/m	Width W/m	Number	W_v/m	H_v/m	Fire type		40	80	120	180	40	80	120	180		40	80	120	180	40	80	120	180
4	4	4	4x4	1.5	Slow	1337	1331	1349	1366	N/F	1331	1349	1366	N/F	N/F	N/F	N/F	N/F	N/F	N/F	N/F	N/F	N/F
					Medium	771	701	719	736	N/F	701	719	736	N/F	N/F	N/F	N/F	N/F	N/F	N/F	N/F	N/F	N/F
					Fast	375	390	405	525	N/F	390	405	525	N/F	412	N/F	N/F	N/F	N/F	N/F	N/F	N/F	N/F
					Ultrafast	202	205	207	210	N/F	205	207	210	N/F	209	N/F	N/F	N/F	N/F	N/F	N/F	N/F	N/F
6	4	4	2x(4+6)	1.5	Slow	N/F	N/F	N/F	N/F	N/F	N/F	N/F	N/F	N/F	N/F	N/F	N/F	N/F	N/F	N/F	N/F	N/F	N/F
					Medium	N/F	N/F	N/F	N/F	N/F	N/F	N/F	N/F	N/F	N/F	N/F	N/F	N/F	N/F	N/F	N/F	N/F	N/F
					Fast	N/F	N/F	N/F	N/F	N/F	N/F	N/F	N/F	N/F	N/F	N/F	N/F	N/F	N/F	N/F	N/F	N/F	N/F
					Ultrafast	N/F	N/F	N/F	N/F	N/F	N/F	N/F	N/F	N/F	N/F	N/F	N/F	N/F	N/F	N/F	N/F	N/F	N/F
4	4	3	3x4	1.5	Slow	1230	1245	1260	1279	1309	1245	1260	1279	1309	1264	1288	1311	1335	1371	1288	1311	1335	1371
					Medium	616	623	630	650	679	623	630	650	679	636	659	683	706	N/F	659	683	706	N/F
					Fast	309	313	321	340	368	313	321	340	368	330	351	372	394	N/F	351	372	394	N/F
					Ultrafast	190	193	195	198	202	193	195	198	202	196	199	202	206	N/F	199	202	206	N/F
6	4	3	4+6+4	1.5	Slow	N/F	N/F	N/F	N/F	N/F	N/F	N/F	N/F	N/F	N/F	N/F	N/F	N/F	N/F	N/F	N/F	N/F	N/F
					Medium	N/F	N/F	N/F	N/F	N/F	N/F	N/F	N/F	N/F	N/F	N/F	N/F	N/F	N/F	N/F	N/F	N/F	N/F
					Fast	N/F	N/F	N/F	N/F	N/F	N/F	N/F	N/F	N/F	N/F	N/F	N/F	N/F	N/F	N/F	N/F	N/F	N/F
					Ultrafast	N/F	N/F	N/F	N/F	N/F	N/F	N/F	N/F	N/F	N/F	N/F	N/F	N/F	N/F	N/F	N/F	N/F	N/F
4	4	2	2x4	1.5	Slow	1129	1146	1164	1182	1210	1146	1164	1182	1210	1161	1183	1206	1228	1261	1183	1206	1228	1261
					Medium	569	578	586	594	607	578	586	594	607	584	594	605	615	633	594	605	615	633
					Fast	287	291	295	299	305	291	295	299	305	295	300	305	310	327	300	305	310	327
					Ultrafast	174	177	180	183	187	177	180	183	187	180	183	187	190	196	183	187	190	196
6	4	2	4+6	1.5	Slow	1280	1309	1337	1365	N/F	1309	1337	1365	N/F	1322	1356	N/F	N/F	N/F	1356	N/F	N/F	N/F
					Medium	651	679	707	735	N/F	679	707	735	N/F	693	726	N/F	N/F	N/F	726	N/F	N/F	N/F
					Fast	342	368	394	420	N/F	368	394	420	N/F	383	412	N/F	N/F	N/F	412	N/F	N/F	N/F
					Ultrafast	199	203	206	210	N/F	203	206	210	N/F	205	209	N/F	N/F	N/F	209	N/F	N/F	N/F
4	4	1	4	1.5	Slow	975	996	1017	1037	1071	996	1017	1037	1071	997	1025	1052	1082	1125	1025	1052	1082	1125
					Medium	491	502	512	522	538	502	512	522	538	504	517	529	540	567	517	529	540	567
					Fast	253	254	258	263	271	254	258	263	271	257	258	262	277	289	258	262	277	289
					Ultrafast	142	143	151	157	164	143	151	157	164	148	251	193	343	168	251	193	343	168
6	4	1	4	1.5	Slow	1070	1101	1131	1161	1208	1101	1131	1161	1208	1103	1140	1179	1216	1275	1140	1179	1216	1275
					Medium	537	551	571	585	607	551	571	585	607	547	575	593	611	648	575	593	611	648
					Fast	277	282	290	296	306	282	290	296	306	288	293	300	308	342	293	300	308	342
					Ultrafast	159	169	172	177	190	169	172	177	190	371	268	179	192	200	268	179	192	200
8	4	1	4	1.5	Slow	1162	1199	1236	1276	1347	1199	1236	1276	1347	1196	1241	1293	1349	N/F	1241	1293	1349	N/F
					Medium	585	603	620	647	718	603	620	647	718	601	622	665	720	N/F	622	665	720	N/F
					Fast	300	304	312	234	299	304	312	234	299	308	314	358	407	N/F	314	358	407	N/F

Table 5-3 (cont'd): Flashover time t_f with smoke extraction system

Length L/m	Width W/m	Number	W_v/m	H_v/m	Fire type	4 m No smoke extraction	4 m Smoke extraction operated at $t_{0.45}$ — 40	80	120	180	4 m Smoke extraction operated at t_{68} — 40	80	120	180	No smoke extraction	5 m Smoke extraction operated at $t_{0.45}$ — 40	80	120	180	5 m Smoke extraction operated at t_{68} — 40	80	120	180
8	4	1	4	1.5	Ultrafast	178	184	194	200	208	184	194	200	208	182	196	202	208	N/F	196	202	208	N/F
10	4		4	1.5	Slow	1245	1295	1349	N/F	N/F	1295	1349	N/F	N/F	1283	1347	N/F	N/F	N/F	1347	N/F	N/F	N/F
					Medium	624	666	719	N/F	N/F	666	719	N/F	N/F	657	718	N/F	N/F	N/F	718	N/F	N/F	N/F
					Fast	328	357	405	N/F	N/F	357	405	N/F	N/F	368	N/F	N/F	N/F	N/F	N/F	N/F	N/F	N/F
					Ultrafast	192	202	208	N/F	N/F	202	208	N/F	N/F	202	208	N/F	N/F	N/F	208	N/F	N/F	N/F
6	6		6	1.5	Slow	1294	1338	N/F	N/F	N/F	1338	N/F	N/F	N/F	1333	N/F	N/F	N/F	N/F	N/F	N/F	N/F	N/F
					Medium	665	708	N/F	N/F	N/F	708	N/F	N/F	N/F	705	N/F	N/F	N/F	N/F	N/F	N/F	N/F	N/F
					Fast	376	396	N/F	N/F	N/F	396	N/F	N/F	N/F	412	N/F	N/F	N/F	N/F	N/F	N/F	N/F	N/F
					Ultrafast	202	207	208	N/F	N/F	207	208	N/F	N/F	207	208	N/F	N/F	N/F	208	N/F	N/F	N/F
4	4		2	2.5	Slow	1074	1105	1128	1149	1173	1105	1128	1149	1173	1117	1145	1169	1273	1297	1145	1169	1273	1297
					Medium	541	554	566	570	583	554	566	570	583	552	558	572	578	622	558	572	578	622
					Fast	270	275	279	284	294	275	279	284	294	284	277	283	303	312	277	283	303	312
					Ultrafast	159	163	167	169	179	163	167	169	179	161	165	172	173	180	165	172	173	180
6	4		2	2.5	Slow	1169	1188	1210	1262	1300	1188	1210	1262	1300	1185	1204	1273	1297	1524	1204	1273	1297	1524
					Medium	576	590	617	632	667	590	617	632	667	581	623	644	665	781	623	644	665	781
					Fast	288	300	310	319	356	300	310	319	356	294	313	333	356	466	313	333	356	466
					Ultrafast	176	181	185	191	198	181	185	191	198	178	185	189	194	365	185	189	194	365
8	4	1	2	2.5	Slow	1222	1282	1321	1345	N/F	1282	1321	1345	N/F	1254	1304	1335	N/F	N/F	1304	1335	N/F	N/F
					Medium	613	652	685	715	N/F	652	685	715	N/F	646	677	707	N/F	N/F	677	707	N/F	N/F
					Fast	314	339	370	402	N/F	339	370	402	N/F	334	365	392	N/F	N/F	365	392	N/F	N/F
					Ultrafast	188	194	201	260	N/F	194	201	260	N/F	193	198	259	N/F	N/F	198	259	N/F	N/F
10	4		2	2.5	Slow	1310	1345	N/F	N/F	N/F	1345	N/F	N/F	N/F	1321	1454	N/F	N/F	N/F	1454	N/F	N/F	N/F
					Medium	678	717	N/F	N/F	N/F	717	N/F	N/F	N/F	693	829	N/F	N/F	N/F	829	N/F	N/F	N/F
					Fast	370	403	N/F	N/F	N/F	403	N/F	N/F	N/F	381	512	N/F	N/F	N/F	512	N/F	N/F	N/F
					Ultrafast	201	209	N/F	N/F	N/F	209	N/F	N/F	N/F	201	297	N/F	N/F	N/F	297	N/F	N/F	N/F
6	6		2	2.5	Slow	1280	1318	1350	N/F	N/F	1318	1350	N/F	N/F	1298	1330	N/F	N/F	N/F	1330	N/F	N/F	N/F
					Medium	652	686	720	N/F	N/F	686	720	N/F	N/F	667	707	N/F	N/F	N/F	707	N/F	N/F	N/F
					Fast	339	380	407	N/F	N/F	380	407	N/F	N/F	358	393	N/F	N/F	N/F	393	N/F	N/F	N/F
					Ultrafast	195	201	269	N/F	N/F	201	269	N/F	N/F	198	209	N/F	N/F	N/F	209	N/F	N/F	N/F
8	6		2	2.5	Slow	1364	N/F	N/F	N/F	N/F	N/F	N/F	N/F	N/F	1362	N/F	N/F	N/F	N/F	N/F	N/F	N/F	N/F
					Medium	731	N/F	N/F	N/F	N/F	N/F	N/F	N/F	N/F	733	N/F	N/F	N/F	N/F	N/F	N/F	N/F	N/F
					Fast	499	N/F	N/F	N/F	N/F	N/F	N/F	N/F	N/F	419	N/F	N/F	N/F	N/F	N/F	N/F	N/F	N/F
					Ultrafast	394	N/F	N/F	N/F	N/F	N/F	N/F	N/F	N/F	309	N/F	N/F	N/F	N/F	N/F	N/F	N/F	N/F
4	4	2	2	2.5	Slow	N/F	N/F	N/F	N/F	N/F	N/F	N/F	N/F	N/F	N/F	N/F	N/F	N/F	N/F	N/F	N/F	N/F	N/F
					Medium	N/F	N/F	N/F	N/F	N/F	N/F	N/F	N/F	N/F	N/F	N/F	N/F	N/F	N/F	N/F	N/F	N/F	N/F
					Fast	N/F	N/F	N/F	N/F	N/F	N/F	N/F	N/F	N/F	N/F	N/F	N/F	N/F	N/F	N/F	N/F	N/F	N/F
					Ultrafast	N/F	N/F	N/F	N/F	N/F	N/F	N/F	N/F	N/F	N/F	N/F	N/F	N/F	N/F	N/F	N/F	N/F	N/F

Table 5-3 (cont'd): Flashover time t_f with smoke extraction system

Length L/m	Width W/m	Number	W_v/m	H_v/m	Fire type	No smoke extraction (4 m)	4 m $t_{0.45}$ 40	80	120	180	4 m t_{68} 40	80	120	180	No smoke extraction (5 m)	5 m $t_{0.45}$ 40	80	120	180	5 m t_{68} 40	80	120	180
4	4	1	2	2	Slow	957	977	1008	1030	1060	977	1008	1030	1060	970	1020	1048	1067	1129	1020	1048	1067	1129
					Medium	478	497	507	518	533	497	507	518	533	499	514	527	537	554	514	527	537	554
					Fast	243	248	253	260	266	248	253	260	266	245	253	258	265	275	253	258	265	275
					Ultrafast	139	143	148	152	158	143	148	152	158	143	148	153	158	165	148	153	158	165
6	4		2	2	Slow	1053	1078	1103	1156	1191	1078	1103	1156	1191	1075	1097	1166	1189	1271	1097	1166	1189	1271
					Medium	528	542	556	570	591	542	556	570	591	540	556	571	586	641	556	571	586	641
					Fast	264	272	279	286	301	272	279	286	301	267	276	284	302	329	276	284	302	329
					Ultrafast	156	162	168	174	183	162	168	174	183	161	168	174	181	190	168	174	181	190
8	4	1	2	2	Slow	1118	1176	1203	1240	1315	1176	1203	1240	1315	1135	1197	1339	1304	1664	1197	1339	1304	1664
					Medium	565	580	598	530	685	580	598	530	685	574	590	643	675	1035	590	643	675	1035
					Fast	283	291	306	324	373	291	306	324	373	284	301	332	363	720	301	332	363	720
					Ultrafast	172	179	186	192	201	179	186	192	201	177	184	192	198	614	184	192	198	614
10	4		2	2	Slow	1203	1235	1308	1345	N/F	1235	1308	1345	N/F	1211	1293	1332	N/F	N/F	1293	1332	N/F	N/F
					Medium	596	617	677	715	N/F	617	677	715	N/F	599	664	703	N/F	N/F	664	703	N/F	N/F
					Fast	299	326	363	401	N/F	326	363	401	N/F	308	353	392	N/F	N/F	353	392	N/F	N/F
					Ultrafast	186	193	200	253	N/F	193	200	253	N/F	189	196	205	N/F	N/F	196	205	N/F	N/F
6	6		2	2	Slow	1174	1205	1237	1306	1464	1205	1237	1306	1464	1190	1222	1302	1339	N/F	1222	1302	1339	N/F
					Medium	579	599	640	675	835	599	640	675	835	585	615	673	710	N/F	615	673	710	N/F
					Fast	291	304	328	367	519	304	328	367	519	293	328	363	396	N/F	328	363	396	N/F
					Ultrafast	180	187	193	200	311	187	193	200	311	184	201	208	263	N/F	201	208	263	N/F
8	6		2	2	Slow	1251	1327	N/F	N/F	N/F	1327	N/F	N/F	N/F	1251	1344	N/F	N/F	N/F	1344	N/F	N/F	N/F
					Medium	624	697	N/F	N/F	N/F	697	N/F	N/F	N/F	625	717	N/F	N/F	N/F	717	N/F	N/F	N/F
					Fast	343	391	N/F	N/F	N/F	391	N/F	N/F	N/F	360	404	N/F	N/F	N/F	404	N/F	N/F	N/F
					Ultrafast	197	204	N/F	N/F	N/F	204	N/F	N/F	N/F	199	208	N/F	N/F	N/F	208	N/F	N/F	N/F
10	6		2	2	Slow	1361	N/F	N/F	N/F	N/F	N/F	N/F	N/F	N/F	1360	N/F	N/F	N/F	N/F	N/F	N/F	N/F	N/F
					Medium	732	N/F	N/F	N/F	N/F	N/F	N/F	N/F	N/F	732	N/F	N/F	N/F	N/F	N/F	N/F	N/F	N/F
					Fast	420	N/F	N/F	N/F	N/F	N/F	N/F	N/F	N/F	451	N/F	N/F	N/F	N/F	N/F	N/F	N/F	N/F
					Ultrafast	210	N/F	N/F	N/F	N/F	N/F	N/F	N/F	N/F	210	N/F	N/F	N/F	N/F	N/F	N/F	N/F	N/F
4	4		1.5	2	Slow	884	906	942	964	995	906	942	964	995	889	952	970	990	1063	952	970	990	1063
					Medium	446	459	470	481	498	459	470	481	498	451	465	478	491	534	465	478	491	534
					Fast	228	233	239	245	253	233	239	245	253	231	238	244	251	262	238	244	251	262
					Ultrafast	126	131	136	141	149	131	136	141	149	131	138	144	149	157	138	144	149	157
6	4		1.5	2	Slow	977	1005	1035	1083	1125	1005	1035	1083	1125	990	1020	1086	1113	1194	1020	1086	1113	1194
					Medium	489	504	531	545	566	504	531	545	566	490	528	548	564	588	528	548	564	588
					Fast	249	257	265	273	285	257	265	273	285	252	261	271	281	294	261	271	281	294
					Ultrafast	145	152	158	165	175	152	158	165	175	152	159	165	172	182	159	165	172	182
8	4		1.5	2	Slow	1045	1100	1134	1185	1240	1100	1134	1185	1240	1045	1117	1177	1223	1321	1117	1177	1223	1321

Table 5-3 (cont'd): Flashover time t_f with smoke extraction system

Cabin		Openings			Fire type	No smoke extraction	4 m Smoke extraction operated at $t_{0.45}$				4 m Smoke extraction operated at t_{68}				No smoke extraction	5 m Smoke extraction operated at $t_{0.45}$				5 m Smoke extraction operated at t_{68}			
Length L/m	Width W/m	Number	W_V/m	H_V/m			40	80	120	180	40	80	120	180		40	80	120	180	40	80	120	180
8	4	1	1.5	2	Medium	526	555	572	591	618	555	572	591	618	548	567	587	608	692	567	587	608	692
					Fast	268	278	288	297	332	278	288	297	332	271	283	294	326	379	283	294	326	379
					Ultrafast	162	170	177	185	194	170	177	185	194	169	176	183	191	201	176	183	191	201
10	4		1.5	2	Slow	1125	1168	1226	1268	1364	1168	1226	1268	1364	1131	1209	1248	1337	N/F	1209	1248	1337	N/F
					Medium	568	589	611	656	734	589	611	656	734	575	599	642	707	N/F	599	642	707	N/F
					Fast	285	297	308	358	419	297	308	358	419	288	301	355	395	N/F	301	355	395	N/F
					Ultrafast	177	185	193	199	211	185	193	199	211	182	189	197	205	N/F	189	197	205	N/F
6	6		1.5	2	Slow	1082	1132	1173	1229	1318	1132	1173	1229	1318	1107	1145	1219	1259	1360	1145	1219	1259	1360
					Medium	553	572	592	613	688	572	592	613	688	562	583	605	674	734	583	605	674	734
					Fast	278	288	298	311	376	288	298	311	376	280	292	311	362	419	292	311	362	419
					Ultrafast	170	178	185	193	202	178	185	193	202	176	183	190	198	312	183	190	198	312
8	6		1.5	2	Slow	1186	1245	1307	N/F	N/F	1245	1307	N/F	N/F	1210	1257	1352	N/F	N/F	1257	1352	N/F	N/F
					Medium	598	622	696	N/F	N/F	622	696	N/F	N/F	602	651	723	N/F	N/F	651	723	N/F	N/F
					Fast	301	323	384	N/F	N/F	323	384	N/F	N/F	302	365	410	N/F	N/F	365	410	N/F	N/F
					Ultrafast	189	197	204	N/F	N/F	197	204	N/F	N/F	192	200	208	N/F	N/F	200	208	N/F	N/F
10	6	1	1.5	2	Slow	1285	1365	N/F	N/F	N/F	1365	N/F	N/F	N/F	1285	N/F	N/F	N/F	N/F	N/F	N/F	N/F	N/F
					Medium	656	736	N/F	N/F	N/F	736	N/F	N/F	N/F	681	N/F	N/F	N/F	N/F	N/F	N/F	N/F	N/F
					Fast	369	420	N/F	N/F	N/F	420	N/F	N/F	N/F	380	N/F	N/F	N/F	N/F	N/F	N/F	N/F	N/F
					Ultrafast	203	211	N/F	N/F	N/F	211	N/F	N/F	N/F	204	N/F	N/F	N/F	N/F	N/F	N/F	N/F	N/F
8	8		1.5	2	Slow	1321	N/F	N/F	N/F	N/F	N/F	N/F	N/F	N/F	1342	N/F	N/F	N/F	N/F	N/F	N/F	N/F	N/F
					Medium	700	N/F	N/F	N/F	N/F	N/F	N/F	N/F	N/F	712	N/F	N/F	N/F	N/F	N/F	N/F	N/F	N/F
					Fast	394	N/F	N/F	N/F	N/F	N/F	N/F	N/F	N/F	399	N/F	N/F	N/F	N/F	N/F	N/F	N/F	N/F
					Ultrafast	206	N/F	N/F	N/F	N/F	N/F	N/F	N/F	N/F	209	N/F	N/F	N/F	N/F	N/F	N/F	N/F	N/F
4	4	2	2	2.5	Slow	1155	N/F	N/F	N/F	N/F	N/F	N/F	N/F	N/F	1187	N/F	N/F	N/F	N/F	N/F	N/F	N/F	N/F
					Medium	582	N/F	N/F	N/F	N/F	N/F	N/F	N/F	N/F	596	N/F	N/F	N/F	N/F	N/F	N/F	N/F	N/F
					Fast	293	N/F	N/F	N/F	N/F	N/F	N/F	N/F	N/F	301	N/F	N/F	N/F	N/F	N/F	N/F	N/F	N/F
					Ultrafast	178	N/F	N/F	N/F	N/F	N/F	N/F	N/F	N/F	184	N/F	N/F	N/F	N/F	N/F	N/F	N/F	N/F
6	4		2	2.5	Slow	1242	N/F	N/F	N/F	N/F	N/F	N/F	N/F	N/F	1277	N/F	N/F	N/F	N/F	N/F	N/F	N/F	N/F
					Medium	622	N/F	N/F	N/F	N/F	N/F	N/F	N/F	N/F	649	N/F	N/F	N/F	N/F	N/F	N/F	N/F	N/F
					Fast	312	N/F	N/F	N/F	N/F	N/F	N/F	N/F	N/F	343	N/F	N/F	N/F	N/F	N/F	N/F	N/F	N/F
					Ultrafast	194	N/F	N/F	N/F	N/F	N/F	N/F	N/F	N/F	199	N/F	N/F	N/F	N/F	N/F	N/F	N/F	N/F
8	4		2	2.5	Slow	1338	N/F	N/F	N/F	N/F	N/F	N/F	N/F	N/F	N/F	N/F	N/F	N/F	N/F	N/F	N/F	N/F	N/F
					Medium	708	N/F	N/F	N/F	N/F	N/F	N/F	N/F	N/F	N/F	N/F	N/F	N/F	N/F	N/F	N/F	N/F	N/F
					Fast	395	N/F	N/F	N/F	N/F	N/F	N/F	N/F	N/F	N/F	N/F	N/F	N/F	N/F	N/F	N/F	N/F	N/F
					Ultrafast	207	N/F	N/F	N/F	N/F	N/F	N/F	N/F	N/F	N/F	N/F	N/F	N/F	N/F	N/F	N/F	N/F	N/F

* N/F: No flashover.

	Energy kW			Q fire kW	Mass kgs^{-1}		
	E$_2$ out		E$_1$ in		M$_2$ out		M$_1$ in
No Ventilation	966		165		2.78		2.82
Forced-ventilation	fan	door			fan	door	
40 Fv	198	749	165	800	0.56	2.44	3.03
50	411	463	112		1.3	1.97	3.32
100	438	231	114		1.29	1.7	2.91
200	646	211	118		2.47	1.11	3.51

Table 7-1: Flux calculations for CFD studies on 'bare cabin' fire operation of smoke extraction system

	CFD simulation		Zone model	
	Model 1	Model 2	Model 1	Model 2
Inflow rate V_1 / m^3s^{-1}	1.57	7.16 10^{-2}	0.35	0.30
Outflow rate V_2 / m^3s^{-1}	1.47	8.00×10^{-2}	0.13	0.27
Neutral plane h_c / m	3.58	3.58	2.90	3.10
Height from floor / m	3.58	3.58	5.80	3.60

Table 8-1: A comparison between the result of CFD simulation and the two zone models

REFERENCES

Alpert, R. L. (1972)

"Calculation of response time of ceiling-mounted fire detectors"

Fire Technology, Vol. 8 (2), 181-195.

Andersen, K. T. (1995)

"Theoretical considerations on natural ventilation by thermal buoyancy"

ASHRAE Transactions, Vol. 101 (2), 1103-1117.

ASHRAE (1985)

"ASHRAE handbook - Heating, ventilating, and air-conditioning systems and applications"

American Society of Heating, Refrigerating and Air-Conditioning Engineers

Australian Standards 1668 (1991)

AS 1668 "The use of mechanical ventilation and air-conditioning in buildings - Mechanical ventilation for acceptable indoor-air quality"

Australian Standards

Baines W.D. (1990)

"Turbulent fountains in an open chamber"

Journal of Fluid Mechanics, Vol. 212, 557-592.

Ball, D. and Campbell, J. (1973)

"Light, heating and ventilation in multi-story and car parks"

Proceedings of Joint Conference on Multi-story and Underground Car Parks,

May 16-17, 1973

The Institution of Structural Engineers and the Institution of Highway Engineers,

35-41.

BCA96 (1996)

"The Building Code of Australia (BCA)"

Australian Building Codes Board (ABCB), Canberra ACT 2601, Australia

Beever, P. (1991)

"Cabins and islands: a fire protection strategy for an international airport

terminal building"

Third International Fire Safety Science Symposium, IAFSS, Edinburgh, Scotland,

U.K., 709-718.

Beever, P. (1995)

"Design in international airport terminals"

Fire East '95 Conference and Exhibition, Hong Kong, 7 November, 4.1-4.5.

Beever, P. (1998)

"The forum"

Journal of Fire Sciences, Vol. 16 (2), 152-153.

Beyler, C.L. (1986)

"Fire plumes and ceiling jets"

Fire Safety Journal, Vol. 11 (1), 53-75.

Birk, D.M. (1991)

"An introduction to mathematical fire modeling"

Technomic Publishing Co., Inc. Lancaster, Pennsylvania, U.S.A.

Brani, D.M. and Black, W.Z. (1992)

"Two-zone model for single-room fire"

Fire Safety Journal, Vol. 19 (2-3), Nos. 2&3, 189-216.

Bressington, P. (1995)

"Railway link to Chek Lap Kok"

Fire East '95 Conference and Exhibition, Hong Kong, 7 November, 5.1-5.8.

Bressington, P. (1999a)

"Assessment of the objectives and effectiveness of hot smoke test"

Seminar on Hot Smoke Test, Regal Kowloon Hotel, Hong Kong, 12 March 1999

Bressington, P. (1999b)

"Retail premise"

Fire Prevention, Vol. 321, June, 22-23.

British Standard 5839 (1995)

BS 5839 Part 6 "Code of practice for the design and installation of fire detection

and alarm systems in dwellings"

British Standards Institution, London, UK

Buchanan, A.H. (1998)

"Five years of performance-based fire safety in New Zealand"

First International Symposium on Engineering Performance-Based Fire Codes

8 September 1998, Hong Kong

Buildings Department (1969)

L.N. 54 (Law Announcement No. 54)

Hong Kong

Buildings Department (1992)

L.N. 79 (Law Announcement No. 79)

Hong Kong

Buildings Department (1995)

"Code of practice for means of access for firefighting and rescue"

Hong Kong

Buildings Department (1996a)

"Code of Practice for the Provision of Means of Escape In Case of Fire"

Hong Kong

Buildings Department (1996b)

"Code of practice for fire resisting construction"

Hong Kong

Buildings Department (1997a)

"Fire code of Hong Kong Chapter 97"

Hong Kong

Buildings Department (1997b)

"Chapter 123 Buildings ordinance"

Hong Kong

Buildings Department (1998)

"Codes of practice for minimum fire service installations and equipment"

Hong Kong Special Administrative Region

Chow, W. K. (1995a)

"Use of zone models on simulating compartmental fires with forced ventilation"

Fire and Materials, Vol. 19, 101-108.

Chow, W. K. (1995b)

"On ventilation design for underground car parks"

Tunnelling and Underground Space Technology, Vol. 10 (2), 225-245.

Chow, W. K. (1995c)

"Aspects of fires for factories in Hong Kong"

Journal of Applied Fire Science, Vol. 5 (1), 17-32.

Chow, W.K. (1995d)

"On the simulation of forced-ventilation fires using three field models"

Proceedings 29th Australian and New Zealand Architectural Science Association

Conference, 11-13 July, University of Canberra, ACT, Australia, 62-66.

Chow, W.K. (1997a)

"A preliminary study on the fire protection aspects of the new airport terminal

building"

Journal of Applied Fire Science, Vol. 6 (4), 327-338.

Chow, W.K. (1997b)

"On the 'cabins' fire safety design concept in the new Hong Kong airport

terminal buildings"

Journal of Fire Sciences, Vol. 15 (5), 404-423.

Chow, W.K. (1997c)

"Assessment of thermal environment in an atrium with air-conditioning"

Journal of Environmental Systems, Vol. 25(4), 409-420.

Chow, W. K. (1998a)

"On the fire plume in a forced-ventilated compartment"

Unpublished Report.

Chow, W.K. (1998b)

"Application of Computational Fluid Dynamics on evaluating 'bare cabin' design for large halls"

The PHOENICS Journal of Computational Fluid Dynamics & Its Applications, Vol. 11(4), 429-453.

Chow, W.K. (1998c)

"Fire safety desired in the new airport terminal"

Lecture for 40th Anniversary, University of Science and Technology of China, Hefei, Anhui, China, 19 September 1998 – in Chinese.

Chow, W.K. (1998d)

"Author's responses to comments"

Journal of Applied Fire Science, Vol. 7(3), 323-327.

Chow, W.K. (1998e)

"The Forum"

Journal of Fire Sciences, Vol. 16(2), 154-157.

Chow, W.K. (1998f)

"Predictability of flashover by zone models"

Journal of Fire Sciences, Vol. 10 (5), 335-350.

Chow, W.K. (1999a)

"A preliminary discussion on engineering performance-based fire codes in the Hong Kong Special Administrative Region"

International Journal on Engineering Performance-Based Fire Codes, Vol. 1 (1), 1-10.

Chow, W.K. (1999b)

"Studies on the stability of thermal stratified layer in a forced-ventilation fire using Computational Fluid Dynamics"

Journal of Applied Fire Science, Vol. 6, 15-25.

Chow, W.K. (1999c)

"PolyU/USTC Atrium: A full-scale burning facility - Preliminary experiments"

Journal of Applied Fire Science, Vol. 8 (3), 229-241.

Chow, W.K. and Fong, N.K. (1991)

"Numerical simulation on cooling of the fire-induced air flow by sprinkler water sprays"

Fire Safety Journal, Vol. 17 (4), 263-290.

Chow, W.K. and Fong, N.K. (1998)

"The PolyU/USTC Atrium: a full-scale burning facility for atrium fire studies"

Proceedings of the First International Symposium on Engineering Performance-Based Fire Codes, Hong Kong Special Administrative Region, 8 September 1998, 186-189.

Chow, W.K. and Ho, P.L. (1990)

"Thermal responses of sprinkler heads"

Building Services Engineering Research and Technology, Vol. 11 (2), 37-47.

Chow, W. K. and Kui, Q. (2000)

"Time to flashover for fires in a 'bare babin' with smoke extraction system"

Architecture Science Review, Vol. 44 (2), 115-121

Christensen, S.M. (1996)

"Resources for computer algebra "

Computers in Physics, Vol. 8 (3), 308-316.

Cooper, L.Y. (1982a)

"A mathematical model for estimating available safe egress time in fire"

Fire and Material, Vol. 6 (3&4), 135-144.

Cooper, L.Y. (1982b)

"Heat transfer from plume to an unconfined ceiling"

Journal of Heat Transfer, Vol. 104 (3), 446-451.

Cooper P. and Linden P.F. (1996)

"Natural ventilation of an enclosure containing two buoyancy sources"

Journal of Fluid Mechanics, Vol. 311, 153-176.

Currie, I. G. (1974)

"Fundamental mechanics of fluids"

McGraw-Hill Book Company Inc.- New York

Davies G.M.J. and Linden P.F. (1992)

"The effects of headwind on buoyancy-driven flow through a doorway"

3rd International Conference on Air Distribution in Rooms, ROOMVENT'92, Vol. 3, 419-433.

Dormand, J. R. and Prince, P. J. (1980)

"A family of embedded Runge-Kutta formulae"

J. Comp. and Appl. Math., Vol. 6, 19-26.

Dormand, J.R. (1996)

"Numerical method for differential equations"

CRC Press, Inc. - New York.

Drysdale, D. (1985)

"An introduction to fire dynamics"

Wiley & Sons Inc. –New York.

Etheridge D. (1990)

"Building ventilation: theory and measurement"

John Wiley & Sons – Chichester

Fire Services Department (1994a)

"Practice of design and commissioning of the smoke control systems for Hong Kong"

Hong Kong

Fire Services Department (1994b)

"Codes of practice for minimum fire service installations and equipment and inspection and testing of installations and equipment "

Hong Kong

FMC (1997)

"FIREWIND user's manual version 3.3"

Fire Modelling & Computing (FMC), 66 Westbrook Avenue, Wahroonga, N.S.W. 2074, Australia.

Galea, E.R., Grandison, A.J. and Patel, M.K. (2001)

"Fire modeling standards/ benchmark"

Report on Phase 1 Simulations, Report No. 01/Im/72, Centre for Numerical Modelling and Process Analysis, University of Greenwich, CMS press-London, U.K.

Hadjisophocleous, G.V. (1998)

"Literature review of performance-based fire codes and design environment"

Journal of Fire Protection Engineering, Vol. 9 (1), 12-40.

Heskestad, G. (1984)

"Engineering relations for fire plumes"

Fire Safety Journal, Vol.7 (1), 25-32.

Heskestad, G. and Smith, H. (1982)

"Plunge test for determination of sprinkler sensitivity"

Research Report JI3A1E2RR, Turnpike: Factory Mutual Corporations, Ma, U.S.A.

Hinkley, P.L. (1971)

"Some notes on the control of smoke in enclosed shopping centers"

Fire research note no. 875, Fire research station"

Borehamwood, Harts, England, May.

Holmes, M.H., Au, Y. and Stayman, J.W. (1995)

"Symbolic and numerical computing for chemical kinetic reaction schemes"

Computers in Physics, Vol. 9 (6), 629-634.

ISO 6241 (1984)

"Performance standards in building -- Principles for their preparation and factors

to be considered"

International Organization for Standardization, Geneva, Switzerland

Jones, J.C. (1998)

"A contribution to the discussion of the cabin fire safety design concept"

Journal of Fire Sciences, Vol. 16 (6), 410-413.

Kong, L. (1979)

"Engineering fluid mechanics"

Water conservancy and electrical power press, China

Koskela, H.K. (1991)

"Comparison between forced-displacement and mixing ventilation in a garage"

ASHRAE Transaction, Part 1A, 1119-1126.

Kui, Q. and Chow, W. K. (2000)

"Bare cabin fires with operation of smoke extraction system"

Proceedings of the Fourth Asia-Oceania Symposium on Fire Science and

Technology, Waseda University, Tokyo, Japan, 22-26 May 2000, 613-620.

Law, M. (1990)

"Fire and smoke models - Their use on the design of some large buildings"

ASHRAE Transactions, Vol. 96, Part 1, 963-971.

Law, M. (1998)

"The forum"

Journal of Fire Sciences, Vol. 16 (2), 149-150.

Law, M. and Beever, P. (1998)

"Letters to the editor"

Journal of Applied Fire Science, Vol. 7 (2), 215-219.

Li, Y. (2000)

"Buoyancy-driven natural ventilation in a thermally stratified one-zone building"

Building and Environment, Vol. 35, 207-214.

Linden, P.F. (1990)

"Emptying filling boxes: the fluid mechanics of natural ventilation"

Journal of Fluid Mechanics, Vol. 212, 309-335.

Linden P.F. and Cooper P. (1996)

"Multiple sources of buoyancy in a naturally ventilated enclosure"

Journal of Fluid Mechanics, Vol. 311, 177-192.

MAPLE V (1998)

MAPLE version 5.1 user's manual, Waterloo Maple Inc., Ontario, Canada

Matsushita, K. (1993)

"An environmental study of underground parking tunnel and lot developments in Japan"

Tunnelling and Underground Space Technology, Vol. 8, 65-73

MATLAB (1997)

Guide and tutor, Version 5, The Mathworks Inc., Massachusetts, USA

Ministry of Construction (1995)

Clause explanation of design code for residential buildings (GB50045-95)

China Ministry of Construction

Ministry of Construction (1999)

Design code for residential buildings (GB50096-1999)

China Ministry of Construction

Ministry of Public Security (1989)

Code for fire protection design of commercial buildings (JGJ48-88, 1989).

Ministry of Public Security, Ministry of Construction, P.R. China

Ministry of Public Security (1995)

Code for fire protection design of buildings (GBJ-16-87, 1995).

Ministry of Public Security, Ministry of Construction, P.R. China

Ministry of Public Security (1997)

Code for fire protection design of tall buildings (GB50045-95, 1997)

Ministry of Public Security, Ministry of Construction, P.R. China

Ministry of Public Security (1998)

Code for fire protection design of garage, motor-repair-shop and parking-area (GB50067-97, 1998)

Ministry of Public Security, Ministry of Construction, P.R. China

Morgan, H.P. (1987)

"Atrium building: smoke flows in atria for smoke-control design"

Fire Safety Journal, Vol. 12 (1), 9-35.

Morton, B.R. (1956)

"Turbulent gravitational convection from maintained and instantaneous sources"

Proceedings of Royal Society, Series A, Vol. 234 (1), 1-23.

NFPA 92A (1992)

"Recommended practice for smoke control system"

National Fire Protection Association, Quincy, MA, U.S.A.

NFPA 92B (1995)

"Guide for smoke management systems in malls, atria and large areas"

National Fire Protection Association, Quincy, MA, U.S.A.

NFPA (1994)

"Life safety code handbook"

National Fire Protection Association, Quincy, MA, U.S.A.

NFPA 92A (2001)

"Recommended practice for smoke control system"

National Fire Protection Association, Quincy, MA, U.S.A.

NFPA 92B (2001)

"Guide for smoke management systems in malls, atria and large areas"

National Fire Protection Association, Quincy, MA, U.S.A.

NFPA (2001)

"Life safety code handbook"

National Fire Protection Association, Quincy, MA, U.S.A.

NIST (1996)

"FASTLite engineering tools for estimating fire growth and smoke transport"

NIST SP 899, NIST, Gaithersburg: Maryland, U.S.A.

NPC (1988)

"Fire Law of People's Republic of China"

National People's Congress (NPC), China

Oxford (1992)

"Computational Ordinary Differential Equations: Based on the proceedings of a

conference on Computational Ordinary Differential equations,"

Oxford Clarendon Press, Oxford University Press - New York.

Peacock, R.D., Reneke, P.A., Bukowski, R.W. and Babrauskas, V. (1999)

"Defining flashover for fire hazard calculations"

Fire Safety Journal, Vol. 32 (4), 331-345.

PHOENICS (2000)

"Documentation for PHOENICS, Version 3.1"

Concentration, Heat & Momentum Limited, Bakery House, 40 High Street,

Wimbledon,

London SW19 5AU, UK.

Quintiere, J. (1995)

"Fundamental of enclosure fire zone models"

SFPE Fire Protection Engineering Handbook, SFPE-NFPA, 7th Edition.

Rehm, R.G. and Forney, G.P. (1992)

"A note on the pressure equations used in zone fire modelling, "

NISTIR 4906, Building and Fire Research Laboratory, National Institute of

Standard and Technology, Gaithersburg, Maryland, USA.

Rouse, H. (1954)

"Gravitational convection from a boundary source"

Tellus, Vol. 4 (3), 201-210.

Shaw, B. H. and Whyte W. (1974)

"Air movement through doorways - the influence of temperature and its control

by forced airflow, Building Services Research Unit"

University of Glasgow, BSE, December, Vol. 42.

Shen, W (2001)

"A glance of U.S. building fire code system"

A special report of National Information Network of Building Technology, November 28, 2001

Stankunas, A. (1989)

"Contaminant level control in parking garages"

ASHRAE Transactions, Vol. 95 (1), 584-605.

Thomas, P.H. (1963-1964)

"Investigations into the flow of hot gases in roof venting"

Fire research technical paper no. 7, London, U.K.

Thomas, P.H. (1995)

"The growth of fire-ignition to full involvement"

Combustion Fundamentals of Fire (Ed. G. Cox) Academic Press - London.

Wang, Y.S. (1989)

"Numerical Calculation on Burning Process"

Science Press, 134-135.

Webster, M.F. (2001)

"General Computational Fluid Dynamics"

Institute for Non-Newtonian Fluid Mechanics, The University of Wales, UK

Wilson, D.J. (1990)

"Gravity driven counterflow through an open door in a sealed room"

Building and environment, Vol. 25 (4), 379-388.

Wong, C. K. (1999)

"Overview for design and commissioning of smoke control system"

Seminar on Hot Smoke Test, Regal Kowloon Hotel, Hong Kong, 12 March 1999

Yih, C.S. (1977)

"Fluid mechanics: A concise introduction to the theory"

West River Press, Ann Arbor, Michigan, USA

Yu, C.Z. (1992)

"Guide to circumstance fluid mechanics"

Tsinghua publish house, China

Zukoski, E.E. (1981)

"Entrainment in fire plume"

Fire Safety Journal, Vol. 3 (2), 107-121.

Appendix A REQUIREMENTS ON DESIGN OF BUILDINGS IN CHINA FIRE CODE

A.1 Basic knowledge of China Fire Codes

Fire codes in China are complex in nature. They can be classified in two main ways: by legal effects and by contents. The details are shown in Table 2-1. For classification by legal effects, there are three types of fire codes: Legislative Laws, Administrative Fire Code and Local Fire Code. Legislative Laws about fire include:

- Fire Law of People's Republic of China (NPC 1998), which is the first and basic law of fire code in China.

- Regulations in Penal Law of China. For example, articles in no. 2, 14, 100, etc ... are focused on fire.

- Public Security Punishment Regulation of P.R.C.

- Administrative Procedural Law of P.R.C.

- City Planning Law of P.R.C

Administrative Fire Codes are constituted by State Council or Ministries based on practical need. These are applied only in areas under their management. Building Codes (Ministry of Public Security 1995 & 1997, Ministry of Construction 1999) are in this category. Local Fire Codes are constituted by all provincial governments and their subordinates, and are applied only in the areas they are in charge of.

For classification by contents, there are three types of fire codes: General Administrative Fire Code, Fire Code of Management and Administration, and Technical Law. General Administrative Fire Code is the Fire Law (NPC 1998) approved by National People's Congress, the legislative body of China. Fire Code of Management and Administration is a good complement to practice constituted by State Council and Ministries. It includes:

- Fire codes issued by State Council.

- Fire codes constituted by the Ministry of Public Security.

- Fire codes jointly-constituted by the Ministry of Public Security and other Ministries.

- Fire codes drafted by specialized ministry.

- Fire codes drafted by local government.

Technical Law is the code of practice. Its contents are:

- Technical fire codes on building.

- Fire codes on petroleum and chemical industry.

- Fire alarm system.

- Fixed fire extinguisher.

- Technical fire codes on fire station.

- Fire technology standard.

Many fire codes in China are related to buildings, among which the three most popularly used are: Code for fire protection design of buildings (GBJ-16-87,

Ministry of Public Security 1995), Code for fire protection design of tall buildings (GB50045-95, Ministry of Public Security 1997), and Design code for residential buildings (GB50096, Ministry of Construction 1999).

A.2   Main requirements on design of building in China Fire Codes

The following requirements are specified in China Code for fire protection design of buildings (GBJ-16-87, Ministry of Public Security 1995)

* **Zoning**

When a fire occurs in a building, it will spread to other places due to the effect of ventilation and radiation. At last, it might become a big fire involving the whole building. It is very important to control a fire in a certain area or zone in a given time. Zoning is an important concept of buildings in China fire code. Zoning is to use some fireproof components to divide a building into different parts, to resist fire spread to other parts in a certain period of time. Zoning can control a fire in a certain area, decrease the loss and make a good condition for egress and extinguishments.

* **Fireproof space between buildings**

The purpose of fireproof space between buildings is to decrease the effect of heat radiation, escaping, and provide a space for fire fighters. The minimum requirements on space between buildings are listed in Table 2-10. The primary factor considered for fireproof space is radiation, which spread the fire among

adjacent buildings. Effect of wind is also considered (Ministry of Construction 1995).

• **Passageway**

Requirements on passageway are based on the consideration of a one-way road, and the width must meet the design of a fire engine. Passageway for fire should be set on the street for buildings which is 150 m facing the street or 220 m in length or their closure yard is 24 m. Passageway is also required for access to water source or fire pools. The passageway should not be less than 3.5 m in width and larger than 160 m in distance to the building. Aerial cables or barriers on the way to fire should not be lower than 4 m. Circle way should link to other driveways with two exits. If using traffic road, the requirement is the same as above.

• **Fireproof class**

Some of the building materials are flammable, others are not or difficult to be burned. The better performance of the material in fire endurance, the higher fireproof class it will be. According to the difference in building structure, fireproof class can be divided into four groups:

Class I: Reinforced concrete floor, roof and wall.

Class II: Steel structure frame.

Class III: Wood roof, reinforced concrete story blank and brick wall.

Class IV: Noncombustible firewalls only, with combustible components.

The performance of burning and the minimum fireproof time limited are shown in Table 2-11. The number of hours in the table is based on 24 case studies of fire (Ministry of Construction 1995). Ninety-one percent of fire burnt continuously for 1 to 2 hours in a single fire zone, another five percent of fire burnt continuously for 2 to 3 hours in a single fire zone.

The relationships between fireproof class and the area, length and stories of the building are shown in Table 2-12.

- **Roof**

For Class I buildings, roof should be built by noncombustible materials. For Class II buildings, steel structure can be considered when common roof cannot reach 0.5 hour minimum fire resistance time (See Table 2-11). Scuttles should be set in each fireproof zone 50 m apart from each one. The way to the roof should be near to the stairs. The requirements are referred to the Japanese Building Code (Ministry of Construction 1995).

A.3   Main requirements on ventilation design of building

To make sure that there is no smoke in the means of escape and fire lifts during a fire, ventilation system and smoke extract system should be installed. Unique ventilation system should be installed to rooms storing combustible or explosive things. A direct ventilation system should be set up every four to six stories. Ventilation tubes should be made of noncombustible materials. Ventilation

systems with heating equipment or close to fire should be made of non-combustible materials. The power switch of the heating equipment should be linked to the wind supply system or other cooling system. Temperature detectors may be considered if necessary. Ventilation system should not be installed through the firewall or other fireproof separate part.

The requirements on both natural and forced ventilations are based on the experiments in the Tianjin Fire Research Institute authorized by the Ministry of Public Security, and also referred to the building codes of other countries (NFPA 1994 & 2001, BCA96 1996), which the requirements are six air changes per hour for rooms less than 600,000 ft^3 and four air changes per hour for rooms larger than 600,000 ft^3 (NFPA 1994 & 2001). The calculation method of ventilation parameters has been illustrated in Clause explanation of design code for residential buildings (GB50045-95) (Ministry of Construction 1995).

A.4   Main requirements on egress design of building

• **Time of escape**

Time of escape means the necessary time for all the people to leave the dangerous building. With experimental simulation and taken in account the reaction factors, the time of escape is limited as:

- 6 minutes for Class I and II buildings

- 2 to 4 minutes for Class III and IV buildings

The results were obtained from a series of experiments in the Tianjin Fire Research Institute authorized by the Ministry of Public Security, and also referred to the Life Safety Code (NFPA 1994 & 2001). Normally, a steel structure building is going to crash in 10 to 20 minutes in a fire according to a former survey (Ministry of Construction 1995).

- **Travel distance**

Travel distance means the distance from the escape spot to the safe place. The time of escape is thus determined by the travel distance. The limitations are listed in Table 2-13.

- The travel distance in buildings with opening corridor can be permitted up to 5 m.

- The travel distance in buildings with sprinklers can be increased by 25%.

- Rooms in the middle of two stairs should be decreased to 5 m. Rooms on the side or at the dead end (end of U type corridor) must be decreased to 2 m.

- The distance from the farthest point of the room to the door should not exceed the distance from the door, which is by the side, or at the end of U type corridor to the exit.

The above requirements were created after referring to other countries' building fire codes (NFPA 1994 & 2001, BCA96 1996). For example, the requirements of travel distance are 25 m in Russia, 9 to 30 m in U.S., 24 m in Hong Kong and 20 m in France. To avoid people crowded together and pushing each other when

escape during a fire, two exits could not be set too close on the same floor. Requirements of exit permitted to install one stair are listed in Table 2-14.

• **Exit**

Exit and egress make people a way out. The requirement of egress width of an exit W_e is related to the number of persons N_{per} and a width index I_w:

$$W_e = \frac{N_{per} I_w}{100}$$

(A-1)

Values of I_w are shown in Tables 2-15 to 2-17.

It is required that the corridor should not be less than 0.9 m in width, based on the consideration of two people passing through the corridor shoulder by shoulder, and one walking on the other one's side.

Two exits are required to be set in the amusement occupancies and karaoke boxes. It is because, if one of the exits is blocked during a fire, people could use the other one for evacuation. The requirements on width of exit, door and corridor are referred to the Building Code of Australia (BCA96 1996) and NFPA Life Safety Code (NFPA 1994 & 2001) (Ministry of Construction 1995).

- **Illumination**

For the convenience of escape at night or in the smoke, illumination of means of escape, stair signs and exit signs should be installed. spared power source or UPS should be ready for illumination, and lasting for more than 20 minutes. Illumination levels shall be at least 0.5 lx and 3 m in sight when a fire occurs. Emergency lighting shall be set on the top of exit, on the wall and the corner of corridor. The position of installation is better to be under the sight line (under 1 m). Sign space should not exceed 20 m. A glass cover for emergency lighting and exit signs should be added for protection. The requirements on illumination for the two codes are the same.

A.5 Main requirements on water supply for fire extinguishment

Water sources are primary facilities for fire extinguishment. Enough water pressure inside the fire hydrant (FH) pipes is very important. The calculation on the usage of water and the water pressure inside the fire hydrant (FH) pipes are illustrated in Clause explanation of design code for residential buildings (GB50045-95) (Ministry of Construction 1995). Water sources for fire are usually from water pipes, natural source or fire water pool. For natural source, it should be sure that the pool can be used in lower level. Water supply is permitted to be cancelled to living zones under 500 people and only two stories buildings. Requirements of water supply system indoor are listed in Table 2-18.

Appendix B   DOORWAY VENTILATION

For future study of forced ventilation, a review of air movement through the doorway is made.

Air flow through open doorways influences the air infiltration heat loss, room air circulation patterns and the distribution of indoor air contaminants between rooms in a building. Estimates of doorway flow rates are required for smoke control in fires. For exterior doorways in residential building, flow induced by the indoor-outdoor temperature difference is usually the most important exchange mechanism.

The counter-flowing streams of incoming cold air and outgoing warm air through an open door can be idealized as a pair of inviscid flows driven by pressure forces produced by density differences (Wilson 1990, Shaw 1974). Inflow and outflow rates are coupled by the requirement that the total volume inflow to a sealed room from all sources must equal the outflow. The low patterns are shown in Figure B-1. The cross-stream mixing in the counter-flowing shear layer has two important effects on the air exchange rate. The inviscid flow is determined with the following assumptions (Wilson 1990):

- There is no mixing or heat transfer between the incoming flow with density ρ_1, temperature T_1 and the outgoing flow with ρ_2 and T_2.

- Air infiltration from other leakage sites in the room is negligible, and there is no mechanical supply or exhaust ventilation.

- Streamlines are straight and parallel at the door orifice, with only hydrostatic pressure differences acting across them. These pressures are assumed to be in equilibrium with the outside in the outgoing flow, and with the inside pressure in the incoming flow $P_1 = P_2$.
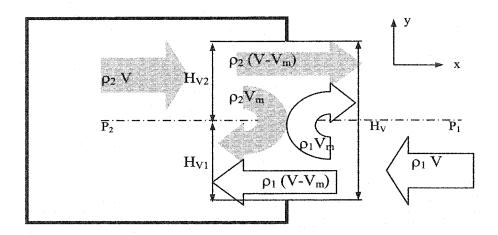
Figure B-1: The mixing between counter-flowing streams

B1. Inviscid flow

For the incoming flow, the Bernoulli equation for an inviscid streamline in the inflow of outdoor air passing through the door is:

$$\frac{P(y)}{\rho_2} + \frac{U_1^{i2}}{2} + gy = \frac{P_1}{\rho_1} \qquad\qquad \text{(B-1)}$$

$$P(y) = P_2 - \rho_2 gy \qquad\qquad \text{(B-2)}$$

$$P_1 = P_2$$

Assumption: Indoor, outdoor pressure equilibrium

Combining equations (B-1) and (B-2),

$$\frac{P_2 - \rho_2 gy}{\rho_1} + \frac{U_1^{i2}}{2} + gy = \frac{P_1}{\rho_1}$$

$$U_1^{i2} = 2(\frac{P_1 - P_2 + \rho_2 gy}{\rho_1} - gy)$$

$$U_1^{i2} = 2(\frac{\rho_2 gy - \rho_1 gy}{\rho_1})$$

$$U_1^{i2} = 2gy(\frac{\rho_2 - \rho_1}{\rho_1})$$

$$U_1^{i2} = 2gy\frac{\Delta\rho}{\rho_1}$$

$$U_1^{i} = \left[2gy\frac{\Delta\rho}{\rho_1}\right]^{0.5} \qquad\qquad \text{(B-3)}$$

where $\Delta\rho = |\rho_1 - \rho_2|$

Integrating velocity to inflow height without outflow,

$$V_1^i = \int_A \int_{V'} v' dA$$

$$= \int_0^{H_v} U_1^i W_v dy$$

$$= \int_0^{H_v} \left[2gy \frac{\Delta\rho}{\rho_1} \right]^{0.5} W_v dy$$

$$= \left[2g \frac{\Delta\rho}{\rho_1} \right]^{0.5} W_v \int_0^{H_v} y^{0.5} dy$$

$$= \frac{2}{3} H_{V1}^{1.5} \left[2g \frac{\Delta\rho}{\rho_1} \right]^{0.5} W_v \qquad (B-4)$$

Similarly: outgoing flow

$$U_2^i = \left[2gy \frac{\Delta\rho}{\rho_2} \right]^{0.5} \qquad (B-5)$$

$$V_2^i = \frac{2}{3} H_{V2}^{1.5} \left[2g \frac{\Delta\rho}{\rho_2} \right]^{0.5} W_v \qquad (B-6)$$

Assumption: Lack of mixing between inflowing outdoor air and the indoor air remaining in the room

Because: the temperature differences between inflow air and indoor air is larger than a few degrees Celsius and there is no mechanical ventilation system installed in the room

Equations (B-4) to (B-6):

$$V_1^i = V_2^i$$

$$\frac{2}{3}H_{V1}^{1.5}\left[2g\frac{\Delta\rho}{\rho_1}\right]^{0.5}W_V = \frac{2}{3}H_{V2}^{1.5}\left[2g\frac{\Delta\rho}{\rho_2}\right]^{0.5}W_V$$

$$\left[\frac{H_{V1}}{H_{V2}}\right]^{\frac{3}{2}} = \left[\frac{\rho_1}{\rho_2}\right]^{\frac{1}{2}}$$

$$\frac{H_{V1}}{H_{V2}} = \left[\frac{\rho_1}{\rho_2}\right]^{\frac{1}{3}} \tag{B-7}$$

Because: Total door height of $H_V = H_{V1} + H_{V2}$

$$\frac{H_V - H_{V2}}{H_{V2}} = \left[\frac{\rho_1}{\rho_2}\right]^{\frac{1}{3}}$$

$$\left[1 + \left(\rho_1\middle/\rho_2\right)^{\frac{1}{3}}\right]H_{V2} = H_V$$

$$H_{V2} = \frac{H_V}{1 + \left(\rho_1/\rho_2\right)^{\frac{1}{3}}} \tag{B-8}$$

Putting equation (B-8) into equation (B-6) gives the inviscid inflow or outflow,

$$V^i = V_2^i = V_1^i$$

Since

$$V_2^i = \frac{2}{3} H_{V2}^{1.5} \left[2g \frac{\Delta \rho}{\rho_2} \right]^{0.5} W_V$$

Putting equation (B-8) into equation (B-6),

$$V_2 = \frac{2}{3} \left[\frac{H_V}{1 + (\rho_1/\rho_2)^{\frac{1}{3}}} \right]^{1.5} \left[2g \frac{\Delta \rho}{\rho_2} \right]^{0.5} W_V$$

$$= \frac{1}{3} \left[\frac{8 H_V^3}{\left[1 + (\rho_1/\rho_2)^{\frac{1}{3}} \right]^3} \bullet g \frac{\Delta \rho}{\rho_2} \right]^{0.5} W_V$$

$$= \frac{W_V}{3} \left[g \frac{\Delta \rho}{\rho_e} H_V^{\ 3} \right]^{0.5} \tag{B-9}$$

Where

$$\rho_e = \frac{\left[1 + (\rho_o/\rho_i)^{\frac{1}{3}} \right]^3}{8} \rho_2 \tag{B-10}$$

B2.   Discharge coefficient

$$C_d = V/V^i$$

$$V = V_2 = V_1$$

With no cross-stream interfacial mixing, from equation (B-9),

$$V = C_d V_2 = C_d \frac{W_v}{3} \left[g \frac{\Delta \rho}{\rho_e} H_v^3 \right]^{0.5}$$

Replacing effective density ρ_e with average density,

$$\rho_a = (\rho_1 + \rho_2)/2$$

$$V = C_d \frac{W_v}{3} \left[g \frac{\Delta \rho}{\rho_a} H_v^3 \right]^{0.5}$$

$$V = C_d V_2 = C_d \frac{W}{3} (g' H_v^3)^{0.5} \qquad \text{(B-11)}$$

where the effective acceleration of gravity is:

$$g' = g \Delta \rho / \rho_a$$

B3. Mixing coefficient

V_n Net flow rate

V_m Mixing flow rate

Defining:

Interfacial mixing coefficient:

$$C_m = V_m / V$$

$$V_n = (V - V_m) = (V - C_m V) = (1 - C_m) V \qquad \text{(B-12)}$$

Doorway orifice coefficient K' is:

$$K' = C_d (1 - C_m) \tag{B-13}$$

$$V_n = (1 - C_m)V$$

$$= \frac{K'}{C_d} V$$

$$= \frac{K'}{C_d} C_d \frac{W_v}{3} (g'H_v^3)^{0.5}$$

$$= \frac{K'}{3} (g'H_v^3)^{0.5} \tag{B-14}$$

Integrating equation (B-14) for the period when the door is moving from a closed position to a 90° open position:

Total air exchange volume:

$$V = V_N t_N$$

$$= \frac{K'}{3} W_v (g'H_v^3)^{0.5} t_N$$

$$= \frac{K'}{3} W_v (g'H_v^3)^{0.5} \int_0^t dt \tag{B-16}$$

Appendix C   DERIVATION OF EQUATIONS FOR SMOKE LAYER INTERFACE HEIGHT AND SMOKE LAYER TEMPERATURE

C.1   Derivation of equations for smoke layer interface height

Consider mass flow rates in the lower cool layer:

$$m_L + m_P + m_e = 0 \tag{C-1}$$

where m_L is the change of mass flow rate in the cool layer; m_P is the plume flow rate; and m_e is the air flow rate through the leakage. m_L is given by averaging the density of the lower layer of air ρ_L as $\rho_L A Z_i$,

$$m_L = \rho_L A \frac{dZ_i}{dt} \tag{C-2}$$

From the plume expression (Wang 1989, Zukoski 1980):

$$m_P = 0.21 \big(Q'(t) \big)^{1/3} \rho_L \sqrt{g Z_i(t)} Z_i^2 \tag{C-3}$$

where

$$Q'(t) = \frac{(1 - L_C)\dot{Q}(t)}{\rho_L C_p T_g \sqrt{g Z_i} Z_i^2} \tag{C-4}$$

Putting equation (C-4) into equation (C-3),

$$m_P = 0.21 \left(\frac{(1-L_C)\dot{Q}(t)}{\rho_L C_p T_g \sqrt{gZ_i} Z_i^2} \right)^{1/3} \rho_L \sqrt{gZ_i} Z_i^2$$

$$m_P = 0.21 \left(\frac{(1-L_C)\dot{Q}(t)g}{\rho_L C_p T_g} \right)^{1/3} \rho_L Z_i^{5/3} \tag{C-5}$$

Equation (C-5) can be rewritten as:

$$m_P = C_2 \dot{Q}(t)^{1/3} \rho_L A_f Z_i^{5/3} \tag{C-6}$$

where

$$C_2 = (0.21/A_f)[(1-L_C)g/(\rho_L C_p T_g)]^{1/3}$$

Equation (C-5) can also be simplified as:

$$m_P = KZ_i^{5/3} \tag{C-7}$$

where

$$K = 0.21 \left(\frac{(1-L_C)\dot{Q}(t)g}{\rho_L C_p T_g} \right)^{1/3} \rho_L$$

K can also be given in terms of the partial vapour pressure of water P_{H_2O}; the partial vapour pressure of carbon dioxide P_{CO_2}; the static pressure of air P; the thickness of the air layer around the plume d_l; and the temperature of the gas T_g (Wang 1989):

$$K = \left(\frac{0.78 + 1.6P_{H_2O}/P}{\sqrt{(P_{H_2O} + P_{CO_2})d_1/P}} - 0.1 \right) \times \left(1 - 0.37\frac{T_g}{1000} \right)\left(P_{H_2O} + P_{CO_2} \right) \quad (C\text{-}8)$$

From the first law of thermodynamics, the rate of heat flowing in is equal to the rate of heat flowing out:

$$q_1 = q_2 \qquad\qquad (C\text{-}9)$$

q_1 is the heat release rate of the fire $\dot{Q}(t)$:

$$q_1 = \dot{Q}(t) \qquad\qquad (C\text{-}10)$$

q_2 is the sum of heat lost through leakage $m_e C_p T_g$ and heat lost by conduction and radiation $L_C\dot{Q}(t)$, where L_C is a conduction and radiation fraction of $\dot{Q}(t)$ of value about 35%. This gives:

$$q_2 = L_C\dot{Q}(t) \qquad\qquad (C\text{-}11)$$

$$\dot{Q}(t) = L_C\dot{Q}(t) + m_e C_p T_g \qquad\qquad (C\text{-}12)$$

or

$$m_e = \frac{\dot{Q}(t)(1-L_C)}{C_p T_g}$$ (C-13)

Putting equations (C-2), (C-7) and (C-13) into equation (C-1),

$$\rho_L A_f \frac{dZ_i}{dt} + \frac{\dot{Q}(t)(1-L_C)}{C_p T_g} + K Z_i^{5/2} = 0$$ (C-14)

where ρ_L is the density of air in the cool layer of 1.293 kgm^{-3}; A_f is the floor area of the room; C_p is the specific heat capacity of air, 1.004 KJ· kg^{-1}· K^{-1}; T_g is the temperature of the cool layer, 300 K; and L_C is the fraction of heat lost by conduction and radiation of $\dot{Q}(t)$ of value 0.35.

For Z_i higher than the height of the fire, taking T_L to be T_g gives:

$$dZ_i / dt = (1/\rho_L A_f)\{-\dot{Q}(t)(1-L_C)/(C_p T_g) - 0.21\rho_L (gZ_i)^{1/2} Z_i^2 \\ \times \left[(1-L_C)\dot{Q}(t)/(\rho_L C_p T_g (gZ_i)^{1/2} Z_i^2)\right]^{1/3}\}$$ (C-15)

This equation can be rewritten as:

$$dZ_N / dt_N = -C_1 q - C_2 q^{1/3} Z_N^{5/3}$$ (C-16)

where C_1 and C_2 are:

$$C_1 = (1 - L_C)/(\rho_L C_p T_g A_f) \tag{C-17}$$

$$C_2 = (0.21/A_f)[(1 - L_C)g/(\rho_L C_p T_g)]^{1/3} \tag{C-18}$$

This equation can be solved numerically as used in the Euler method with:

$$\begin{cases} \dfrac{dZ_i}{dt} = f(Z_i, t) \\ Z(t_0) = Z_0 \end{cases} \tag{C-19}$$

$$Z_{n+1} = Z_n + h\, f\,(t_n, Z_n) \tag{C-20}$$

C.2   Derivation of equations for smoke layer temperature

From the eleven basic equations of the two-layer zone model, the hot smoke layer temperature could be expressed as:

$$\frac{dT_h}{dt} = \frac{1}{C_p \rho_h V_h}\left[\left(q_h - C_p m_h T_h\right) + V_h \frac{dP}{dt}\right] \tag{C-21}$$

According to the ASET model assumption,

$$\frac{dP}{dt} = 0$$

Equation (C-21) can be simplified as:

$$\frac{dT_h}{dt} = \frac{1}{C_p \rho_h V_h} \left(q_h - C_p m_h T_h \right) \qquad \text{(C-22)}$$

The energy of hot layer q_h comes from two parts, the fire $(1 - L_C)\dot{Q}(t)$, and the plume $C_p m_P T_g$.

$$q_h = (1 - L_C)\dot{Q}(t) + C_p m_P T_g \qquad \text{(C-23)}$$

Putting in equation (C-22),

$$\frac{dT_h}{dt} = \frac{1}{C_p \rho_h V_h} \left((1 - L_C)\dot{Q}(t) + C_p m_P T_g - C_p m_h T_h \right) \qquad \text{(C-24)}$$

Hot smoke layer volume V_h can be expressed as:

$$V_h = A_f (H - Z_i) \qquad \text{(C-25)}$$

For no ventilation:

$$m_h - m_P = 0$$

or $\qquad m_h = m_P$ (C-26)

$$P = R'\rho_h T_h = R'\rho_L T_g$$

$$\rho_h = \rho_L \frac{T_g}{T_h}$$ (C-27)

Putting equations (C-25), (C-26) and (C-27) into equation (C-24):

$$\frac{dT_h}{dt} = \frac{T_h}{C_p \rho_L A_f (H - Z_i) T_g} \left((1 - L_C)\dot{Q}(t) + C_p m_P (T_g - T_h) \right)$$ (C-27)

or

$$\frac{dT_h}{dt} = \frac{T_h}{(H - Z_i)} \left(\frac{(1 - L_C)\dot{Q}(t) + C_p m_P T_g}{C_p \rho_L A_f T_g} - \frac{T_h m_P}{\rho_L A_f T_g} \right)$$ (C-28)

This equation can be rewritten as:

$$dT_N / dt_N = T_N [C_1 q + (1 - T_N / T_g) C_2 q^{1/3} Z_N^{5/3}] / (H - Z_N)$$ (C-29)

Appendix D MAPLE V AND MATLAB PROGRAM LISTINGS

D.1 MAPLE V program listing

[1] Main program for constant fire:

```
> A:=10;

> H:=3.5;

> Q:=800000;

> Lc:=0.35;

> Cp:=1004;

> k:=600;

> Tg:=300;

> g:=9.8;

> pL:=1.293;

>

> TMAX1:=sqrt(Q/1000/1000)*k;

> TMAX:=trunc(TMAX1);

>

> C1:=(1-Lc)/(Cp*Tg*pL*A);

> C2:=0.21*((1-Lc)*g/(pL*Cp*Tg))^(1/3)/A;

>

> with(share);

> with(ODE);
```

```
> S0:=[0.0,H];

> eq0:=(t,Z)->-C2*(Q)^(1.0/3.0)*Z^(5.0/3.0)-C1*Q;

> Z1:=rungekuttahf(eq0,S0,0.1,1);

> Zt:=Z1[1];

> RS:=[Zt[1],Zt[2],Tg];

> dppts3:=array(0..909);

> dppts3[1]:=RS;

> for n from 1 by 1 while RS[2]>=0.001 do

>   for i from 1 by 1 while i<=10 do

>     eq12:=(t,Z,T)->-C2*(Q)^(1.0/3.0)*Z^(5.0/3.0)-C1*Q;

>     eq22:=(t,Z,T)->T/(H-Z)*(C1*(Q)+C2*

> ((Q)^(1.0/3.0))*(1.0-T/300)*Z^(5.0/3.0));

>     rkpts2:=rungekuttahf([eq12,eq22],RS,0.1,1);

>     RS:=rkpts2[1];

>   od;

>   dppts3[n]:=RS;

> od;

> plot(makelist(dppts3));
```

[2] Main program for t^2 fire:


```
> A:=10;

> H:=3.5;

> Q:=800000;
```

```
> Lc:=0.35;

> Cp:=1004;

> k:=600;

> Tg:=300;

> g:=9.8;

> pL:=1.293;

>

> TMAX1:=sqrt(Q/1000/1000)*k;

> TMAX:=trunc(TMAX1);

>

> C1:=(1-Lc)/(Cp*Tg*pL*A);

> C2:=0.21*((1-Lc)*g/(pL*Cp*Tg))^(1/3)/A;

>

> with(share);

> with(ODE);

> S0:=[0.0,H];

>eq0:=(t,Z)->-C2*(1000*(t/k)^2.0*1000.0)^(1.0/3.0)*Z^(5.0/3.0)-

C1*1000*(t/k)^2.0*1000.0;

> Z1:=rungekuttahf(eq0,S0,0.1,1);

> Zt:=Z1[1];

> RS:=[Zt[1],Zt[2],Tg];

> dppts3:=array(0..909);

> dppts3[1]:=RS;

> for m from 1 by 1 to TMAX while RS[2]>=0.001 do
```

```
>   for i from 1 by 1 while i<=10 do

>     eq11:=(t,Z,T)->-C2*((1000*(t/k)^2.0*1000.0)^(1.0/3.0))*(Z^(5.0/

>     3.0))-C1*1000*(t/k)^2.0*1000.0;

>     eq21:=(t,Z,T)->T/(H-Z)*(C1*1000*(t/k)^2.0*1000.0+C1*

>  ((1000*(t/k)^2.0*1000.0)^(1.0/3.0))*(1.0-T/300)*(Z^(5.0/3.0)));

>     rkpts1:=rungekuttahf([eq11,eq21],RS,0.1,1);

>     RS:=rkpts1[1];

>   od;

>   dppts3[m]:=RS;

>   od;

> for n from 1 by 1 while RS[2]>=0.001 do

>   for i from 1 by 1 while i<=10 do

>     eq12:=(t,Z,T)->-C2*(Q)^(1.0/3.0)*Z^(5.0/3.0)-C1*Q;

>eq22:=(t,Z,T)->T/(H-Z)*(C1*(Q)+C2*((Q)^(1.0/3.0))*(1.0-

T/300)*Z^(5.0/3.0));

>     rkpts2:=rungekuttahf([eq12,eq22],RS,0.1,1);

>     RS:=rkpts2[1];

>   od;

>   dppts3[m+n-1]:=RS;

> od;

> plot(makelist(dppts3));
```

D.2 MATLAB program listing

[1] Main program for constant fire:

COMMAND-File

clear; clf;

% initial conditions

H = 3.5;

A = 10;

Tg = 300;

Q = 800;

g = 9.8;

Lc = 0.35;

Cp = 1004;

pcl = 1.293;

p = 1.013;

k = 600;

% C1 and C2

C1=(1-Lc)/(pcl*Cp*Tg*A);

C2=0.21/A*((1-Lc)*g/(pcl*Cp*Tg))^(1/3);

% calculate first step for avoiding divided by zero when Z(1) = H

```
Z0(1)=H;

[t,Z] = ode15s('asetsub1',[1:1:800],[Z0],[],Tg,H,Q,k,C1,C2);

zrelt = [t,Z];


% time step of Z > 0, te

for i = 1:1:800

    if zrelt(i,2)> 0.1      ta = i;

    end

end

te = fix(ta);


% initial Z

Ze = zrelt(2,2);


% calculate other steps

Z0(1)=Ze;

Z0(2)=300;


[t,Z] = ode15s('asetsub',[1:1:te],[Z0],[],Tg,H,Q,k,C1,C2);


    result = [t,Z];


% plot figures and ending

plot(t,Z(:,1),'k-');
```

figure

plot(t,Z(:,2),'k-');

save aset.dat Z -ascii

M-File

function dZ = asetsub1(t,Z,options,Tg,H,Q,k,C1,C2)

% dZ/dt is dZ(1)

dZ = zeros(1,1);

dZ(1)= -C1*(1000*Q)-C2*(1000*Q)^(1/3)*Z(1)^(5/3);

function dZ = asetsub(t,Z,options,Tg,H,Q,k,C1,C2)

% dZ/dt is dZ(1)

% dT/dt is dZ(2)

dZ = zeros(2,1);

dZ(1)= -C1*(1000*Q)-C2*(1000*Q)^(1/3)*Z(1)^(5/3);

dZ(2) = Z(2)/(H-Z(1))*(C1*(1000*Q)+C2*(1000*Q)^(1/3)*Z(1)^(5/3)*(1-Z(2)/Tg));

[2] Main program for t^2 fire:

COMMAND-File

clear; clf;

% initial conditions

D-7

```matlab
H = 3.5;

A = 100;


Tg = 300;

Q = 800;

g = 9.8;


Lc = 0.35;

Cp = 1004;

pcl = 1.293;

p = 1.013;

k = 600;


% C1 and C2

C1=(1-Lc)/(pcl*Cp*Tg*A);

C2=0.21/A*((1-Lc)*g/(pcl*Cp*Tg))^(1/3);


% calculate first step for avoiding divided by zero when Z(1) = H

Z0(1)=H;

[t,Z] = ode15s('aset2sub1',[1:1:800],[Z0],[],Tg,H,Q,k,C1,C2);

zrelt = [t,Z];


% time step of Z > 0, te

for i = 1:1:800
```

```matlab
    if zrelt(i,2)>0
      ta = i;
    end
end
te = fix(ta);


% initial Z
Ze = zrelt(2,2);


% calculate other steps
Z0(1)=Ze;
Z0(2)=300;


    [t,Z] = ode15s('aset2sub',[1:1:te],[Z0],[],Tg,H,Q,k,C1,C2);


    result = [t,Z];


% plot figures and ending
plot(t,Z(:,1),'k-');
figure
plot(t,Z(:,2),'k-');


save aset2.dat Z -ascii
```

<u>M-File</u>

```
function dZ = aset2sub1(t,Z,options,Tg,H,Q,k,C1,C2)


% dZ/dt is dZ(1)

dZ = zeros(1,1);

dZ(1)= -C1*(1000*(t/k)^2*1000)-C2*(1000*1000*(t/k)^2)^(1/3)*Z(1)^(5/3);


function dZ = aset2sub(t,Z,options,Tg,H,Q,k,C1,C2)

% dZ/dt is dZ(1)

% dT/dt is dZ(2)

dZ = zeros(2,1);

dZ(1)= -C1*(1000*(t/k)^2*1000)-C2*(1000*1000*(t/k)^2)^(1/3)*Z(1)^(5/3);

dZ(2)=Z(2)/(H-

Z(1))*(C1*(1000*1000*(t/k)^2)+C2*(1000*1000*(t/k)^2)^(1/3)*Z(1)^(5/3)*(1-

Z(2)/Tg));
```

Appendix E   DERIVATION   OF   NAVIER-STOKES EQUATIONS

E.1   An introduction of Navier-Stokes equation

The physical aspects of any fluid flow are governed by three fundamental principles: conservation of mass; Newton's second law and conservation of energy. These fundamental principles can be expressed in terms of mathematical equations, which in their most general form are usually partial differential equations. CFD is the science of determining a numerical solution to the governing equations of fluid flow whilst advancing the solution through space or time to obtain a numerical description of the complete flow field of interest (Webster 2001).

The governing equations for Newtonian fluid dynamics, the unsteady Navier-Stokes equations, have been known for over a century. However, the analytical investigation of reduced forms of these equations is still an active area of research, as is the problem of turbulent closure for the Reynolds averaged form of the equations. For non-Newtonian fluid dynamics, theoretical developments of chemically reacting flows and multiphase flows are not so advanced.
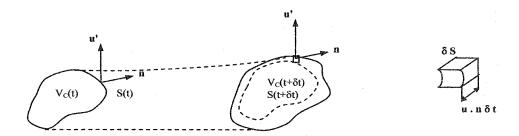
The role of CFD in engineering predictions has become so popular that it may be viewed as a new tool of fluid dynamics, besides classical experimental and analytical approaches.

The development of more powerful computers has furthered the advances being made in the field of CFD. Consequently, CFD is now the preferred means of testing alternative designs in many engineering consulting companies before carrying out experiments.

On the discretized mesh, the Navier-Stokes equations take the form of a system of non-linear equations. Transforming into a discrete set of equations would bring problems in both physics and numerical analysis. For example, it is important to maintain conservation of mass in the difference equations. Up to 20 variables on the pressure, the three velocity components, density, temperature and others such as chemical species concentrations will be encountered at each node. Furthermore, capturing important physical phenomena such as small-scale turbulence structure requires extremely fine meshes with 20,000 to 2,000,000 nodes, leading to about 40,000,000 unknowns (Webster 2001).

E.2   Basic physical laws

The Navier-Stokes equation was derived from basic physical laws. Several basic methods have been selected and used in deriving the equation (Currie 1974).

Normally, there are two ways to derive the motion of fluid equation. One is to approach the question from the molecules point of view. The fluid is treated as consisting of molecules, which is governed by the laws of dynamics. The macroscopic behavior of the fluid is predicted from the laws of mechanics and probability theory. The coefficient of viscosity and the thermal conductivity could be applied. The theory is well developed for light gases, but it is incomplete for poly-atomic gas molecules and liquids (Currie 1974).

Another method is to derive the equation by the use of continuum concept. Individual molecules are ignored and it is assumed that the fluid is consisted of continuous matter. It is required to satisfy the conservation laws of mass, momentum and energy, and field variables including velocity, pressure, density and others will be solved. The mean free path of the molecules should be very small compared with the smallest physical length scale of the flow field. It is widely used to solve fluid mechanics problems including liquids and gases.

Normally, the fluid is assumed to be incompressible, and the dynamic viscosity is assumed to be constant.

The density and the velocity at a point in the continuum are defined as:

$$\rho = \lim_{\Delta v_C \to \epsilon} \left(\frac{\sum \Delta m_C}{\Delta V_C} \right) \qquad \text{(E-1)}$$

$$u = \lim_{\Delta V_C \to \varepsilon} \left(\frac{\sum v \Delta m_C}{\Delta m_C} \right) \tag{E-2}$$

where ε is a sufficiently small volume compared with the smallest significant length scale in the flow field but is sufficiently large to contain a large number of molecules.

Mass in control volume is given by:

$$\int_{V_C} \rho \, dV_C \tag{E-3}$$

E.3   Reynolds' transport theorem

Material derivatives of volume integrals will be encountered in the combination of the arbitrary control volume and the Lagrangian coordinate system. It is necessary to transform such terms into equivalent expression involving volume integrals of Eulerian derivatives. The theorem, which would permit such a transformation is called the Reynolds' transport theorem (Currie 1974).

Any quantity of fluid α (such as mass, momentum in some direction or energy) is a function of t, $\alpha = \alpha(t)$. The rate of change of the integral of α is defined as follows:

$$\frac{D}{Dt}\int_{V_C(t)}\alpha(t)dV_C = \lim_{\delta t \to 0}\left\{\frac{1}{\delta t}\left[\int_{V_C(t+\delta t)}\alpha(t+\delta t)dV_C - \int_{V_C(t)}\alpha(t)dV_C\right]\right\} \qquad \text{(E-4)}$$

where $V_C(t)$ is the control volume containing the specified mass of fluid. The quantity $\alpha(t+\delta)$ integrated over $V_C(t)$ is subtracted.

$$\frac{D}{Dt}\int_{V_C(t)}\alpha(t)dV_C$$
$$= \lim_{\delta t \to 0}\left\{\frac{1}{\delta t}\left[\int_{V_C(t+\delta t)}\alpha(t+\delta t)dV_C - \int_{V_C(t)}\alpha(t+\delta t)dV_C\right] + \frac{1}{\delta t}\left[\int_{V_C(t)}\alpha(t+\delta t)dV_C - \int_{V_C(t)}\alpha(t)dV_C\right]\right\}$$

$$\text{(E-5)}$$

The expression for the Lagrangian derivative of the integral of α may be written in the following form:

$$\frac{D}{Dt}\int_{V_C(t)}\alpha(t)dV_C = \lim_{\delta t \to 0}\left\{\frac{1}{\delta t}\left[\int_{V_C(t+\delta t)-V_C(t)}\alpha(t+\delta t)dV_C\right]\right\} + \int_{V_C(t)}\frac{\partial\alpha}{\partial t}dV_C \qquad \text{(E-6)}$$

The distance from an inner surface to the outer surface is $u' \times n \times \delta t$, element of surface area is δS, element of volume change is $\delta V_C = u'\, n\, \delta t\, \delta S$. The surface enclosing $V_C(t)$ is denoted by $S(t)$. At any point on this surface, the velocity may be denoted by u' and the normal unit vector by n.

$$\frac{D}{Dt}\int_{V_C(t)}\alpha(t)dV_C = \lim_{\delta t \to 0}\left\{\left[\int_{S(t)}\alpha(t+\delta t)u'\cdot ndS\right]\right\} + \int_{V_C(t)}\frac{\partial\alpha}{\partial t}dV_C$$

$$= \int_{S(t)}\alpha(t)u'\cdot ndS + \int_{V_C(t)}\frac{\partial\alpha}{\partial t}dV_C \qquad \text{(E-7)}$$

The foregoing form of Reynolds' transport theorem is put in this desired form by converting the surface integral to a volume integral by the use of Gauss' theorem. In this way, the surface-integral term would become:

$$\int_{S(t)} \alpha(t)u' \cdot n dS = \int_{V_c(t)} \nabla \cdot (\alpha u') dV_C \qquad \text{(E-8)}$$

Substituting the result into the above expression and combining the two volume integrals would give the preferred form of Reynolds' transport theorem:

$$\frac{D}{Dt} \int_{V_c} \alpha dV_C = \int_{V_c} \left[\frac{\partial \alpha}{\partial t} + \nabla \cdot (\alpha u'_k) \right] dV_C \qquad \text{(E-9)}$$

or in tensor notation,

$$\frac{D}{Dt} \int_V \alpha dV = \int_V \left[\frac{\partial \alpha}{\partial t} + \frac{\partial}{\partial x_k} (\alpha u'_k) \right] dV \qquad \text{(E-10)}$$

E.4   Conservation of mass

The principle of mass conservation is: if the given fluid mass is followed as it flows, the mass of flow would remain unchanged when its size and shape are observed to change (Currie 1974).

$$\int_{V_c} \rho dV_C = 0 \qquad \text{(E-11)}$$

$$\frac{D}{Dt} \int_{V_C} \rho dV_C = 0 \qquad\qquad (E\text{-}12)$$

Converting this equation to a volume integral which contains only Eulerian derivatives by using Reynolds' transport theorem (E-10):

$$\int_{V_C} \left[\frac{\partial \rho}{\partial t} + \frac{\partial}{\partial x_k}(\rho u'_k) \right] dV_C = 0 \qquad\qquad (E\text{-}13)$$

The only way to satisfy the equation is, for all possible choices of V_C for the integrand to be 0.

$$\frac{\partial \rho}{\partial t} + \frac{\partial}{\partial x_k}(\rho u'_k) = 0 \qquad\qquad (E\text{-}14)$$

The momentum conservation equation comes from applying Newton's second law of motion to an element of the fluid. For a given mass of fluid in a Lagrangian frame of reference, the rate of momentum change of the fluid mass is equal to the net external force.

The net external body force acting on a mass of volume V_C is:

$$\int_{V_C} \rho f dV_C \qquad\qquad (E\text{-}15)$$

where f is a vector representing the resultant of the body forces per unit mass. The net external surface force acting on the surface S containing V is:

$$\int_S P_S dS \qquad\qquad\qquad\qquad (E\text{-}16)$$

where P_S is a surface vector which represents the resultant surface force per unit area.

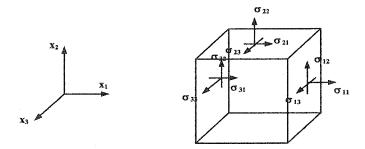The momentum contained in the volume V_C is:

$$\int_{V_C} \rho u' dV_C \qquad\qquad\qquad\qquad (E\text{-}17)$$

The rate of change of momentum of the mass contained within V_C is:

$$\frac{D}{Dt} \int_{V_C} \rho u' dV_C \qquad\qquad\qquad\qquad (E\text{-}18)$$

The mathematical equation resulted from imposing the physical law of conservation of momentum is:

$$\frac{D}{Dt} \int_{V_C} \rho u' dV_C = \int_S P_S dS + \int_{V_C} \rho f dV_C \qquad\qquad (E\text{-}19)$$

Generally, there are nine components of stress at a given point, one normal component and two shear components on each coordinate plane.

The stress is represented by the quantity σ_{ij}, where i and j refer to the stress at a point which may be represented by a tensor of rank 2.

There would be a surface force vector P_S at each point which is related to the stress tensor σ_{ij} on different plane. The unit normal vector acting on this surface is n_i, the resulting force acting in the x_1, x_2, x_3 direction is $P_{S1} = \sigma_{11}n_1$, $P_{S2} = \sigma_{12}n_1$, the surface force will be given by $P_{Sj} = \sigma_{ij}n_i$ where i is summed from 1 to 3. The equation of conservation of momentum is:

$$\frac{D}{Dt}\int_{V_C} \rho u_j dV_C = \int_S \sigma_{ij}n_i dS + \int_{V_C} \rho f dV_C \qquad (E\text{-}20)$$

By using Reynolds' transport theorem (E-10), the fluid property α here is the momentum per unit volume $\rho u'_j$ in the x_j direction.
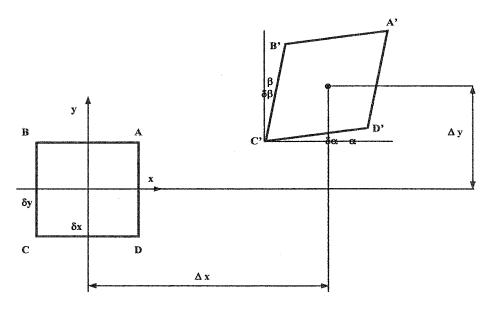
$$\int_{V_C}\left[\frac{\partial}{\partial t}(\rho u'_j) + \frac{\partial}{\partial x_k}(\rho u'_j u'_k)\right]dV_C = \int_{V_C}\frac{\partial \sigma_{ij}}{\partial x_i}dV_C + \int_{V_C}\rho f_j dV_C$$

$$\frac{\partial}{\partial t}(\rho u'_j) + \frac{\partial}{\partial x_k}(\rho u'_j u'_k) = \frac{\partial \sigma_{ij}}{\partial x_i} + \rho f_j$$

E-9

$$\rho \frac{\partial u'_j}{\partial t} + u'_j \frac{\partial \rho}{\partial t} + u'_j \frac{\partial}{\partial x_k}(\rho u'_k) + \rho u'_k \frac{\partial u'_j}{\partial x_k} = \frac{\partial \sigma_{ij}}{\partial x_i} + \rho f_j$$

According to equation (E-14), the sum of $u'_j \frac{\partial \rho}{\partial t}$ and $u'_j \frac{\partial}{\partial x_k}(\rho u_k)$ is zero,

$$\rho \frac{\partial u'_j}{\partial t} + \rho u_k \frac{\partial u'_j}{\partial x_k} = \frac{\partial \sigma_{ij}}{\partial x_i} + \rho f_j \qquad (E-21)$$

E.5 Rotation and rate of shear

The rotation of a fluid element about its own axis and the shearing of a fluid element is considered, and the tensor quantities which represent these physical quantities are identified in this part. A two-dimensional element of fluid, which is a rectangle with δx and δy at time $t = 0$ is shown in the above figure. After a short time interval δt, the center of the fluid element is moved to a new position. The distance of the two centers before and after the movement x is (Currie 1974):

$$\Delta x = \int_0^{\delta t} u'[x(t), y(t)]dt \qquad (E-22)$$

x and y must be close to zero for short times as δt, the velocity component u can

be expanded in Taylor series about the point (0,0):

$$\Delta x = \int_0^{\delta t} [u'(0,0) + x(t)\frac{\partial u}{\partial x}(0,0) + y(t)\frac{\partial u'}{\partial y}(0,0) + ...]dt \qquad (E-23)$$

Integrating the equation,

$$\Delta x = u'(0,0)\delta t + \int_0^{\delta t} [x(t)\frac{\partial u'}{\partial x}(0,0) + y(t)\frac{\partial u'}{\partial y}(0,0) + ...]dt = u'(0,0)\delta t + ... \quad (E-24)$$

Similarly,

$$\Delta y = v'(0,0)\delta t + ... \qquad (E-25)$$

The fluid element would rotate and be distorted as indicated by the corners while

the fluid body is moving, t = δt. The angle δα and δβ indicate the two sides of

the element, where α and β are positive when measured counterclockwise and

clockwise individually.

$$\delta\alpha = \tan^{-1}\left(\frac{y_{D'C'}}{x_{D'C'}}\right) = \tan^{-1}\left\{\frac{[v'(\frac{1}{2}\delta x,-\frac{1}{2}\delta x)\delta t + ...] - [v'(-\frac{1}{2}\delta x,-\frac{1}{2}\delta x)\delta t + ...]}{\delta x + ...}\right\}$$

$$(E-26)$$

where v' is evaluated first at point D at coordinates $(\frac{1}{2}\delta x,-\frac{1}{2}\delta x)$ and secondly at

point C, at coordinates $(-\frac{1}{2}\delta x,-\frac{1}{2}\delta x)$.

Expanding the velocity component v' in Taylor series about the point (0,0):

$$\delta\alpha = \tan^{-1}\left\{\frac{[v'(0,0) + \frac{1}{2}\delta x(\frac{\partial v'}{\partial x})(0,0) - \frac{1}{2}\delta y(\frac{\partial v'}{\partial y})(0,0) + ...]\delta t}{\delta x(1+...)}\right.$$

$$\left. -\frac{[v'(0,0) - \frac{1}{2}\delta x(\frac{\partial v'}{\partial x})(0,0) - \frac{1}{2}\delta y(\frac{\partial v'}{\partial y})(0,0) + ...]\delta t}{\delta x(1+...)}\right\}$$

$$= \tan^{-1}\left\{\frac{[\delta x(\frac{\partial v'}{\partial x})(0,0) + ...]\delta t}{\delta x(1+...)}\right\}$$

$$= \tan^{-1}\left\{\frac{[(\frac{\partial v'}{\partial x})(0,0) + ...]\delta t}{(1+...)}\right\}$$

$$= \tan^{-1}\left\{\left[(\frac{\partial v'}{\partial x})(0,0) + ...\right]\delta t\right\} \qquad \text{(E-27)}$$

Since the argument of the arctangent is small:

$$\delta\alpha = \left[(\frac{\partial v'}{\partial x})(0,0) + ..\right]\delta t + ...$$

$$\frac{\delta\alpha}{\delta t} = (\frac{\partial v'}{\partial x})(0,0) + ..$$

This expression represents the change in the angle α per unit time so that in the limit of δx, δy, and δt all tend to zero.

$$\alpha = \frac{\partial v'}{\partial x}(0,0) \qquad \text{(E-28)}$$

where α is the time derivative of the angle α. Similarly, the time derivative of the angle β is given by:

$$\beta = \frac{\partial u'}{\partial x}(0,0) \qquad \text{(E-29)}$$

The rate of clockwise rotation of the fluid element about its center is:

$$\frac{1}{2}(\dot{\beta} - \dot{\alpha}) = \frac{1}{2}\left(\frac{\partial u'}{\partial y} - \frac{\partial v'}{\partial x}\right) \qquad \text{(E-30)}$$

The shearing action is measured by the rate at which the sides B'C' and D'C' are approaching each other and is therefore given by the quantity:

$$\frac{1}{2}(\dot{\beta} + \dot{\alpha}) = \frac{1}{2}\left(\frac{\partial u'}{\partial y} + \frac{\partial v'}{\partial x}\right) \qquad \text{(E-31)}$$

The analysis above is carried out in two dimensions which may be considered as the projection of a three-dimensional element on the xy plane. If the analysis is carried out in the other planes, it can be verified that the rotation of rate of element is about its own axes.

$$\text{Rate of rotation} = \frac{1}{2}\left(\frac{\partial u'}{\partial y} - \frac{\partial v'}{\partial x}\right) \qquad \text{(E-32)}$$

$$\text{Rate of shearing} = \frac{1}{2}\left(\frac{\partial u'}{\partial y} + \frac{\partial v'}{\partial x}\right) \qquad \text{(E-33)}$$

Both the rate of rotation and the rate of shearing may be represented by tensors of rank 2.

Deformation-rate tensor e_{ij} is defined as:

$$e_{ij} = \frac{\partial u_i'}{\partial x_j} = \frac{1}{2}\left(\frac{\partial u_i'}{\partial x_j} - \frac{\partial u_j'}{\partial x_i}\right) + \frac{1}{2}\left(\frac{\partial u_i'}{\partial x_j} + \frac{\partial u_j'}{\partial x_i}\right) \qquad \text{(E-34)}$$

That is the antisymmetric part of the deformation-rate tensor which represents the rate of rotation of a fluid element in that flow field about its own axes while the symmetric part of the deformation-rate tensor represents the rate of shearing of the fluid element.

E.6   Constitutive equations

Nine elements of the stress tensor σ_{ij} are related to the nine elements of the deformation-rate tensor e_{kl} by a set of parameters (Currie 1974).

The stress tensor is supposed to satisfy the following conditions (Currie 1974):

- The stress is hydrostatic and the pressure exerted by the fluid is the thermodynamic pressure, when the fluid is at rest.

$$\sigma_{ij} = -P\delta_{ij} + \tau_{ij} \qquad \text{(E-35)}$$

where τ_{ij} is called the shear-stress tensor, which is dependent on the motion of the fluid only, P is the thermodynamic pressure, and δ_{ij} is the Kronecker delta.

- The stress tensor σ_{ij} is linearly related to and dependent only on the deformation-rate tensor e_{kl}.

E-15

- No shear stresses will act during the motion, since there is no shearing action in a solid-body rotation of the fluid.

- There are no preferred directions in the fluid, so that the fluid properties are point functions.

There are nine elements in the shear-stress tensor τ_{ij} and each of these elements can be written as linear combination of the nine elements in the deformation-rate tensor e_{kl}. The 81 (9 x 9) parameters have relation between τ_{ij} and e_{kl}. General form of τ_{ij} is:

$$\tau_{ij} = \alpha_{ijkl} \frac{\partial u'_k}{\partial x_l} \qquad (E\text{-}36)$$

As shown in the previous section, $\dfrac{\partial u'_k}{\partial x_l}$ can be broken down into an antisymmetric part and a symmetric part. The antisymmetric part corresponds to the rate of rotation of a fluid element and the symmetric part corresponds to the shearing rate. According to condition 3, if the flow field is executing a simple solid-body rotation, there could be no shear stresses in the fluid. But for a solid-body rotation, the antisymmetric part of $\dfrac{\partial u'_k}{\partial x_l}$, namely $\dfrac{1}{2}(\dfrac{\partial u'_k}{\partial x_l} - \dfrac{\partial u'_l}{\partial x_k})$ is not zero.

To satisfy condition 3, the coefficients of this part of the deformation-rate tensor must be zero. So the constitutive relation for stress is:

$$\tau_{ij} = \frac{1}{2} \beta_{ijkl} \left(\frac{\partial u'_k}{\partial x_l} + \frac{\partial u'_l}{\partial x_k} \right) \tag{E-37}$$

β_{ijkl} is the 81 elements of the fourth-rank tensor and still undetermined. Condition 4, which is so called the condition of isotropy, has been imposed, which guarantees that the results obtained should be independent of the orientation of the coordinate system chosen. Most general isotropic tensor of rank 4 is in the form of:

$$\lambda' \delta_{ij} \delta_{kl} + \mu' (\delta_{ik} \delta_{jl} + \delta_{il} \delta_{jk}) + \gamma' (\delta_{ik} \delta_{jl} + \delta_{il} \delta_{jk}) \tag{E-38}$$

where λ', μ', and γ' are scalars.

In this way, the 81 quantities contained in the general tensor are reduced to three independent quantities in the isotropic case. In the case of the fourth-rank tensor which relates the shear-stress tensor to the deformation-rate tensor, β_{ijkl} will be not only isotropic, but symmetric in view of condition 3. That means γ' must be zero. The shear stress now becomes:

$$\tau_{ij} = \frac{1}{2} [\lambda' \delta_{ij} \delta_{kl} + \mu' (\delta_{ik} \delta_{jl} + \delta_{il} \delta_{jk})] \left(\frac{\partial u'_k}{\partial x_l} + \frac{\partial u'_l}{\partial x_k} \right) \tag{E-39}$$

$\delta_{kl} = 0$, unless $l = $ k,

E-17

$$\frac{1}{2}\lambda'\delta_{ij}\delta_{kl}\left(\frac{\partial u'_k}{\partial x_l}+\frac{\partial u'_l}{\partial x_k}\right)=\lambda'\delta_{ij}\frac{\partial u'_k}{\partial x_k}\qquad\text{(E-40)}$$

and l has been replaced by k. Similarly, replacing k by i, and l by j.

$$\frac{1}{2}\mu'\delta_{ik}\delta_{jl}\left(\frac{\partial u'_k}{\partial x_l}+\frac{\partial u'_l}{\partial x_k}\right)=\frac{1}{2}\mu'\left(\frac{\partial u'_i}{\partial x_j}+\frac{\partial u'_j}{\partial x_i}\right)\qquad\text{(E-41)}$$

Replacing l by i and k by j:

$$\frac{1}{2}\mu'\delta_{il}\delta_{jk}\left(\frac{\partial u'_k}{\partial x_l}+\frac{\partial u'_l}{\partial x_k}\right)=\frac{1}{2}\mu'\left(\frac{\partial u'_j}{\partial x_i}+\frac{\partial u'_i}{\partial x_j}\right)\qquad\text{(E-42)}$$

Hence, the expression for the shear-stress tensor is:

$$\tau_{ij}=\lambda'\delta_{ij}\frac{\partial u'_k}{\partial x_k}+\mu'\left(\frac{\partial u'_i}{\partial x_j}+\frac{\partial u'_j}{\partial x_i}\right)\qquad\text{(E-43)}$$

So, the constitutive relation for stress in a Newtonian fluid is:

$$\sigma_{ij}=-P\delta_{ij}+\lambda'\delta_{ij}\frac{\partial u'_k}{\partial x_k}+\mu'\left(\frac{\partial u'_i}{\partial x_j}+\frac{\partial u'_j}{\partial x_i}\right)\qquad\text{(E-44)}$$

The equation of momentum conservation (E-21) together with the constitutive relation for a Newtonian fluid (E-44) yield the famous Navier-Stokes equation, which is the principal condition to be satisfied by a fluid as it flows. The term $\partial \sigma_{ij} / \partial x_i$ which appears in equation (E-21) can be evaluated explicitly as:

$$\frac{\partial \sigma_{ij}}{\partial x_i} = \frac{\partial}{\partial x_i}\left[-P\delta_{ij} + \lambda'\delta_{ij}\frac{\partial u'_k}{\partial x_k} + \mu'\left(\frac{\partial u'_i}{\partial x_j} + \frac{\partial u'_j}{\partial x_i}\right)\right]$$

$$= -\frac{\partial P}{\partial x_j} + \frac{\partial}{\partial x_j}\left(\lambda'\frac{\partial u'_k}{\partial x_k}\right) + \frac{\partial}{\partial x_i}\left[\mu'\left(\frac{\partial u'_i}{\partial x_j} + \frac{\partial u'_j}{\partial x_i}\right)\right] \qquad \text{(E-45)}$$

In the first two terms of the equation above, i has been replaced by j, since it is only when $i = j$ that these terms are non-zero. Substituting this result in equation (E-21):

$$\rho\frac{\partial u'_j}{\partial t} + \rho u'_k\frac{\partial u'_j}{\partial x_k} = -\frac{\partial P}{\partial x_j} + \frac{\partial}{\partial x_j}\left(\lambda'\frac{\partial u'_k}{\partial x_k}\right) + \frac{\partial}{\partial x_i}\left[\mu'\left(\frac{\partial u'_i}{\partial x_j} + \frac{\partial u'_j}{\partial x_i}\right)\right] + \rho f_j \qquad \text{(E-46)}$$

Equation (E-46) is known as the Navier-Stokes equation. There are three scalar equations corresponding to the three possible values of the free subscript j.

Normally, the fluid can be assumed to be incompressible and the dynamic viscosity to be constant.

$\dfrac{\partial}{\partial x_j}\left(\lambda' \dfrac{\partial u'_k}{\partial x_k}\right)$ is identically zero, the viscous-shear term is:

$$\frac{\partial}{\partial x_i}\left[\mu'\left(\frac{\partial u'_i}{\partial x_j}+\frac{\partial u'_j}{\partial x_i}\right)\right]=\mu'\left[\frac{\partial}{\partial x_j}\left(\frac{\partial u'_i}{\partial x_i}\right)+\frac{\partial^2 u'_j}{\partial x_i \partial x_i}\right]=\mu'\frac{\partial^2 u'_j}{\partial x_i \partial x_i} \qquad \text{(E-47)}$$

This term is proportional to the Laplacian of the velocity vector, and the constant of proportionality is the dynamic viscosity. The Navier-Stokes equation for an incompressible fluid of constant density is:

$$\rho\frac{\partial u'_j}{\partial t}+\rho u'_k \frac{\partial u'_j}{\partial x_k}=-\frac{\partial P}{\partial x_j}+\mu'\frac{\partial^2 u'_j}{\partial x_i \partial x_i}+\rho f_j \qquad \text{(E-48)}$$

Neglecting viscous effects, it becomes:

$$\rho\frac{\partial u'_j}{\partial t}+\rho u'_k \frac{\partial u'_j}{\partial x_k}=-\frac{\partial P}{\partial x_j}+\rho f_j \qquad \text{(E-49)}$$

Appendix F   DERIVATION OF THEORETICAL ZONE MODEL

F.1   Derivation of key equations in the zone model

The two-layer zone model is shown in Figure 8-2. The point heat source is taken as at the center on the floor. The following assumptions were made:

- The rate of entrainment at the edge of the plume is proportional to some characteristic velocity at that height.

- The profiles of mean vertical velocity and mean buoyancy force in horizontal sections are of similar form at all heights.

- The largest local variations of density in the field of motion are small in comparison with some chosen reference of density, this reference being taken as the density of the ambient fluid at the level of the source.

- The scale of the initial laminar zone is small compared with the subsequent zone of turbulent convection.

- The pressure is hydrostatically distributed throughout the field of motion.

- Transverse forces are ignored in comparison with those in the vertical direction.

- Turbulent mixing in the vertical direction is ignored in comparison with that in the horizontal.

- No mixing between the plume and ambient air flow.

- Floor, ceiling and walls of the chamber are made of adiabatic materials.

Under the assumptions above, the mass balance equation of zone model is:

$$\rho_0 A_{c1} v_{c1} = \rho_2 A_{c2} v_{c2} \tag{F-1}$$

$$A_{c1} = C_{c1} A_1$$

$$A_{c2} = C_{c2} A_2$$

Energy equation is:

$$Q = \rho_0 C_p A_{c2} v_{c2} \Delta T \tag{F-2}$$

$$\Delta T = T_2 - T_0$$

h_c is defined as the height of the neutral plane.

$$\Delta P_1 = \Delta \rho g h_c$$

$$\Delta P_2 = \Delta \rho g (h' - h_c)$$

$$\frac{\Delta P_1}{\rho_0} = \frac{1}{2} \zeta v_{c1}^2$$

$$v_{c1} = \sqrt{\frac{2 \Delta P_1}{\rho_0}} = \sqrt{\frac{2 \Delta \rho g h_c}{\rho_0 \zeta}} \tag{F-3}$$

$$\frac{\Delta P_2}{\rho_2} = \frac{1}{2} \zeta v_{c2}^2$$

$$v_{c2} = \sqrt{\frac{2\Delta P_2}{\rho_0}} = \sqrt{\frac{2\Delta\rho g(h' - h_c)}{\rho_0 \zeta}} \qquad (F\text{-}4)$$

The volume flow rate equation for inflow is:

$$V_1 = A_{c1}v_{c1} = C_{c1}A_1\sqrt{\frac{2\Delta\rho gh_c}{\rho_0 \zeta}} = C_{d1}A_1\sqrt{\frac{2\Delta\rho gh_c}{\rho_0}} \qquad (F\text{-}5)$$

where $C_{d1} = C_{c1}/\zeta^{1/2}$

and the volume flow rate equation for outflow is:

$$V_2 = A_{c2}v_{c2} = C_{c2}A_2\sqrt{\frac{2\Delta\rho g(h' - h_c)}{\rho_2 \zeta}} = C_{d2}A_2\sqrt{\frac{2\Delta\rho g(h' - h_c)}{\rho_2}} \quad (F\text{-}6)$$

where $C_{d1} = C_{c1}/\zeta^{1/2}$

From equations (F-1) to (F-4), it is simply known that

$$\frac{\rho_0}{\rho_2} = \frac{T_2}{T_0} = \frac{V_2}{V_1} \qquad\qquad \frac{\Delta T}{T_0} = \frac{\Delta\rho}{\rho_2} \qquad\qquad \frac{\Delta T}{T_2} = \frac{\Delta\rho}{\rho_0}$$

$$\Delta T = T_2 - T_0$$

$$V_1 = C_{d1}A_1\sqrt{\frac{2\Delta Tgh_c}{T_2}} \tag{F-7}$$

$$V_2 = C_{d2}A_2\sqrt{\frac{2\Delta Tg(h'-h_c)}{T_0}} \tag{F-8}$$

From equation (F-2),

$$\Delta T = \frac{Q}{\rho_0 C_p V_2} = \frac{Q}{\rho_0 C_p C_{d2}A_2\sqrt{\frac{2\Delta Tg(h'-h_c)}{T_0}}}$$

$$\Delta T^3 = \frac{Q^2 T_0}{(\rho_0 C_p C_{d2}A_2)^2 2g(h'-h_c)}$$

The temperature difference between the upper layer and the lower layer is:

$$\Delta T = \left(\frac{Q}{\rho_0 C_p C_{d2}A_2}\right)^{2/3}\left(\frac{T_0}{2g(h'-h_c)}\right)^{1/3} \tag{F-9}$$

Defining the buoyancy flux B:

$$B = \frac{Qg}{C_p \rho_0 T_0}$$

$$T_2 = \frac{Q}{\rho_0 C_p V_2} + T_0$$

$$V_2 = C_{d2}A_2 \sqrt{\frac{2Qg(h'-h_c)}{\rho_0 C_p V_2 T_0}}$$

$$V_2^3 = (C_{d2}A_2)^2 \frac{2Qg(h'-h_c)}{\rho_0 C_p T_0}$$

$$V_2 = (C_{d2}A_2)^{2/3}(2B(h'-h_c))^{1/3} \qquad\qquad\qquad (F-10)$$

Similarly,

$$V_1 = (C_{d1}A_1)^{2/3}(2Bh_c)^{1/3} \qquad\qquad\qquad (F-11)$$

The neutral level h_c is defined as the height where the pressure difference across the building envelope is zero.

From equation (F-1),

$$\rho_0 V_1 = \rho_2 V_2$$

Combining with equations (F-7) and (F-8),

$$\rho_0 C_{d1}A_1 \sqrt{\frac{2\Delta Tgh_c}{T_2}} = \rho_2 C_{d2}A_2 \sqrt{\frac{2\Delta Tg(h'-h_c)}{T_0}}$$

$$(\rho_0 C_{d1} A_1)^2 T_0 2\Delta Tgh_c = (\rho_2 C_{d2} A_2)^2 T_2 2\Delta Tg(h' - h_c)$$

$$h_c = \frac{(\rho_2 C_{d2} A_2)^2 T_2 h'}{(\rho_0 C_{d1} A_1)^2 T_0 + (\rho_2 C_{d2} A_2)^2 T_2}$$

$$h_c = \frac{h'}{\dfrac{T_2}{T_0}(\dfrac{C_{d1} A_1}{C_{d2} A_2})^2 + 1} = \frac{h'}{n+1} \qquad \text{(F-12)}$$

where

$$n = \frac{T_2}{T_0}(\frac{C_{d1} A_1}{C_{d2} A_2})^2$$

$$V_1 = (C_{d1} A_1)^{2/3} (2Bh_c)^{1/3}$$

$$V_2 = (C_{d2} A_2)^{2/3} (2B(h' - h_c))^{1/3}$$

The equation of thermal plume above a fire was developed by Rouse (1954) and Yih (1977):

$$M = 0.153\rho_2 [Qg/(\rho_2 C_p T_0)]^{1/3} (h' - (h' - h_c))^{5/3}$$

$$M = 0.153\rho_2 [Qg/(\rho_2 C_p T_0)]^{1/3} h_c^{5/3} \qquad \text{(F-13)}$$

$$M = \rho_2 A_2 v_2 = \rho_2 V_2$$

$$V_2 = \frac{M}{\rho_2} = \frac{0.153\rho_2[Qg/(\rho_2 C_p T_0)]^{1/3} h_c^{5/3}}{\rho_2} = 0.153B^{1/3}h_c^{5/3} \qquad \text{(F-14)}$$

Combining equations (F-10) and (F-14),

$$V_2 = (C_{d2}A_2)^{2/3}(2B(h'-h_c))^{1/3} = 0.153B^{1/3}h_c^{5/3}$$

$$(C_{d2}A_2)^2 \, 2(h'-h_c) = 0.153^3 h_c^5$$

$$C_{d2}A_2 = \sqrt{\frac{0.153^3 h_c^5}{2(h'-h_c)}}$$

$$\frac{C_{d2}A_2}{h'^2} = \sqrt{\frac{0.153^3 (\frac{h_c}{h'})^5}{2(1-\frac{h_c}{h'})}}$$

$$\frac{C_{d2}A_2}{h'^2} = 0.042318\sqrt{\frac{(\frac{h_c}{h'})^5}{(1-\frac{h_c}{h'})}} \qquad \text{(F-15)}$$

That is the relationship between the neutral level height h_c and the outlet area A_2.

F.2   MATLAB listing

```
dT=zeros(1,9);

V=zeros(1,9);

y1=zeros(1,9);

y2=zeros(1,9);

y3=zeros(1,9);

h1=0;

i=0;

j=0;

A1=1;

A2=1;

e=0.1;

h=5;

T0=300;

E=500;

Cd=0.6;

cp=1010;

p=1.293;

g=9.8;

pi=3.14;


B=E*g/(cp*p*T0);


while e< 0.8
    i=i+1;
    e=e+0.1;
    y1(i)=0.042318/Cd*(F^5/(1-e)).^(1/2)  ;
    y2(i)=(Cd*y1(i))^(2/3)*(2*B*(1-e))^(1/3)*h^(5/3);
```

```
end


i=0;

j=0;

while h1 < (F-0.2)

    h1=h1+0.1;

    i=i+1;

      dT(i)=(F/(p*cp*Cd*A2))^(2/3)*(T0/(2*g*(F-h1)))^(1/3);

end


e=0.2:0.1:1;

plot(y1,e);

xlabel('A/h2');

ylabel('hc/h');


figure(2)

e=0.2:0.1:1;

plot(y1,y2);

xlabel('A/h2');

ylabel('V2');


e=0.1:0.1:h1

plot(F,dT);

xlabel('hc');

ylabel('dT');


dT=dT';
```

Appendix G   DERIVATION OF PLUME EQUATIONS

G.1   Derivation of equations for volume flux, momentum flux and energy flux

A typical plume model is shown in Figure 9-3. Taking the point heat source on the floor, $S_0 = 0$. Under the assumptions, the fundamental equation of vertical acceleration in two-dimensional flow is:

$$\rho v \frac{\partial v}{\partial y} + \rho u \frac{\partial v}{\partial x} = -\Delta B + \frac{\partial \tau}{\partial x} \qquad (G-1)$$

where τ is the shear stress, proportional to the mean product of the turbulent velocity components, and ΔB is the unit buoyant force.

The equation of continuity is:

$$\frac{\partial v}{\partial y} + \frac{\partial u}{\partial x} = 0 \qquad (G-2)$$

Assuming the horizontal cross-section of the pool is round, according to the conservation law of motion, the volume flux V can be written as:

$$V = 2\pi \int_0^\infty vxdx \qquad (G-3)$$

The momentum of the pool is:

$$M = \int_0^R \rho v^2 \cdot 2\pi x dx = \rho v_0^2 \pi R_0^2 \qquad\qquad (G-4)$$

where v_0 is the vertical velocity in the cross-section of the pool and R_0 is the radius of the cross-section of the pool.

The momentum flux M of the plume is:

$$M = 2\pi \int_0^\infty \rho v^2 r dr \qquad\qquad (G-5)$$

The energy flux E of the plume is:

$$E = 2\pi \int_0^\infty \frac{\rho v^3}{2} x dx \qquad\qquad (G-6)$$

The buoyancy flux is defined as:

$$B = \frac{Qg}{C_p \rho T} \qquad\qquad (G-7)$$

Four cases of simulations were done for studying this case. The results of velocity distribution, pressure distribution and temperature distribution are

shown in Figures 9-4 to 9-6 respectively. The results of plume vertical velocity

probability curves are plotted in Figure 9-7, showing the distributions of v.

As a result, for the condition of axial symmetry model, the vertical velocity v has

the following relationship with x and h (Rouse 1954):

$$\frac{v}{(B/h)^{1/3}} = f\left(\frac{x}{h}\right) \tag{G-8}$$

Suppose the velocity distribution is uniform, according to both the simulation

above and the experimental results (Beyler 1986, Drysdale 1985, Rouse 1954,

Heskestad 1984, Hinkley 1971, Morton 1956, Morgan 1987, Thomas 1963, Yih

1977, Yu 1992, Zukoski 1981), the velocity distribution could be expressed as

Gaussian distribution.

$$v = v_{max} \exp\left(-\frac{x^2}{R^2}\right) \tag{G-9}$$

where R is the specified plume radius.

Then, the velocity distribution can be written as:

$$v = \alpha\left(\frac{B}{h}\right)^{1/3} \exp\left(-65\frac{x^2}{h^2}\right) \tag{G-10}$$

where α is a coefficient related to height h, it is defined in Figure 9-8, expressed as terms of a character for length l_c (taken as 1 m) as:

$$\alpha = -1.379 \, (h / l_c)^3 + 8.032 \, (h / l_c)^2 - 16.427 \, (h / l_c) + 17.029$$

Putting this result into equations (G-3), (G-5) and (G-6), then the following equations are obtained:

Volume flux

$$V = 0.0483 \alpha B^{1/3} h^{5/3} \qquad \text{(G-11)}$$

Momentum flux

$$M = 0.02415 \alpha^2 \rho B^{2/3} h^{4/3} \qquad \text{(G-12)}$$

Energy flux

$$E = 0.00805 \alpha^3 \rho B h \qquad \text{(G-13)}$$

From the result of this simulation, it is found that in the main part of the plume, normally $\alpha = 4.0$.

So equations (G-10) to (G-13) could be simplified as:

Velocity distribution

$$v = 4.0 \left(\frac{B}{h} \right)^{1/3} \exp \left(-65 \frac{x^2}{h^2} \right)$$ (G-14)

Volume flux

$$V = 0.1932 B^{1/3} h^{5/3}$$ (G-15)

Momentum flux

$$M = 0.3864 \rho B^{2/3} h^{4/3}$$ (G-16)

Energy flux

$$E = 0.5152 \rho B h$$ (G-17)

G.2   Derivation of central axis equation

Assuming the parallel flow has no effect on the vertical velocity of the plume, then the forced ventilation of the ambient air flow has no effects on the velocity distribution in each horizontal level, so that only the position of the plume central axis would be changed.

Central axis can be seen as a link of many points. Each point was taken as forces from both horizontal direction (which is from the forced ventilation of ambient air) and vertical direction (which is from the buoyant).

Horizontal force from ventilation of ambient air:

$$\frac{1}{2}\rho w^2 = ma_x \qquad\qquad\qquad (G-18)$$

Vertical force from buoyant:

$$(\rho_0 - \rho)Hg = ma_y \qquad\qquad\qquad (G-19)$$

So that the movement of each point in central axis can be written as:

$$x = wt + \frac{1}{2}a_x t^2 = wt + \frac{1}{2}\left(\frac{\rho_0 w^2}{2m}\right)t^2 \qquad\qquad (G-20)$$

$$h = vt + \frac{1}{2}a_y t^2 = vt + \frac{1}{2}\left(\frac{(\rho_0 - \rho)Hg}{m}\right)t^2 \qquad (G-21)$$

In the plume,

$$Q = mC_p\Delta T$$

$$m = \frac{Q}{C_p\Delta T} \qquad (G\text{-}22)$$

Putting equation (G-22) into equations (G-20) and (G-21),

$$x = wt + \frac{C_p\Delta T\rho_0 w^2}{4Q}t^2 \qquad (G\text{-}23)$$

$$h = vt + \frac{1}{2}\left(\frac{(\rho_0 - \rho\ )HgC_p\Delta T}{Q}\right)t^2 \qquad (G\text{-}24)$$

In the plume,

$$\frac{\rho}{\rho_0} = \frac{T_0}{T} \qquad (G\text{-}25)$$

Putting equation (G-25) into equation (G-24),

$$\left\{\begin{array}{l} x = wt + \dfrac{C_p\Delta T\rho_0 w^2}{4Q}t^2 \\[2em] h = vt + \dfrac{(1-\dfrac{T_0}{T})\rho_0 HgC_p\Delta T}{2Q}t^2 \end{array}\right. \qquad (G\text{-}26)$$

In a special case, when w is constant and the plume has no effects on the forced ventilation from ambient air, equation (G-20) can be simplified to:

$$x = wt$$

and if the temperature inside the plume is uniform, equation (G-24) can be simplified to:

$$h = vt$$

Then, the plume central axis equation can be written as:

$$x = \frac{w}{v} h \qquad\qquad\qquad (G-27)$$

Appendix H   PUBLICATIONS FROM THIS STUDY

- Chow, W.K. and Kui, Q., "Preliminary review on fire safety codes in China", First International Symposium on Engineering Performance-Based Fire Codes, The Hong Kong International Trade & Exhibition Center, Hong Kong, 8 September 1998, pp 213-219.

- Kui, Q. and Chow, W.K., "Bare cabin fires with operation of smoke extraction system", Proceedings of the Fourth Asia-Oceania Symposium on Fire Science and Technology, Waseda University, Tokyo, Japan, 22-26 May 2000, pp 613-620.

- Chow, W.K. and Kui, Q., "Time to flashover for fires in a 'bare babin' with smoke extraction system", Architecture Science Review, 2000, pp 115-121.

- Kui, Q., "Brief review on forced-ventilation requirements in China fire codes", International Journal on Engineering Performance-Based Fire Codes, Vol. 5, No.1, 2003, pp 7-19.

- Kui, Q., Chow, W. K., Gao, Y. and Liu, S. L., "A study on plume equation in a chamber with forced ventilation", International Journal on Architectural Science - Accepted to publish, May (2003).